Optimising performance in clinical capsule endoscopy

Koulaouzidis, Anastasios

2020

Document Version:
Publisher's PDF, also known as Version of record

Optimising performance in clinical capsule endoscopy

ANASTASIOS KOULAOUZIDIS
DEPARTMENT OF CLINICAL SCIENCES, MALMÖ | LUND UNIVERSITY

Printed by Media-Tryck, Lund 2020 NORDIC SWAN ECOLABEL 3041 0903

LUND UNIVERSITY

FACULTY OF MEDICINE

Department of Clinical Sciences, Malmö

Lund University, Faculty of Medicine
Doctoral Dissertation Series 2020:75
ISBN 978-91-7619-937-4
ISSN 1652-8220

Optimising performance in clinical capsule endoscopy

Anastasios Koulaouzidis

LUND
UNIVERSITY

DOCTORAL DISSERTATION
by due permission of the Faculty of Medicine, Lund University, Sweden.
To be defended at Diagnostiskt centrum, Carl-Bertil Laurells gata 9,

Skåne University Hospital Malmö.

9 June 2020 at 09.00.

Faculty opponent
Professor Gunnar Baatrup

Organization LUND UNIVERSITY Faculty of Medicine Department of Clinical Sciences, Malmö	**Document name** DOCTORAL DISSERTATION **Date of issue** June 9, 2020
Author(s): Anastasios Koulaouzidis, MD DM	Sponsoring organization

Title and subtitle Optimising performance in clinical capsule endoscopy

Abstract

Video capsule endoscopy (VCE), perfomed by ingesting a small vitamin-sized camera pill, was developed over a period of a couple of decades and –since its introduction in clinical practice at the dawn of the millennium– has become an essential tool in the diagnosis and management of small bowel (SB) diseases. At the same time, other fields such as minimally invasive diagnosis of other parts of the gastointestinal (GI) tract has been or is currently explored as future applications of this technology. As a pure imaging modality, VCE 'suffers' from lack of additional on-board data that could allow higher diagnostic accurary. This could be either advanced image enhancement or biochemical sensors that could provide relevant info. Furthermore, as VCE clips reading remains manual, it is heavily dependent on the reviewer's experience. Historically, VCE lesion miss rates have been reported at levels between 6% and 18%. There is also poor agreement on interobserver agreement and subsequent management decision-making.

The aim of this thesis was to increase the knowledge and to critically evaluate the importance of existing applications as well as exploring and developing new applications to optimize use and diagnostic outcomes of VCE in clinical practice. More specifically, to investigate the correlation between VCE imaging and faecal calprotectin (FC); to develop a model for prediction of VCE results based on FC levels; to investigate and consolidate existing clinical data on the utility of Fujinon Intelligent Chromoendoscopy (FICE) in improving delineation and detection rate for pathological findings in VCE compared to conventional reading; to develop and validate a novel database aiming to provide a reference for research on the development of medical decision support system (MDSS) for VCE; and to develop an approach to capsule localisation and to provide estimations of relative movement of the VCE during its passage through the GI tract.

Results of the studies showed that in patients with strong clinical suspicion of SB inflammation and negative (conventional) bidirectional endoscopy, VCE should not be limited to patients with elevated biomarkers only. Moreover, the correlation between FC levels and GI inflammation –as detected by VCE– was moderate and FC=>76 mcg/g may be associated with appreciable SB inflammation on VCE in patients with negative prior diagnostic workup. Furthemore, FICE seems to perform better for pigmented lesions such as angiectasias, both in lesion delineation and detection. However, overall using the three FICE modes did not significantly improve detection rate or the quality of visualization of the most common pathological findings seen on SB VCE. We developed KID, the first database of VCE images and videos with both graphic and semantic annotations, developed specifically for MDSS research. KID provides a platform for data sharing and software development. The experiments detailed are proof-of-principle studies demonstrating the potential for KID to fulfil this role. Moreover, we presented methods for both 2D and 3D localisation of capsules using visual information alone. Such methods are feasible and have potential to be of clinical use.

Key words: Capsule endoscopy, small bowel, innovation, image improvement, software, localisation, KID, FICE

Classification system and/or index terms (if any)

Supplementary bibliographical information	Language English
ISSN and key title 1652-8220 Lund University, Faculty of Medicine Doctoral Dissertation Series: 2020:75	ISBN 978-91-7619-937-4

Recipient's notes	Number of pages 124	Price
	Security classification	

Signature 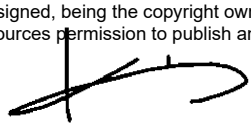 Date 2020-04-17

Optimising performance in clinical capsule endoscopy

Anastasios Koulaouzidis

LUND
UNIVERSITY

Cover photo by Anastasios Koulaouzidis

Faculty of Medicine
Department of Clinical Sciences Malmö
Lund University

Lund University, Faculty of Medicine Doctoral Dissertation Series 2020:75
ISBN 978-91-7619-937-4
ISSN 1652-8220

Printed in Sweden by Media-Tryck, Lund University, Lund 2020

To my brother, Henrik and Ervin

Table of Contents

Abbreviations

AI	Artificial intelligence
ALICE	Augmented Live-body Image Colour-Spectrum Enhancement
AVC	Advanced video coding
BM	Blue mode
BRIEF	Binary Robust Independent Elementary Features
CAD	Computer-aided detection/diagnosis
CD	Crohn's disease
CE	Capsule endoscope
CECDAI	Capsule endoscopy Crohn's disease activity index
CEST	Capsule endoscopy structured terminology
CIE-Lab	Commission Internationale de l'eclairage-Lab
CMOS	Complementary metal-oxide-semiconductor
CRP	C-reactive protein
DY	Diagnostic yield
ELISA	Enzyme-linked immunosorbent assay
FAST	Features from Accelerated Segment Test
FC	Faecal calprotectin
FICE	Flexible spectral imaging colour enhancement
FOV	Field of view
fps	Frames per sec
GI	Gastrointestinal
IBD	Inflammatory bowel disease
IQR	Inter-quartiles range
IT	Information technology

JI	Jaccard index
KID	κάψουλα interactive database
LED	Light emitting diode
LRAC	Localized region-based active contour
LS	Lewis score
MAE	Mean absolute error
MDSS	Medical decision support systems
MLAs	Machine learning algorithms
MRE	Magnetic resonance enterography
NBI	Narrow band imaging
NPV	Negative predictive value
ORB-SLAM	Oriented FAST and Rotated BRIEF – Simultaneous Localisation and Mapping
OWL DL	Ontology web language description logics
POI	Point(s) of interest
PPV	Positive predictive value
P	Probability
QUADAS	Quality Assessment of Diagnostic Accuracy Studies
RF	Radio frequency
ROC	Receiver operating characteristic
ROI	Region(s) of interest
SB	Small bowel
SfS	Shape-from-Shading
VCE	Video capsule endoscopy
WLE	White light endoscopy
WLI	White light imaging
2D	2-dimensional
3D	3-dimensional

Lists of papers

This thesis is based on the following papers, which will be referred to in the text by their Roman numerals. All papers were reprinted with permission from the respective publishers.

I. **Koulaouzidis A**, Sipponen T, Nemeth A, Makins R, Kopylov U, Nadler M, Giannakou A, Yung DE, Johansson GW, Bartzis L, Thorlacius H, Seidman EG, Eliakim R, Plevris JN, Toth E. Association Between Fecal Calprotectin Levels and Small-bowel Inflammation Score in Capsule Endoscopy: A Multicenter Retrospective Study. Digestive Diseases and Sciences 2016; 61(7):2033-40.

II. Yung DE, Boal Carvalho P, Giannakou A, Kopylov U, Rosa B, Rondonotti E, Toth E, Plevris JN, **Koulaouzidis A**. Clinical validity of flexible spectral imaging color enhancement (FICE) in small-bowel capsule endoscopy: a systematic review and meta-analysis. Endoscopy 2017; 49(3):258-269.

III. **Koulaouzidis A**, Iakovidis DK, Yung DE, Rondonotti E, Kopylov U, Plevris JN, Toth E, Eliakim A, Wurm Johansson G, Marlicz W, Mavrogenis G, Nemeth A, Thorlacius H, Tontini GE. KID Project: an internet-based digital video atlas of capsule endoscopy for research purposes. Endoscopy International Open 2017; 5(6):E477-E483.

IV. **Koulaouzidis A**, Iakovidis DK, Yung DE, Mazomenos E, Bianchi F, Karagyris A, Dimas G, Stoyanov D, Thorlacius H, Toth E, Ciuti G. Novel experimental and software methods for image reconstruction and localization in capsule endoscopy. Endoscopy International Open 2018; 6(2):E205-E210.

Introduction

The concept of a swallowable capsule first appeared in 1957 in Jacobson and Mackay's ground-breaking paper on radiofrequency (RF) transmission of temperature and pressure from within the human body (MacKay et al., 1957). From this point onward, the combination of significant incremental progress, ingenuity and interdisciplinary collaborations led to the development new type of video-telemetry capsule endoscope, small enough to be swallowed (Iddan et al., 2000).

Once a capsule endoscope (CE) is ingested, transmission of colour images begins, resulting in a large volume of imaging data. Video capsule endoscopy (VCE) remains the first-line diagnostic tool for screening of small bowel (SB) diseases (Vasilakakis et al., 2019). Despite several incremental technical advancements, VCE sequences are still manually read, a task that is both time-consuming –typically lasting 45-90min– and prone to errors as it requires the undivided concentration of the reader (Koulaouzids et al., 2015[a]). The latter is the result of natural limitation(s) imposed by the ceiling of human capabilities (Iakovidis et al., 2014[b]). In fact, over the past few years, several studies indicated that despite the reported diagnostic yield (DY), the true sensitivity of VCE is difficult to determine due to the lack of an adequate gold standard (Iakovidis et al., 2015). Therefore, although the current commercially available capsules offer convenience and an acceptable DY, they have several drawbacks (Vasilakakis et al., 2020).

Traversing the gastrointestinal (GI) tract in a passive manner is –perhaps– the most important of them; VCE readers are neither able to interfere with the CE movement(s) nor the speed of the pill-sized device as it moves in the lumen of the GI tract propelled by bowel contractions (Koulaouzidis et al., 2012[d]). As bowel peristalsis is a complex, cumulative event of five contractile patterns, *i.e.*, peristaltic waves, stationary contractions, clusters of contractions (Phase III), giant contractions and anti-peristalsis waves, its impact on CE locomotion (speed, position and orientation) is unpredictable (Koulaouzidis et al., 2015[a]). In other words, it's not possible to stop or navigate the CE towards an area (or point) of interest, for further thorough inspection (Vasilakakis et al., 2020). Furthermore, extrapolating from the advancements/strides in conventional (flexible/wired) endoscopy –since the introduction of the latter in regular clinical practice more than five decades ago–, the prospect for wireless devices should be considered as anything but optimistic (Koulaouzidis et al., 2015[c]). The lack of additional data,

aside white light imaging (WLI), that could add to an increased diagnostic certainty is another important technology drawback (Koulaouzidis et al., 2015[a]).

Therefore, pairing images with biochemical data, for instance faecal calprotectin (FC), could assist in the clinical interpretation of pathology recorded in VCE sequences.

Furthermore, because of its inherent technological limitations VCE continues to miss lesions such as ulcers and submucosal tumors and/or other SB malignancies. Developments in software for image and video processing might help to increase the DY of SB VCE. Flexible spectral imaging color enhancement (FICE; also known as Fujinon Intelligent Chromoendoscopy; Fujinon, Saitama, Japan) is a digital processing algorithm which takes white-light endoscopy (WLE) images and mathematically processes the image by emphasizing certain ranges of wavelengths (Pohl et al., 2010; Krystallis et al., 2011). Therefore, computational methods, which are integral to the reviewing software interface of all WLI VCE, could contribute not only to the reduction of the time required for VCE reading but also diminishing human errors in VCE sequence interpretation.

Such computational methods first appeared in the early 2000s in the form of automatic polyp detection using conventional video-endoscopy images (Iddan et al., 2000; Iakovidis et al., 2015). In fact, back in 2015, we had mentioned, that several other approaches for the detection and/or characterization of abnormalities have been proposed by computer scientists and engineers to support medical decision-making (Iakovidis et al., 2014[b]). At that time, artificial intelligence (AI) in VCE was still in its early stages. These methods were based on *processing* and/or *analysis* of videos from VCE procedures (Koulaouzidis et al., 2020). Processing involves transformation of video signals to enhance relevant information or suppress irrelevant information, for example, to enhance the outlines of the lesions or to suppress noise. Analysis involves automatic detection of relationships between sets of pixels or video frames, such as pixels belonging to a lesion or recognition of image contents i.e. lesion recognition (Iakovidis et al., 2015).

Hence, AI system development is based on machine learning algorithms (MLAs) for automatic detection, localisation, and recognition of pathology in VCE images and videos. A large amount of data, in the form of annotations, is required to train MLAs. However, a limited number of datasets composed of images with graphic annotations have become available in the context of information technology (IT) studies.

Background

It has been almost two decades since the appearance of the first commercial CE in 2001 (Iddan et al., 2000; Cummins et al., 2019). CE has had a remarkable impact on clinical practice by offering a minimally invasive, hence well-tolerated, alternative to conventional 'wired' endoscopy for visualisation of the entire GI tract (Vasilakakis et al., 2020). VCE devices have a shape similar to that of a large vitamin pill, and their volume is roughly 2 cm^3 (Koulaouzidis et al., 2013[b]). Nowadays, there are five leading companies in the market of VCE, which provide diagnostic tools for non-invasive exploration of the SB as well as CEs for oesophageal, stomach and colonic examinations. One of these companies, Medtronic Inc., has developed the third version of its SB CE, called the PillCam®SB3 (Vasilakakis et al., 2020). Also, it has developed the PillCam®Crohn's capsule, used for the visualisation of SB and colonic mucosa for the assessment of Crohn's disease (CD), as well as the Pillcam®COLON2 and the PillCam®UpperGI for the examination of the respective parts of the upper GI tract.

The MC2000 and the EndoCapsule® (EC-S10) are the latest versions of SB capsule endoscopes manufactured by Intromedic (Koulaouzidis et al., 2013[b;] Vasilakakis et al., 2019) and Olympus Corporation (Koulaouzidis et al., 2015[a]), respectively. Interestingly, the CapsoCam®Plus (Koulaouzidis et al., 2013[a]) by Capsovision provides a 360° side-on panoramic field view due to the four cameras placed in the centre of its body. Jinshan Science & Technology, Chongqing, China has developed the OMOM Capsule 2 (Koulaouzidis et al., 2013[b]; Rondonotti et al., 2018). Recently, ANKON focusing mostly on robotic gastroscopy, has captured the attention with the significant promise of providing a non-invasive, robotic based approached in upper GI tract diagnosis.

Capsule technology

The first CE-system (mouth-to-anus; M2A®) was developed by Given®Imaging Ltd (Yoqneam, Israel) and it was approved (for clinical use in humans) in Europe and the USA in August 2000. Initially, its battery life was only about 6 h. The first generation of commercially available PillCam®SB (essentially the renamed M2A®) was released in 2001, while the second generation of PillCam®SB was released in 2007 (PillCam®SB2). The latest, commercial PillCam®SB CE model

(PillCam®SB3) was released in 2013 (Rondonotti et al., 2018). PillCam®SB2, which is still used in few centres around the globe, measures 11×26 mm and weighs<4 g (Koulaouzidis et al., 2015[b]). It contains a miniature colour video Complementary metal-oxide-semiconductor (CMOS) camera with four illuminating Light emitting diodes (LEDs), two batteries, a RF transmitter and an antenna. Images are captured at a rate of 2 frames per sec (fps) for PillCam®SB or 4 fps for PillCam®SB2 and an adjustable frame rate of 2-6 fps for the third version of the PillCam®SB (Rondonotti et al, 2018), while the battery life is between 8 h (PillCam®SB) and 12 h (PillCam®SB2), and in the newer model >12h (Koulaouzidis et al., 2015[b]).

Due to increased field of view (FOV) (156°), PillCam®SB2/SB3 has a broader mucosal coverage, as compared with 140° of its predecessor i.e. PillCam®SB, and an effective visibility distance of 30 mm (Omori et al., 2018). The image resolution of all PillCam®SB iterations, save for the last, is at 256×256 pixels. Advanced optics and automatic light control provide optimal image quality and illumination. Therefore, at a reference working distance of 4.5 mm, the coverage mucosal area of PillCam®SB2 is 1100mm^2 as compared with 500 mm^2 of its predecessor (Metzger et al., 2009).

The second most commonly used in Europe system is the MiroCam® (which stands for Micro Intelligent Robotic Object Camera) which has been developed by the intelligent Microsystem centre established by the Korea Ministry of Science & Technology in Seoul, South Korea, which was renamed to IntroMedic Co Ltd in 2006 (Koulaouzidis et al., 2015[a]). The company's SB CE device passed the European medical standards and received certification (CE mark) in 2007; it also received the US Food & Drug Administration approval in May 2011 (Koulaouzidis et al., 2013[b]). MiroCam® (currently version 3, released in 2014), utilizes a novel transmission technology, the electric field propagation. This technology uses the capsule itself to generate an electrical field and the human body as a conductive medium for data transmission, in the so-called *human body communication* (Vasilakakis et al., 2019). Perhaps this, in conjunction with the set array of sensors, is the main reason for the persistent failure of this CE model to capture upper oesophageal and gastro-oesophageal junction (Z-line) images (Koulaouzidis, 2012; Bartzis et al., 2014). Specifications of the MiroCam® CE device include a size of 10.8×24.5mm, weight of 3.4 g, a FOV of 170°. For further technology specifications and details of the rest of the commercially available systems (Figure 1).

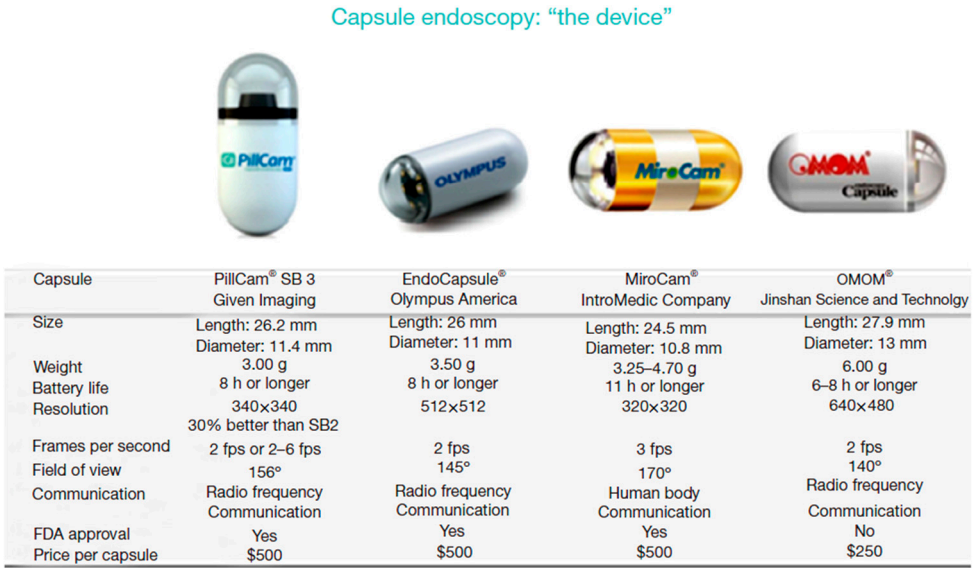

Capsule	PillCam® SB 3 Given Imaging	EndoCapsule® Olympus America	MiroCam® IntroMedic Company	OMOM® Jinshan Science and Technolgy
Size	Length: 26.2 mm Diameter: 11.4 mm	Length: 26 mm Diameter: 11 mm	Length: 24.5 mm Diameter: 10.8 mm	Length: 27.9 mm Diameter: 13 mm
Weight	3.00 g	3.50 g	3.25–4.70 g	6.00 g
Battery life	8 h or longer	8 h or longer	11 h or longer	6–8 h or longer
Resolution	340×340 30% better than SB2	512×512	320×320	640×480
Frames per second	2 fps or 2–6 fps	2 fps	3 fps	2 fps
Field of view	156°	145°	170°	140°
Communication	Radio frequency Communication	Radio frequency Communication	Human body Communication	Radio frequency Communication
FDA approval	Yes	Yes	Yes	No
Price per capsule	$500	$500	$500	$250

Figure 1. Illustration and specifications of the commercially-available and most commonly-used VCE systems (courtesy of Prof. Rami Eliakim and the Annals of Translational Medicine).

Reading software

The proprietary reading software of Given®Imaging Ltd is the RAPID®Reader and through repeated developments it has now reached its ninth version. This software interface provides single, dual or quadruple window video review as well as additional diagnostic features and study reviewing aids. It contains an improved user interface similar to the ribbon toolbar concept used in Microsoft®products, the Lewis Score (LS) calculator (Koulaouzidis et al., 2015[b]), the FICE (Koulaouzidis et al., 2015[c]), the suspected blood indicator (Yung et al., 2017), QuickView (Koulaouzidis et al., 2012[c]), a thumbnail comparison feature, backward compatibility with studies from previous RAPID® software versions and an improved progress indicator/localisation guide (Koulaouzidis et al., 2015[a]).

Several IT groups have proposed software for detection of SB lesions/bleeding, reducing reading time, lesion localisation, motility assessment, video enhancement and/or data management (Koulaouzidis et al., 2015[a]; Iakovidis et al., 2015). Reducing reading time is beneficial, especially in high volume centres. Previous work has shown that readers’ experience does not improve detection of lesions in VCE (Zheng et al., 2012). Therefore, computer-aided detection/diagnosis (CAD) can improve DY.

Despite prolific IT research, incorporating AI systems into CE reading remains difficult (Iakovidis et al., 2015). The backbone of AI system development is based

on MLAs) for automatic detection, localisation, and recognition of pathology in CE images and videos. A large amount of data, in the form of annotations, is required to train MLAs. Semantic annotations describe the content of VCE videos and images, whereas graphic annotations are pixel-level labels indicating regions of interest (ROIs), (Figure 2). Although there are some online databases (available from this link: http://www.endoatlas.com/websites.html), these usually include the necessary semantic annotations, but lack graphic annotations of ROIs. Therefore, such material cannot be directly used by IT scientists for intelligent systems' training or as a reference for their evaluation.

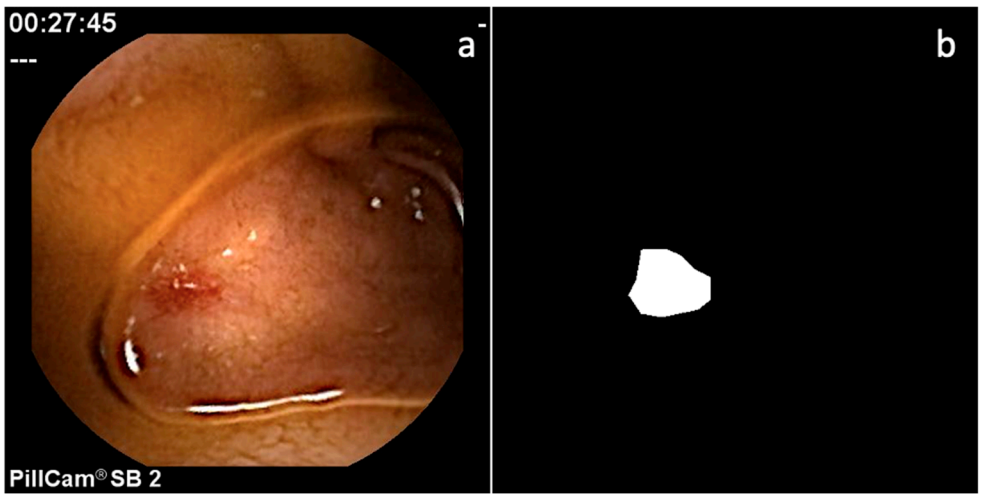

Figure 2. Semantic annotation (angiectasia) and (b) graphic annotation of the same image indicating region of interest in the (a) image.

A limited number of datasets composed of images with graphic annotations have become available in the context of IT studies (Iakovidis et al., 2015; Cong et al., 2015). A novel database, KID (***κάψουλα* interactive database**; based on Greek word for "capsule") (http://is-innovation.eu/kid/) was developed to fill this gap (Figure 3). It is available online, upon free registration, aiming to provide a reference for research on the development of medical decision support systems (MDSS) for VCE, including the study of the performance of human observers in comparison to others and CAD.

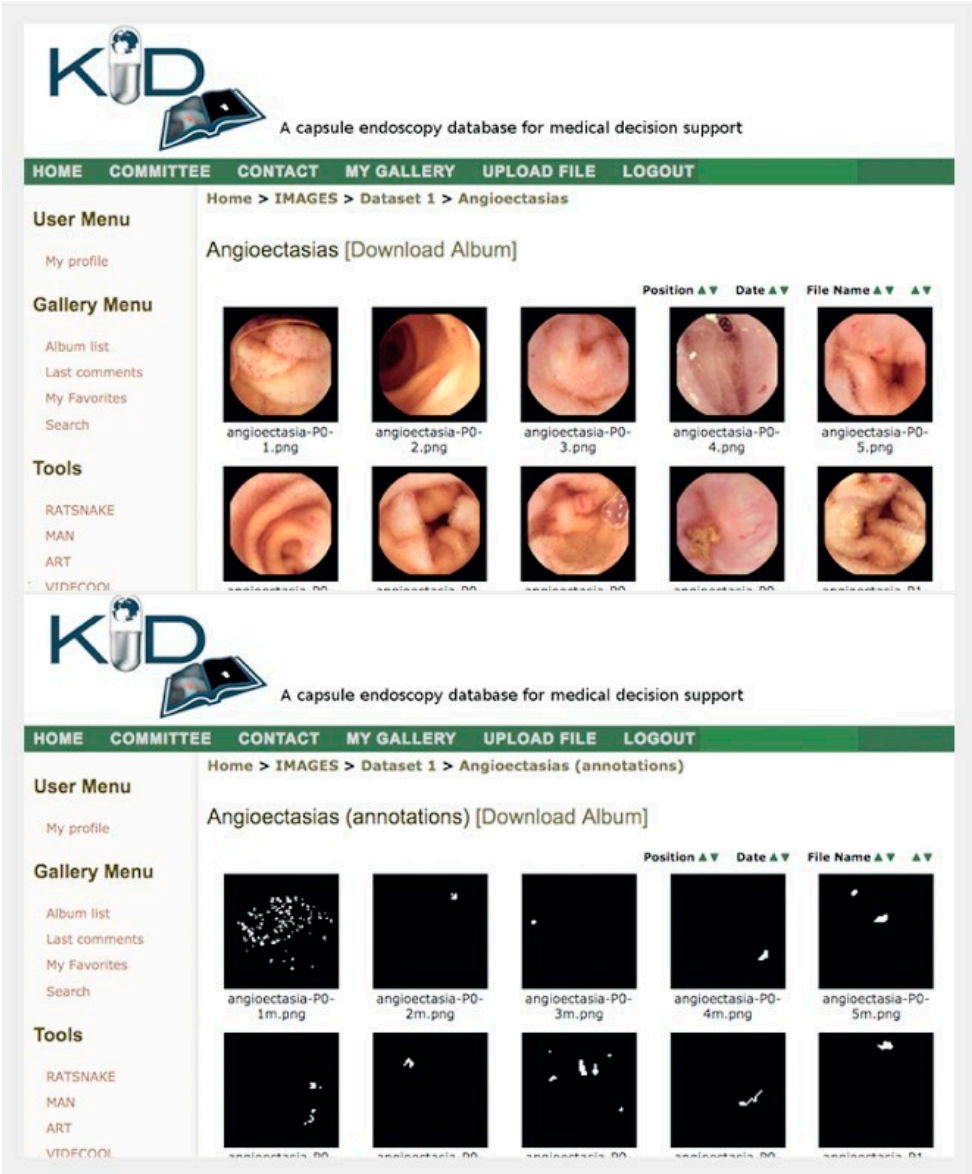

Figure 3. One of the sets of angiectasia images (top) with their corresponding graphic annotations (black and white, bottom), seen within the KID (*κάψουλα* interactive database) website interface.

In order to standardise reporting of SB inflammation using VCE, two scoring indices have been developed: the Lewis score (LS) (Figure 4) and the Capsule Endoscopy Crohn's Disease Activity Index (CECDAI) (Gralnek et al., 2008; Niv et al., 2012; Koulaouzidis et al., 2012[b]). Both scores are based on parameters and descriptors of inflammatory changes and have been externally validated in several

reports (Rosa et al., 2012; Cotter et al., 2015; Höög et al., 2014; Koulaouzidis et al., 2012[b]). However, they are of limited discriminatory ability, and it is still unclear how accurately they measure the degree of mucosal inflammation (Cotter et al., 2015; Gurudu et al., 2012).

Figure 4. Lewis score (LS) calculator, as seen with the Rapid®Reader software (Medtronic); image courtesy of Prof. Martin Keuchel.

Calprotectin and faecal calprotectin

Calprotectin was first isolated from human granulocytes by Fagerhol (Fagerhol et al., 1980) (Figure 5). Calprotectin is a major component of the cytosol of neutrophils and –to a lesser extent– monocytes and macrophages, released in faeces upon leukocyte activation (Sipponen, 2013; Sipponen et al., 2015; Logan 2010). In the presence of calcium, calprotectin is resistant to degradation and stable in faeces at room temperature for up to 7 days (Sipponen, 2013; Røseth, 2003). FC 'leaks' into the gut lumen through inflamed mucosa therefore reflecting the amount of leukocyte cell activation, migration, and death in the bowel wall (Sipponen et al., 2012).

Although FC is not disease specific, a recent meta-analysis showed an excellent correlation of FC with the severity of mucosal inflammation. At a cut-off level of 100 mcg/g, FC can distinguish inflammatory bowel disease (IBD) from non-inflammatory conditions (van Rheenen et al., 2010). Therefore, many field experts consider FC a reliable and highly specific biomarker of intestinal inflammation (Gurudu et al., 2012; Sipponen, 2013). There are conflicting reports suggesting that the correlation between FC and mucosal inflammation may be weaker in SB

inflammation in comparison with the colon. Monoclonal, polyclonal, and combination enzyme-linked immunosorbent assay (ELISA) (quantitative), and bedside immunochromatographic (semi-quantitative) methods have been developed –and validated– for FC measurement (Sipponen et al., 2015).

Figure 5. Crystal structure of human Calprotectin molecule (source: https://www.ncbi.nlm.nih.gov/Structure/pdb/1XK4)

Recently, we showed that measurement of FC levels prior to referral for CE is a useful tool to select patients with possible SB IBD (Koulaouzidis et al., 2011). In this single-centre study, FC >100 mcg/g is good predictor of positive SB VCE findings, while FC >200 mcg/g was associated with higher VCE DY (65%) and

confirmed SB inflammation in 50% of cases (Koulaouzidis et al., 2011). Hence, it is reasonable to consider that strong correlation should exist between FC levels and LS (Koulaouzidis et al., 2012[b]; Gurudu et al., 2012). However, in a separate cohort of patients with suspected, isolated SB disease, LS showed strong correlation with FC <100 mcg/g (Koulaouzidis et al., 2012[b]). The overall correlation between FC and LS is moderate at best (Kopylov et al., 2015). This is certainly consistent with the high negative predictive value (NPV) of FC (Gurudu et al., 2012). Nonetheless, in individuals with higher FC levels, LS does not correlate well, and this can have impact on both patient selection for VCE as well as with final outcomes.

Flexible spectral imaging colour enhancement

FICE is a digital processing algorithm which takes WLE images and mathematically processes the image by emphasizing certain ranges of wavelengths. Three single-wavelength images can be selected and assigned to Red, Green, and Blue monitor inputs to display a composite colour-enhanced image (Table 1, Figure 6) (Manfredi et al., 2015). FICE virtual chromoendoscopy is hypothesized to thereby enhance surface patterns, improving visualization and detection of mucosal lesions (Mishkin et al., 2006). FICE has been applied to endoscopy of the upper and lower GI tract, as well as in double-balloon enteroscopy (Imagawa et al., 2011[a]; Neumann et al., 2009), with the aim of increasing detection of neoplastic lesions. However, there has been a lack of conclusive evidence for its clinical effectiveness in enhancing lesion visualization and detection in SB VCE (Koulaouzidis et al., 2013[b]).

Table 1. FICE settings 1–3 used in SB VCE: wavelengths in nm for the red, green, and blue (RGB) channels.

	Red	Green	Blue
Mode			
FICE 1	595	540	535
FICE 2	420	520	530
FICE 3	595	570	415

FICE, Flexible spectral imaging colour enhancement; SBVCE, small-bowel video capsule endoscopy; nm, nanometre.

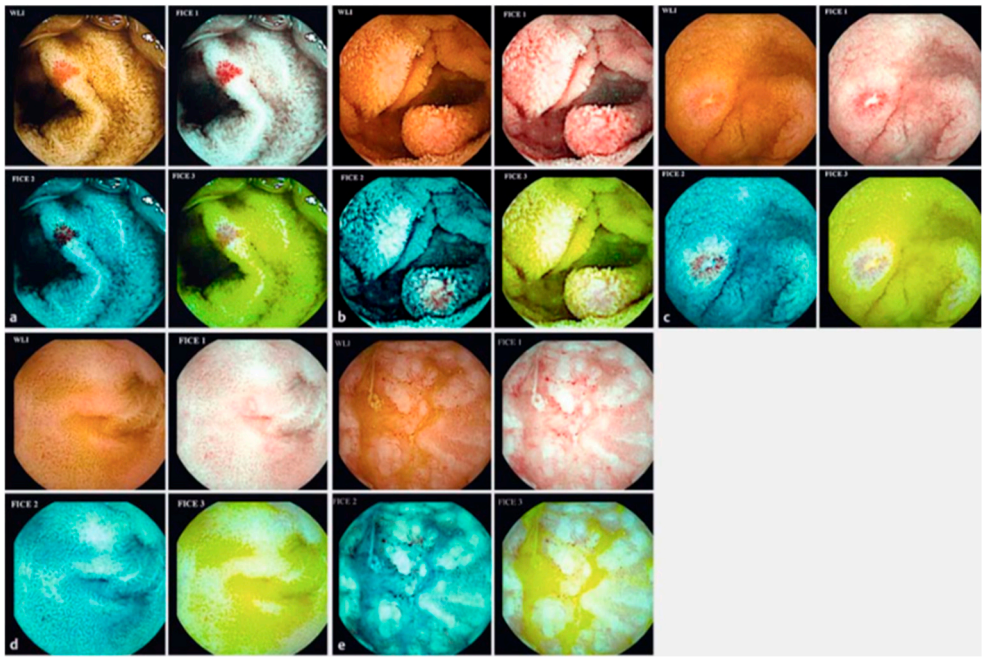

Figure 6. Pathological findings seen at small bowel video capsule endoscopy (SB VCE), as visualized with white-light imaging (WLI) and flexible spectral imaging color enhancement (FICE) settings 1, 2 and 3: a) angiectasia; b) polyp; c) ulcer; d) mucosal erosions; e) nodular lymphoid hyperplasia. (PillCam®SB2 used for part b images; PillCam®SB3 for the rest of the images in the panel).

VCE reading

Reducing reading time is beneficial, especially in high volume centres. Previous work has shown that readers' experience does not improve detection. Therefore, CAD can improve DY. Despite prolific IT research, incorporating AI systems into VCE reading remains difficult (Iakovidis et al., 2015). The backbone of AI system development is based on MLAs for automatic detection, localisation, and recognition of pathology in VCE images and videos. A large amount of data, in the form of annotations, is required to train MLAs. Semantic annotations describe the content of VCE clips and images, whereas graphic annotations are pixel-level labels indicating ROIs (Figure 2). Although there are some online databases, these usually include the necessary semantic annotations, but lack graphic annotations of ROIs. Therefore, such material cannot be directly used by IT scientists for either the training of intelligent systems or as a reference for their evaluation. A limited number of datasets composed of images with graphic annotations have become available in the context of IT studies (Iakovidis et al., 2015; Cong et al., 2015).

CE localisation

VCE continues to face several technological limitations including lack of reliable lesion localisation capability (Iakovidis et al., 2015) and the 2-dimensional (2D) nature of VCE images which hampers lesion characterisation (Grove, 2013; Van Rijn et al., 2006). Consequently, it is difficult to determine the precise location of lesions detected within the body. This information is vital to establish prognosis and for treatment planning, e.g. deciding the appropriate route for device-assisted enteroscopy. Earlier such approaches include topographic video segmentation, i.e. division of video frames into a number of consecutive segments corresponding to different parts of the GI tract (Baptista et al., 2014). Later approaches were based on motion estimation to localise the CE with respect to anatomical landmarks (Iakovidis et al., 2015). CE localisation system based on landmark or feature extraction and tracking in consecutive video frames (Spyrou et al., 2014). This system implements visual odometry to provide estimations of relative movement of the CE during its passage through the GI tract (Spyrou et al., 2015); this information can also be used to achieve 3-dimensional (3D) reconstruction of the SB lumen.

Aims

General aim

The overall aim of the dissertation was to increase the knowledge and critically evaluate the importance of existing applications and to explore and develop new applications to optimize the use and diagnostic outcomes of VCE in clinical practice.

Specific aims

- To investigate the correlation between LS and FC in a large group of patients undergoing VCE for suspected or known SB IBD.
- To develop a model for prediction of VCE results (LS) based on FC levels.
- To investigate and consolidate existing clinical data on the utility of FICE in improving delineation and detection rate for SB pathological findings in VCE compared to conventional WLE reading.
- To develop and validate a novel database, available online, aiming to provide a reference for research on the development of MDSS for VCE.
- To study the performance of human observers in comparison to others and CAD.
- To develop and evaluate an approach to CE localisation and to provide estimations of relative movement of the CE during its passage through the GI tract.

Methods and patients

Procedure and preparation

VCE was performed with PillCam®SB2/SB3 (Given®Imaging Ltd, Yokneam, Israel) and MiroCam® (IntroMedic Co, Seoul, South Korea), according to local hospital protocols. The technical characteristics of these systems can be found elsewhere in the literature (Sliker et al., 2014; Koulaouzidis et al., 2015[a]). According to the local hospital routine, CE were performed after 8hours fast and with or without bowel cleansing preparation. Cleansing preparation, where/when used, was polyethylene glycol PEG 2 or 4 lt. Prokinetics, where used, was in the form of domperidone (5-10 mg orally) and/or metoclopramide (10 mg intramuscularly) (Koulaouzidis et al., 2013[c]). All videos were reviewed by experienced VCE readers (each >500 readings).

Faecal calprotectin and C-reactive protein

FC was measured with monoclonal/polyclonal ELISA (CALPRO AS, Lysaker, Norway; reference range 0-50 mcg/g) or immunochromatographic assay (Buhlmann's Quantum Blue, Basel, Switzerland; reference range: normal <50 mcg/ g; 'grey zone' 51-99 mcg/g; and positive >100 mcg/g) (Sipponen, 2013). For the purpose of further statistical analysis, where FC<20 mcg/ g, i.e., undetectable, the value 0 was used; for the semi-quantitative assays, for values >300 mcg/g, the 300 mcg/g was used. The C-reactive protein (CRP) and monocyte count were normal across sites if levels were <5 and <0.8 ng/l, respectively.

Lewis score

LS was calculated using the integrated LS Calculator (RAPID®, Given®Imaging Ltd, Yokneam, Israel) under white light or blue mode review (Koulaouzidis et al., 2012[a]); where the calculator was not available (MiroView®, IntroMedic Co, Seoul, South Korea), the calculation was performed manually (Figure 5). LS is based on the number and distribution of intestinal segments with villous oedema, ulceration,

and stenosis. To calculate the LS, the small bowel is first divided into equal transit thirds (tertiles). The final LS represents the highest tertile or the score with stenosis, if demonstrated (Kopylov et al., 2014). Eventually, the LS allows SB inflammatory activity to be classified into three grades: (1) normal or clinically insignificant mucosal inflammatory change (LS <135); (2) mild disease (135<= LS < 790); and (3) moderate-to-severe disease (LS =>790) (Gralnek et al., 2008; Rosa et al., 2012; Cotter et al., 2015). The VCE date, FC measurement date, and time difference in days between the two was also calculated (Koulaouzidis et al., 2012[b]).

Study I

Patients and study design

This was a retrospective, multicentre study. The study cohort included all consecutive patients who underwent SB VCE in five academic referral centres (UK, Finland, Sweden, Canada, and Israel) and a large district general hospital (UK), from January 2010 to December 2013, with clinical suspicion of IBD or for IBD reassessment. Patients having normal ileocolonoscopy, without histological confirmation of CD on any biopsy material examined, were also eligible. A FC measurement within 3 months from the time of VCE was considered necessary for inclusion. The absence of a bidirectional digestive endoscopy in the preceding period (up to a year before VCE) was considered an exclusion criterion. Other causes of raised CRP or monocytes were excluded following review of patient case notes. Clinical and demographic data on age, gender, and VCE indications were extracted from the patients' files and/or electronic hospital records. A small part of the UK and Swedish data may have been used in a previous publication (Koulaouzidis et al., 2015[b]).

Study II

Patients and study design

A comprehensive literature search was conducted using the PubMed and Embase databases (January 2000 to November 2015). The search was performed on December 12, 2015. In order to capture as many full-text articles and abstracts as possible, a broad search strategy was employed, using the terms '***capsule endoscopy***', '***small bowel***', '***FICE***', and '***chromoendoscopy***' in various combinations. The initial search was performed with no limitations. Primary selection was based on titles and abstracts; further selection involved reading the full texts of any relevant publications (Figure 7).

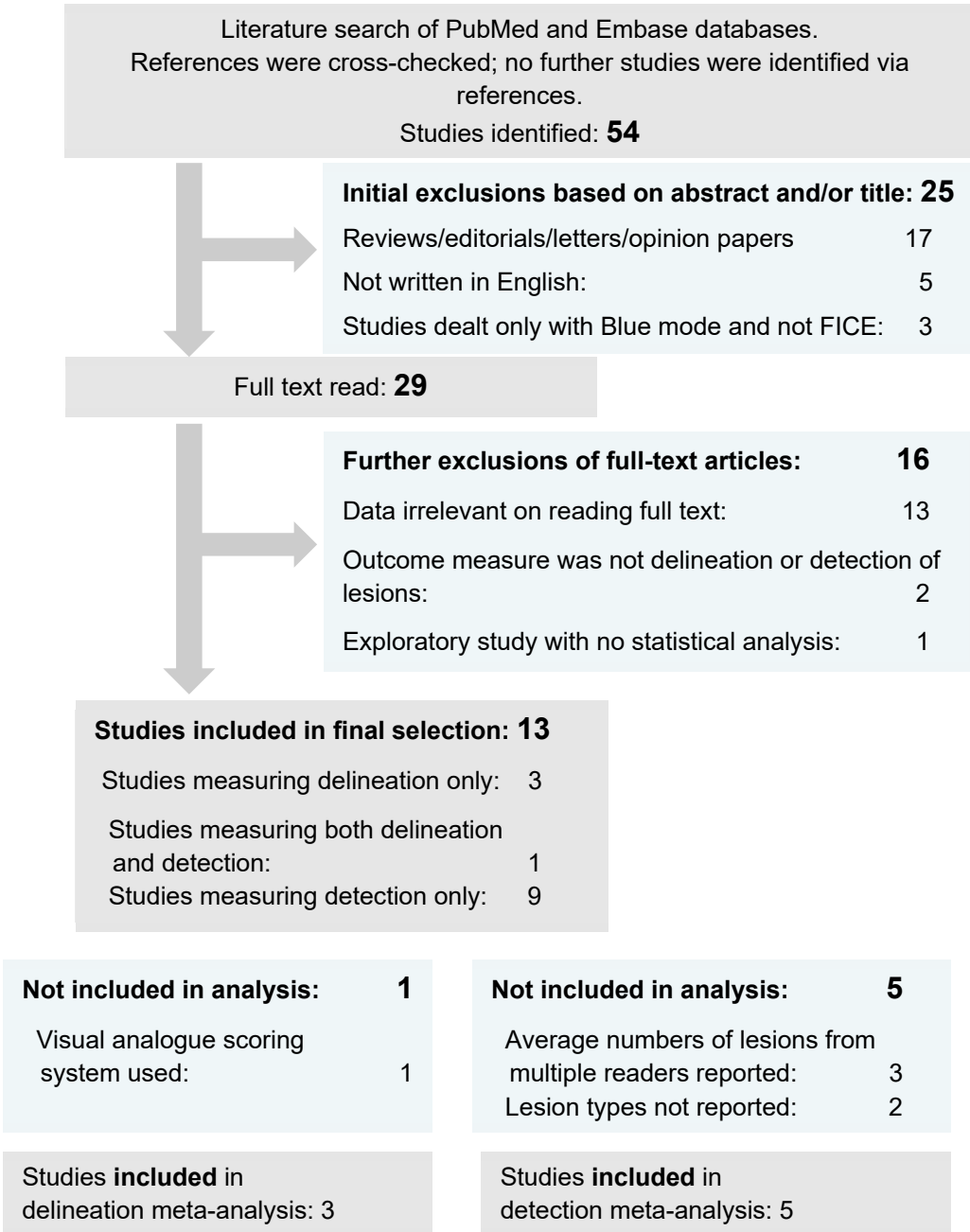

Figure 7. Selection of studies for inclusion; Flexible spectral imaging enhancement (FICE) and improvement of delineation and detection of pathological findings in small-bowel video capsule endoscopy (SB VCE).

For a study to be included in this meta-analysis, the following criteria were considered necessary: (a) complete articles published in English; (b) articles where capsule endoscopy was used to investigate SB pathology only; and (c) articles where one or more of the three FICE modes was used on VCE images and/or videos. Lastly, we included studies that investigated: (i) changes in image delineation or (ii) changes in lesion detection, using FICE.

Data extraction and quality control were performed independently by two reviewers (DY, PBC). A third reviewer (AK), expert in capsule endoscopy and the content material, was involved if there was any uncertainty about the data. When additional data were required, primary (first and/or senior) authors of the specific manuscript(s) were contacted by email with relevant questions.

Outcome measures

Lesion delineation

The outcome measure was the pooled rate of improvement in lesion visualization based on reader rating (individual or average), as measured against the original WLE image for: (a) each of the FICE settings (1-3), and (b) the two main pathological findings consistently presented across all studies: angiectasias and SB mucosal ulcers/erosions. Images where visualization was deemed ‘similar to’ or ‘worse’ than with images obtained with WLE were grouped together as “lack of improvement.”

Lesion detection

We analysed studies where each video was viewed only once by one reader. The outcome measure was whether there was any significant difference between the average number of lesions detected across the three FICE modes and the WLI, for angiectasias and mucosal ulcers/erosions.

Study III

Database creation

Open-source database (Oracle MySQL; https://www.mysql. com/) and web-gallery development software (Coppermine; http://coppermine-gallery.net/) were used. Software tools for video manipulation and image annotation were added to the KID website. To date, six centres (the KID working group) have contributed anonymized, annotated VCE images/videos from various CE models; more than 2,500 annotated VCE images and 47 videos have been uploaded. These include

images of (a) normal VCE; (b) vascular lesions including angiectasias and/or bleeding; (c) inflammatory lesions, including mucosal aphthae and ulcers, erythema, cobble stoning, and luminal stenosis; (d) lymphangiectasias; and (e) polypoid lesions (Figure 8a).

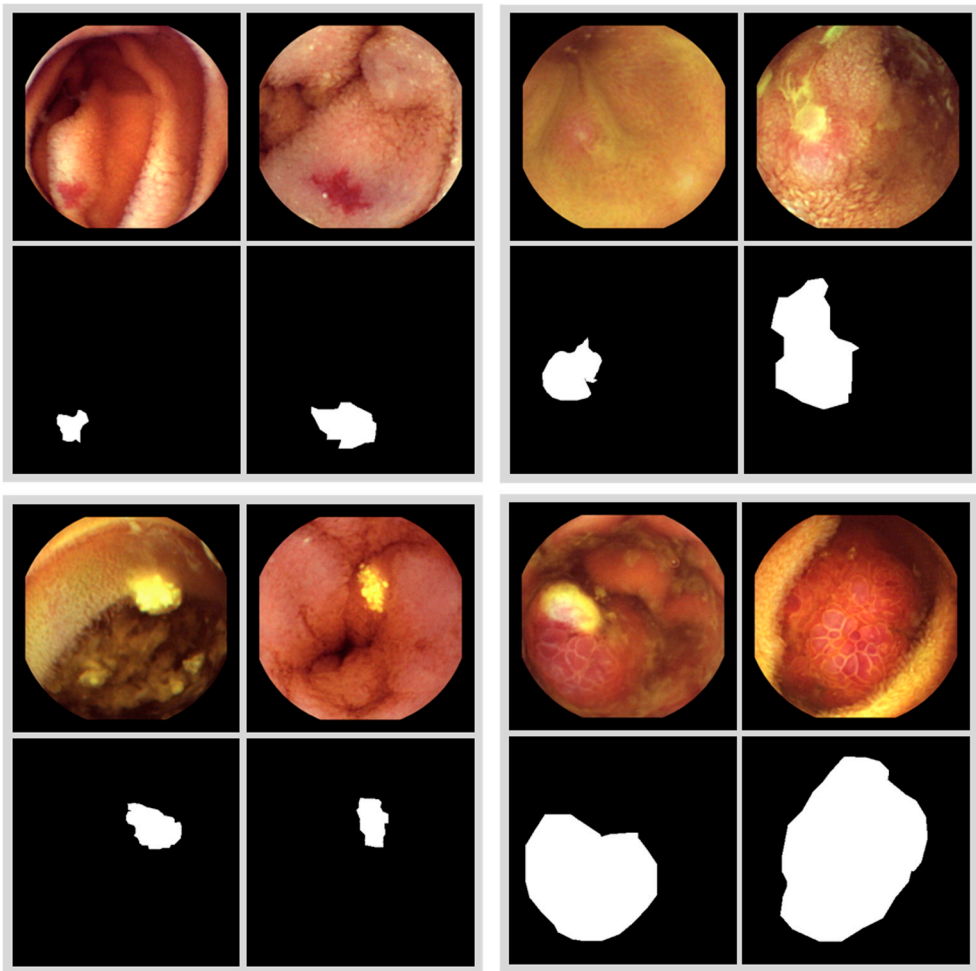

Figure 8. Annotations panel; Top row (from left to right); P1 and P2 angiectasias, aphtha and mucosal ulcers; second row: corresponding graphic annotations made using Ratsnake beneath each of the images of the top row, showing the position, size and shape of the lesions in the relevant images; third row (from left to right): 2 images of nodular lymphangiectasias and 2 images of polypoid lesions; bottom row: graphic annotations of the lesions in third row.

Image and video standards

Lesion categorization is based on the VCE Structured Terminology (CEST) (Korman et al., 2005). Contributions are of high quality (original resolution), not distorted by additional compression. For images, the recommended standard is ISO/IEC 15948 Portable Network Graphics, a popular platform-independent format

with lossless compression. Other acceptable standards include the ISO/IEC, 14496-10, MPEG-4, Advanced Video Coding and H.264. Supported formats for videos include Flash video (F4V & FLV).

Image annotation

The usefulness of KID relies on image annotations. Semantic and graphic annotations are supported by an open access, platform-independent annotation tool (Ratsnake) (Iakovidis et al., 2014[a]). The graphic annotation process is shown below, (Figure 9). Semantic annotation is done through textual labels and using standard web ontology language description logics (OWL DL) (Freitas et al., 2009). The quality of data and annotations submitted to KID are scrutinized by an international scientific committee (http://is-innovation.eu/kid/committee.php); contributions not meeting the aforementioned standards are rejected.

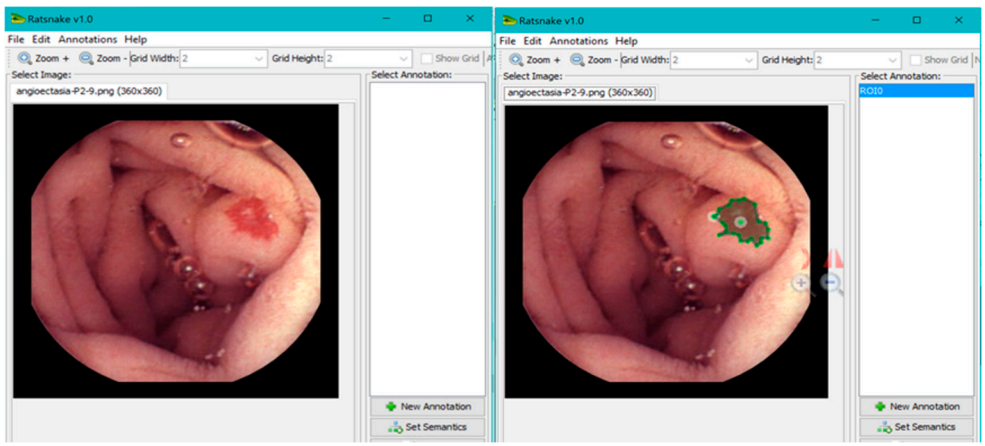

Figure 9. Use of Ratsnake annotation tool to perform graphical annotation of an angiectasia on video capsule endoscopy (VCE).

Experiment using the KID database

Computer-aided lesion size measurements based on colour image segmentation

A total of 64 images of GI lesions taken with MiroCam® (IntroMedic Co., Seoul, Korea) were used. The lesions were: angiectasias (n=27), lymphangiectasias (n=9), ulcers (n=9), chylous cysts (n=8), polypoid lesions (n=6), and SB aphthae (n=5). Graphic annotations made by expert readers (AK, ER, ET; >2000 VCE readings each) were used as lesion surface size reference standards. The images were automatically segmented into two regions: a ROI, i.e. the lesion in question, and the rest of the image.

Localized Region-based Active Contour

The Localized Region-based Active Contour (LRAC) (Lankton et al., 2008) algorithm is capable of segmenting regions characterized by heterogeneity in grayscale images for a stepwise graphic presentation (Figure 10). The reader initializes the LRAC by defining a circular contour roughly on or around the lesion, starting at a random point in the image. The lesion did not need to be fully included in the initial contour. The algorithm calculates contours based on intensity histogram information (i.e. information on image brightness and intensity) from the regions inside and outside the contour. The calculations are performed locally, around each point along the contour. The algorithm continues to run until the overall similarity of the histograms inside and outside the contour is minimized.

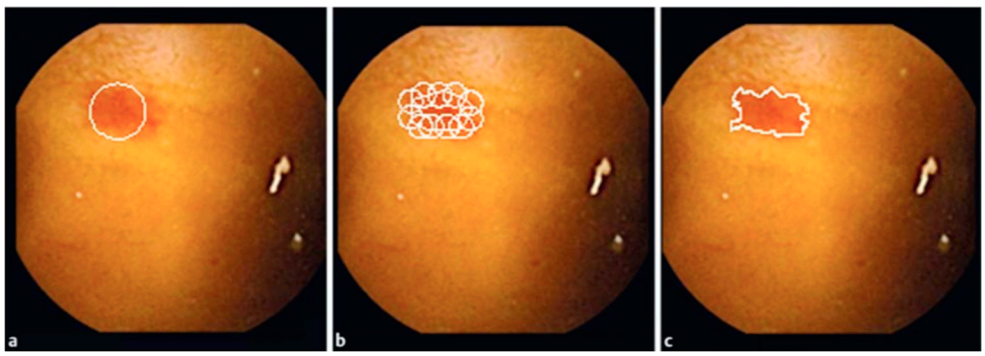

Figure 10. Segmentation of image using the Localized Region-based Active Contour (LRAC) algorithm. **a.** User defined initial contour. **b.** Contour deformation/morphing based on local histogram information on brightness and intensity in the various circular neighborhoods at each point on the contour. **c.** segmented image obtained.

International Commission of Lighting-Lab

In this experiment, we extended the algorithm to the three components of the Commission internationale de l'éclairage-Lab (CIE-Lab) colour space representation (instead of the standard RGB) (Iakovidis et al., 2014[b]). Components of this space represent lightness (L), which is ap- proximately equivalent to the respective grayscale image, quantity of red (a>0) or quantity of green (–a>0), quantity of yellow (b>0) or quantity of blue (–b>0) of a pixel (Figure 11).

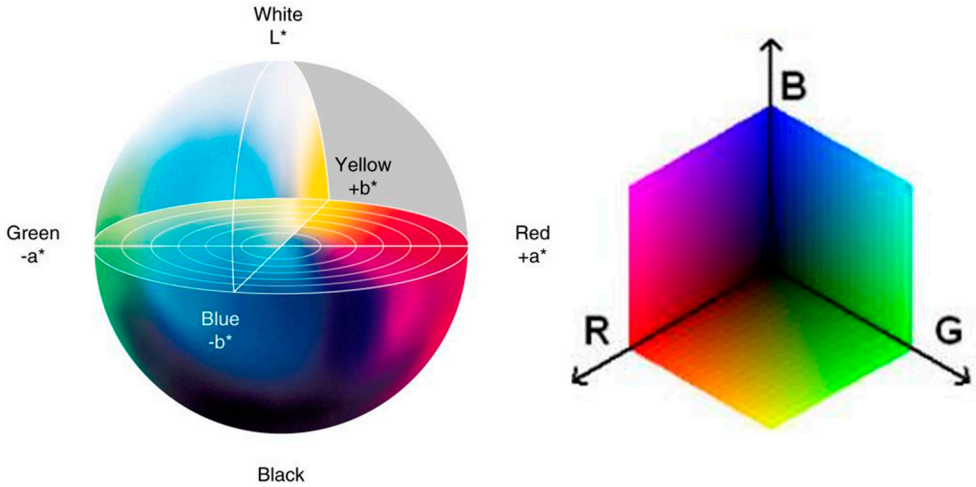

Figure 11. CIE-Lab colour wheel (left) compared to the RGB colour wheel (right).

The results of image segmentation using this algorithm applied to the 'a' component of CIE-Lab, compared to in RGB (Figure 12).

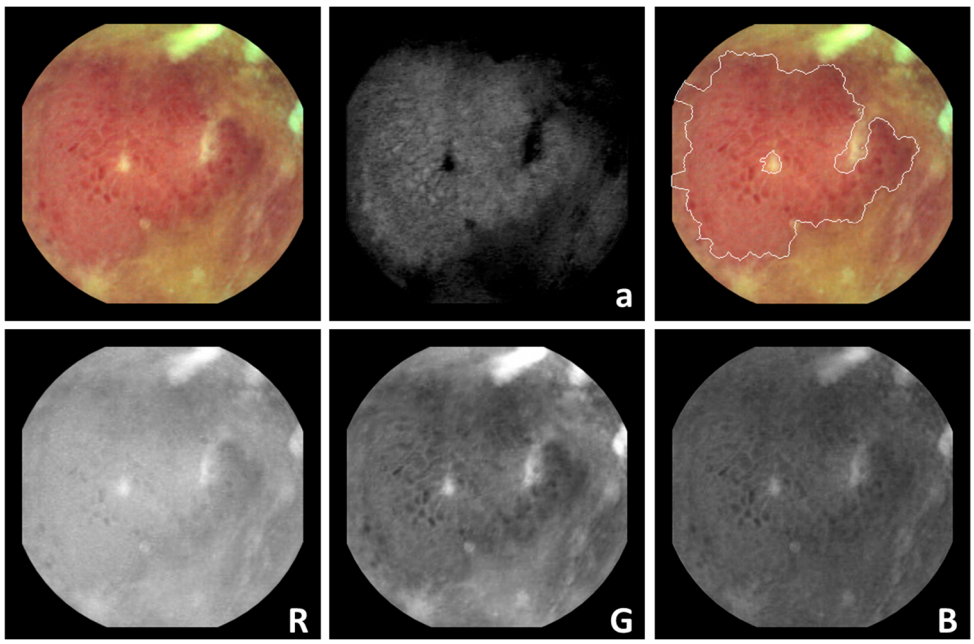

Figure 12. Image segmentation by Localised Region-based Active Contour (LRAC) algorithm. Top row, from left: original image of mucosal break with surrounding erythema; image segmentation using the a component of CIE-Lab; the final result of image segmentation where the contours have been defined and marked. Bottom row, from left: the image when broken down into red (R), green (G), and blue (B) channels under the traditional RGB system.

The Jaccard Index (JI) (Pont-Tuset et al., 2016) was used to assess the similarity of the ROI obtained with the aid of LRAC compared to the graphically annotated ROI obtained by the expert readers (gold standard) per image, i.e. the agreement between the expert human readers and the algorithm. The JI is considered to be the most suitable and popular measure for the assessment of image segmentation algorithms (Pont-Tuset et al., 2016). It quantifies the overlap between two ROIs as the ratio of their intersection to their union with respect to the human readers. Therefore, it is independent from the measurement unit, e. g. pixels^2 or mm^2, used to quantify the measured area. An illustrative example is presented herein (Figure 13).

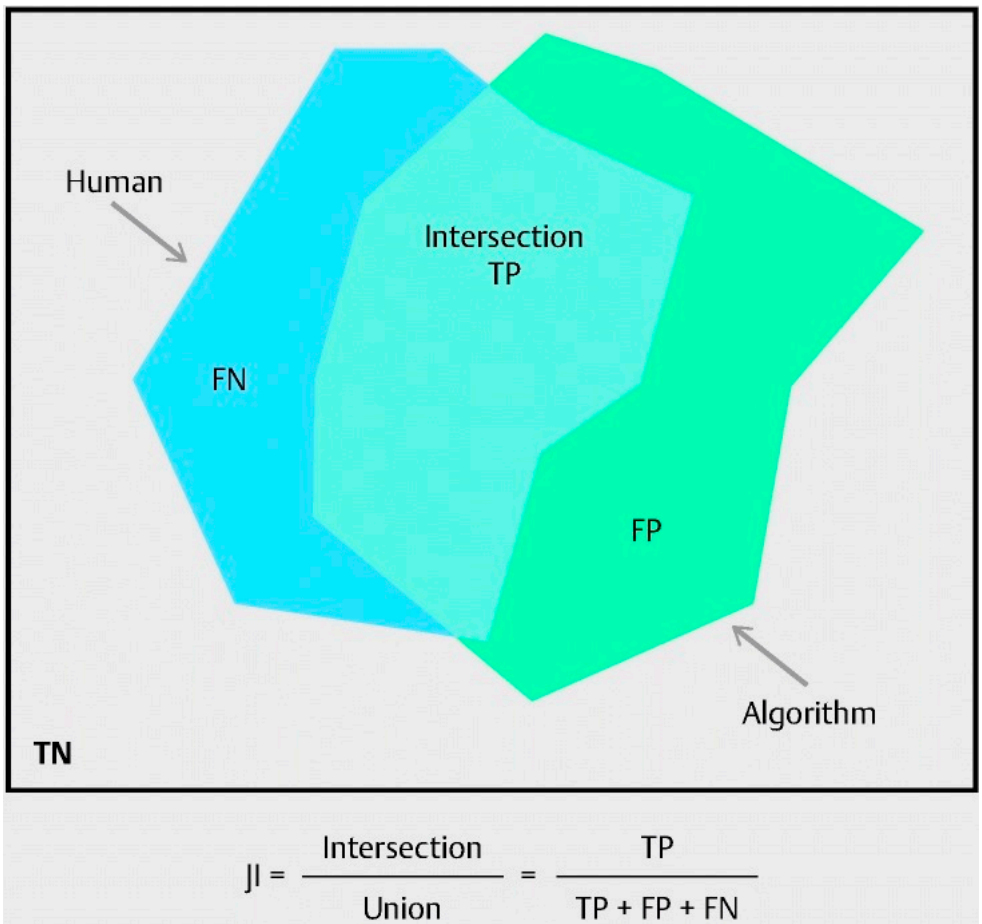

Figure 13. Agreement between a human reader and the algorithm as quantified by the Jaccard index (JI). Given a region annotated by a human expert (left) and a region annotated by the algorithm (right), the intersection of the 2 regions corresponds to the abnormality. The union of the 2 regions corresponds to the sum of the False Negative (FN), the False Positive (FP), and the true Positive (TP). Thus, if the 2 regions perfectly coincide, FN=0, FP=0 and their intersection i.e. TP becomes equal to their union, resulting in JI of 100%. If there is no match between the 2 regions, then TP=0 and JI will be 0.

Study IV

Experimental procedure

The experiment was performed in a controlled setting using a commercially available CE fixed to a robotic arm which was used to move the capsule through an in vitro bowel phantom. The setup modules are detailed below and in (Figure 14):

- High-precision robotic arm (RV-3SB robot, Mitsubishi, Tokyo, Japan): able to move the capsule forwards and back- wards through the bowel phantom at programmed velocities.
- Straight plastic rod attached to the robotic arm, with the capsule fixed to one end; the rod was longer than the total length of the model to allow the capsule to traverse the entire lumen. The capsule was aligned to the centre of the lumen.
- Pillcam®SB3 (Medtronic, Minneapolis, USA) capsule with camera resolution 320×320 pixels, variable frame rate of 2-6 fps, and 156° FOV.
- 30-cm lifelike bowel model (LifeLike BioTissue Inc, Ontario, Canada); the model was fixed and suspended in a custom-made support. The internal diameter was about 23 mm, consistent with that of adult humans.

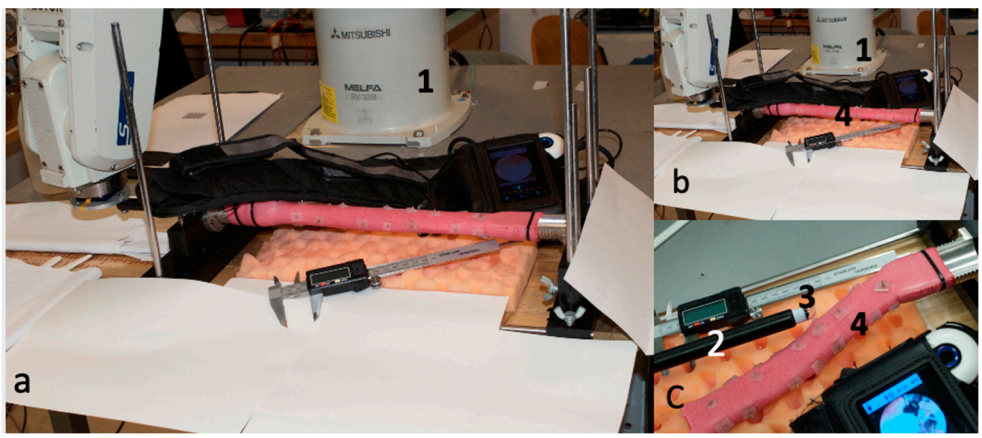

Figure 14. Experimental setup overview before opaque covering was placed over the model bowel for VCE recording (**a**) 1, robotic arm; (**b**)1, robotic arm; 4, Lifelike bowel; (**c**) 2, plastic hollow rod holding the CE; 3, CE and 4, Lifelike Bowel.

The setup was covered with an opaque plastic box to minimize external illumination, similar to in vivo conditions. The real-time viewer used to show the images captured by the Pillcam®SB3 CE. Coloured thumbtacks (diameter 0.95 mm)

were secured in four rows along the lumen and the appearance and location of each marker from the rim of the model were carefully documented. Normal gut peristalsis was not simulated at this stage to ensure accurate measurements of distances and therefore the reproducibility of results in this preliminary experiment.

Calibration and estimation of 2D trajectory

Camera calibration is a fundamental process for determining the unknown intrinsic parameters of a camera, such as its focal length. It is used by the 3D reconstruction software to produce estimates of camera position in real-world units (meters). Calibration is usually performed only once, during system development, for a given camera model. Following activation of the PillCam®SB3, calibration was performed before beginning the experiment, to correct for lens distortion and calculate the unspecified intrinsic parameters of the camera including focal length. The set-up used images of a chessboard with 3-mm squares arranged in a 10×13 configuration (Figure 15). The capsule was mounted on the plastic rod and robotically navigated into the model lumen. It was moved forwards and backwards in a straight line through the length of the model. Several passes were made at different constant velocities of 0.5-8 mm/sec.

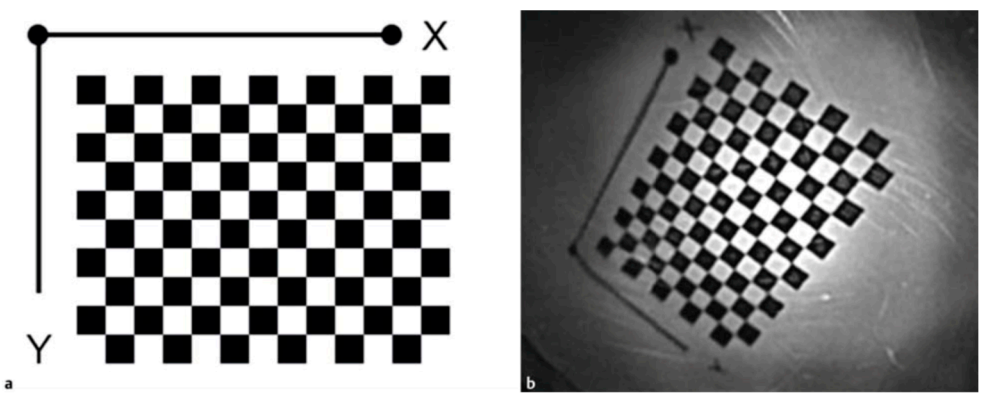

Figure 15. Checkboard pattern used for the initial CE calibration. The CE calibration pattern as printed (**a**) and the CE calibration pattern as viewed from the CE lens (**b**).

Calibration was performed using Kannala and Brandt's method, best suited for the calibration of conventional, wide-angle and fish-eye lenses (Kannala et al., 2006). The motion estimation algorithm detects corresponding points of interest (POI) in consecutive video frames; represented by the drawing pins lining the bowel wall. Relative distances between the POI and camera lens were used to estimate actual distances travelled by the capsule. The mean absolute error (MAE) of localisation

was used to quantify accuracy, calculated as the mean of the absolute difference between estimated and actual travel distances of the capsule.

3D reconstruction and shape-from-shading

The 2D images obtained from the capsule were then processed to achieve 3D reconstruction of the bowel model. A modified Shape-from-Shading (SfS) technique was used to reconstruct a 3D surface from 2D images. SfS refers to a computer vision technique that recovers 3D shape and depth information from 2D digital images by investigating the variation of illumination across the image. The major assumption that this technique is based on is that the amount of reflected light is dependent on the orientation (shape) of the scene that is imaged. The majority of SfS approaches assume a light source either coinciding with the optical centre or infinitely far away from the scene. However, these conditions are unrealistic for endoscopic recordings.

Despite the small distance between camera and light source, the observed tissue is also very close to the camera and images are therefore affected by small illumination changes. To overcome this limitation, the method used approximates the position of the light source at the tip of the endoscope and uses the position directly in the algorithm. Given the small size and the density of the circular LED array of the capsule, its overall illumination can be considered equivalent to that of such a single light source following an approximately uniform illumination aggregation model (Cool et al., 2015).

Traditional SfS can recover depth up to an unknown scale factor, using the albedo of the imaged surface (Ciuti et al., 2012). Albedo is a physical measure of reflectance or brightness of a surface. For a given surface, albedo is defined as the ratio of the reflected irradiance to the incident irradiance and it is dimensionless. Irradiance is a physical measure defined as the radiant flux (power) received by a surface per unit area. Furthermore, in our technique, because we consider the camera and light source as separate entities, we can model the SfS problem such that the unknown albedo is parameterized and calculated, thus providing a more accurate metric estimation of depth (Visentini-Scarzanella et al., 2012).

Oriented FAST and Rotated BRIEF

The ORB-SLAM (Oriented FAST and Rotated BRIEF – Simultaneous Localisation and Mapping) is used to estimate the pose (location and orientation) of a camera by finding matching points in image sequences as in videos (Mur-Artal et al., 2015). From these matching points and the known calibration parameters of the camera, an estimation of the camera's pose as well as a sparse 3D reconstruction (mapping) of the environment can be extracted. Using a sequence of images from the VCE video, the entire trajectory ('tracks') of the CE can be estimated. In ORB-SLAM the

matching points in consecutive images are extracted using a specific type of customized image features called ORB. ORB features include Features from Accelerated Segment Test (FAST), used for detection of points of interest within the image (Rosten et al., 2006) and Binary Robust Independent Elementary Features (BRIEF) (Calonder et al., 2015), used for the representation of image content at the points of interest. These features offer the advantage of fast calculation, facilitating the real-time operation of SLAM, as well as being invariant to viewpoint rotation and scale changes.

Ethics

All studies were conducted in accordance with the ethical principles of the Declaration of Helsinki, in compliance with good clinical practice and local regulations and were approved by the local Ethics Committees.

Statistics

Study I: Baseline quantitative data are presented as median and inter-quartiles range (IQR). For nominal variables, the Chi-square test or Fisher's exact test were used as appropriate. Student's t test was used for quantitative variables with normal distribution. Spearman's rank correlation coefficient (rho; r*s*) was used to assess the correlation between LS and FC. The strength of correlation was defined as follows: r*s* values <=0.1 were considered to denote no correlation; 0.1-0.3 weak to modest; 0.3-0.49 moderate; 0.5-0.79 strong; and, =>0.8 very strong correlation (http://www.statstutor.ac.uk/resources/uploaded/spearmans.pdf.). In order to detect the association between FS and LS adjusted for other factors, a multivariate linear regression analysis was used. The initial model contained age and monocyte count as adjustment factors of time lag between FC measurement and SB VCE. The model was subjected to a backwards elimination procedure using a multivariate linear regression analysis using the likelihood ratio test. A two-tailed probability (P) value <0.05 was considered to be statistically significant. In addition, a receiver operating characteristic (ROC) analysis was conducted in order to determine the optimum cut-off point of FC results using the dichotomization of LS as explained in the previous paragraph. Statistical analyses were carried out in R statistical package.

Study II: Data on the diagnostic yield of SB VCE were extracted, pooled, and analysed. Pooled results with corresponding 95% confidence interval (95%CI) were derived using the fixed-effects model (Mantel – Haenszel method) unless significant

heterogeneity was detected, in which case, a random-effects model (DerSimonian – Laird) was used. We used the Q statistic of χ^2 test and I^2 to estimate the heterogeneity of individual studies contributing to the pooled estimate. I^2 values were used to evaluate whether the differences across the studies were greater than could be expected by chance alone. A P value <0.05 suggests the presence of heterogeneity beyond what could be expected by chance alone. I^2 values of 20%-50% or of >50% suggest moderate and high heterogeneity, respectively. Forest plots were constructed for visual display of individual study and pooled results (Higgins et al., 2002). Repeated-measures analysis of variance with ANOVA was used to measure the difference in lesion detection between WLE and the three FICE modes based on the findings from the videos in WLE mode and using FICE settings 1-3.

The F statistic was used to determine significance in repeated-measures ANOVA. P<0.05 for the F-statistic was considered statistically significant (Misangyi et al., 2006). Statistical analysis was performed by using the Metan package of STATA version 12.1 (StataCorp, College Station, Texas, US).

Assessment of study bias: Methodological quality and potential bias of the included studies was evaluated by using the Quality Assessment of Diagnostic Accuracy Studies (QUADAS) 2 scale (Whiting et al., 2011). The use of FICE was the 'index test' and capsule endoscopy imaging or video review under WLE was taken to be the 'reference standard'.

Study III: The Jaccard Index (JI) (Pont-Tuset et al., 2016) was used to assess the similarity of the ROI obtained with the aid of LRAC compared to the graphically annotated ROI obtained by the expert readers (gold standard) per image, i.e. the agreement between the expert human readers and the algorithm. The JI is considered to be the most suitable and popular measure for the assessment of image segmentation algorithms (Pont-Tuset et al., 2016). It quantifies the overlap between two ROIs as the ratio of their intersection to their union with respect to the human readers. Therefore, it is independent from the measurement unit, e. g. $pixels^2$ or mm^2, used to quantify the measured area.

Study IV: The SfS (Shape-from-Shading) and ORB-SLAM (Oriented FAST and Rotated BRIEF – Simultaneous Localisation and Mapping) described above and in relevant literature (Visentini-Scarzanella et al., 2012; Mur-Artal et al., 2015).

Results

Study I

In the aforementioned period, 333 (119M/214F; median age: 41 years; IQR: 25) patients who fulfilled the study inclusion criteria were referred for VCE due to clinical suspicion of SB IBD (n=287; 98M/189F; median age: 41 years; IQR: 26) or suspicion of SB inflammation reactivation in patients with known CD (n = 46; 21M/25F; median age: 34.5 years; IQR: 24). Two different SB VCE systems were used (PillCam®SB:150/MiroCam®:183); in 3 patients the CE (2 PillCam®SB, 1 MiroCam®) was retained in the stomach for the entire period of the recording, hence no LS data were available. These cases were excluded from further analysis. Symptoms were mainly diarrhea, anaemia, weight loss, and/or abdominal pain, (Table 2).

Table 2. Cohort's indications for referral for small-bowel video capsule endoscopy (SB VCE); please note that numbers do not add up to study size of 333 as many patients had more than one indication for referral.

Indication(s)	Number of patients (% of total)
Diarrhoea	112 (33.6)
Abdominal pain(s)	104 (31.2)
Iron deficiency anaemia	62 (18.6)
Raised FC	26 (7.8)
Weight loss	23 (6.9)
OGIB	19 (5.7)
Abnormal Radiological investigation(s)	11 (3.3)
Background of coeliac, autoimmune, and/or IBD	11 (3.3)
Nutritional deficiency/malabsorption e.g., B12/folate, albumin	9 (2.7)
Family history of IBD	6 (1.8)
Perianal fistula(e)	6 (1.8)

FC, faecal calprotectin; IBD, inflammatory bowel disease; OGIB, obscure gastrointestinal bleeding.

Faecal Calprotectin - Clinically Important FC Thresholds

FC measurements were performed with a quantitative ELISA in 280 patients and with semiquantitative assays in the remainder (n=50). Overall, for the entire dataset (n=330), correlation between FC and LS was weak (r_s: 0.232, $P<0.001$). When the two clinically significant FC thresholds of 100 and 250 mcg/g were examined

(Sipponen, 2013; Koulaouzidis et al., 2011), irrespective of the FC assay used, the r*s* between FC and LS for the two threshold levels was 0.247 (weak) and 0.337 (moderate), respectively (P=0.307). The median values (with range; IQR) for FC, LS and the time interval between FC measurement and SB VCE were 90(15,255; 240) mcg/g, and 0(0,337.5; 337.5) and 0(0,62.75; 62.75) days, respectively. Furthermore, no LS/FC correlation difference was recorded between the 2 SB VCE systems, (P=0.118).

In the quantitative FC (ELISA) subgroup (n=280), the correlation between FC and LS was moderate (r*s*: 0.385, P: 0.001), as previously shown (Koulaouzidis et al., 2012[b]; Koulaouzidis et al., 2015[b]). The median values (with range; IQR) for FC, LS, and the time interval between FC measurement and SB VCE were 28(9,220; 211) mcg/g, and 0(0,339.75; 339.75) and 14.5(0,46.75; 46.75) days, respectively. In this subgroup, 150 VCEs were performed with MiroCam® and the remainder (n=130) with PillCam®SB. No statistical difference between FC levels (100.37±191.24 vs 90.71 mcg/g; P=0.649), time interval between FC/VCE (28.4±39.4 vs 20.63±29.5 days; P=0.059), prokinetic use (P=0.547), or bowel prep use (P=0.717) between the two CE model subgroups was noted, (Table 3, 4).

Table 3. Breakdown of results by comparing subgroup of FC kits used.

	Quantitative FC	**Semiquantitative FC**
Number of cases	280	50
Median FC (mcg/g) (range IQR)	28 (9-220; 211)	145 (105.75-300; 194.25)
Median LS (range IQR)	0 (0-339.75; 339.75)	135 (0-287; 287)
Median time from FC to VCE (days) (range IQR)	14.5 (0-46.75; 46.75)	25 (0-474; 474)

FC, faecal calprotectin; IQR, inter-quartile range; LS, Lewis score; SD, standard deviation; VCE video capsule endoscopy.

In the subgroup of semiquantitative FC (n=50), there was no correlation between FC and LS (r*s*: -0.130, P=0.377). In this subgroup, the median values (with range and IQR) for FC and LS were 145(105.75,300; 194.25) mcg/g and 135(0,287; 287), respectively. PillCam®SB was used in 18 patients and MiroCam® in 32 patients. Furthermore, the median interval between SB VCE and FC was 25(0-474; 474) days (i.e. not significantly different from the quantitative FC group; P=0.07).

Table 4. Comparison of MiroCam® vs. PillCam®SB2 subgroups in the quantitative FC subgroup.

	MiroCam®	PillCam®SB2	P value
Number of cases	150	130	
Median FC (mcg/g, SD)	100.37 ±191.24	90.71 ±166.1	0.547
Time from FC to VCE (days, SD)	28.4 ±39.4	20.63 ±29.5	0.059
Prokinetic use	55	42	0.547
Bowel prep used	54	42	0.717

FC, faecal calprotectin; IQR, inter-quartile range; LS, Lewis score; SD, standard deviation; VCE video capsule endoscopy.

Monocytes and C-reactive protein

The median (range; IQR) monocyte and CRP counts were 0.535(0.41, 0.72; 0.31) and 7(3,15; 12), respectively. The correlation between monocyte count and LS was weakly negative (r*s*: -0.019, P=0.732), while the relevant value for CRP was r*s*: -0.095, P=0.086. It has been reported that the CRP/monocyte ratio represents the acute phase of inflammation (Bolanis et al., 2011). There were 73 complete datasets (ratio, FC and LS) with measurements obtained ±7 days around the CE (median: 0 days, IQR: 0 days). The median value of the ratio was 12(5.21, 24.47; 24.25), and the correlation of the ratio with FC and LS was r*s*: 0.14(P=0.235) and r*s*: 0.02(P=0.865), respectively.

Model Creation

In order to investigate the potential association between LS and FC, both variables were log-transformed. The final model for the association of LS and FC was found to be:

$$\text{Log}(LS + 1) = -1.05 - 0.0087 \times \text{time lag simplistic} + 1.0471 \times \log(FC + 1)$$

Other predictors such as age (P=0.902) and monocyte count (P=0.805) were eliminated from the initial model during the backwards elimination procedure. The results of the final model (Table 5), where the intercept (P=0.269) was kept as it was found that the normality of the residuals was violated when this was removed. Furthermore, the model is interpreted as an increase of 1 point in FC gives an increase of 1.0471 in log(LS + 1) (95%CI: 0.679; 1.415). The latter translates to 0.389 points increase in LS (95%CI: 0.159; 0.832) for a constant FC/CE time lag simplicity of zero. Also an increase of 1 point in FC/CE time lag gives a decrease of -0.0087 (95%CI: -0.016; -0.001) in log(LS + 1).

Table 5. Model for the association of FC and LS.

Model	Coefficients	SE	t value	Pr(> |t|)	95% CI
Intercept	-1.0513	0.9466	-1.11	0.269	-2.907; 0.804
Time lag FC/VCE	-0.0087	0.0039	-2.24	0.027	-0.016; -0.001
Log (FC + 1)	1.0471	0.1876	5.58	<0.001	0.679; 1.415

FC,faecal calprotectin; VCE,video capsule endoscopy; SE,Standard error; Pr,probability; CI,confidence interval.

Optimum Cut-off Point of FC

The analysis using ROC curves gave that the dichotomization of LS at 135 for clinically significant (LS <135) or negative (LS =>135) for SB inflammation gave an optimum cut-off point of FC 76 at mcg/g with sensitivity 0.59 and specificity 0.41 (Figure 16).

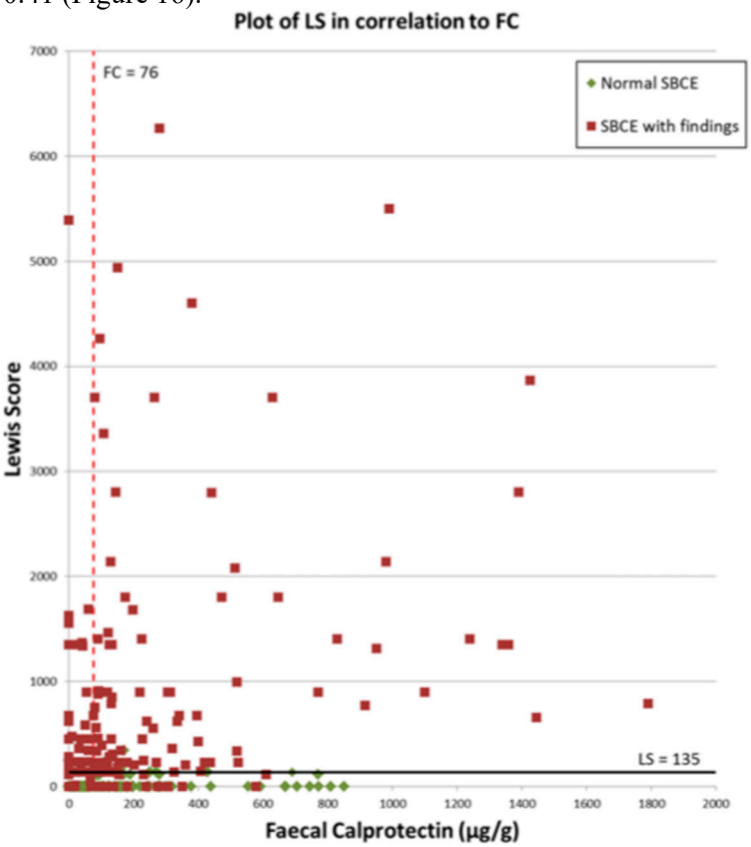

Figure 16. Plot of Lewis score in correlation to Faecal calprotectin.

Study II

The initial search yielded 54 publications of which; 39 were excluded for the following reasons: articles were reviews/ editorials/letters/opinion papers (n=17); data found to be irrelevant on reading of full text (n=13); not in English language (n=5); studies dealt exclusively with other chromoendoscopy techniques (e. g. Blue mode) and not FICE (n=3); outcome measure not delineation or detection of lesions (n=2) (Rimbaş et al., 2015; Maeda et al, 2014); study was exploratory with no statistical analysis (n=1) (Pohl et al., 2010).

Eventually, 13 studies were included in the final review, with 8 then included in meta-analyses (Table 6, Table 7) (Imagawa et al., 2011[a]; Krystallis et al., 2011; Sato et al., 2014; Imagawa et al., 2011[b]; Duque at al., 2012; Kobayashi et al., 2012; Matsumura et al., 2012; Sakai et al., 2012; Konishi et al., 2014; Boal Carvalho et al., 2016; Gupta et al., 2011; Dias de Castro et al., 2015; Cotter, 2014). The countries of origin for the studies were: Japan (n=7) (Imagawa et al., 2011[a];Sato et al., 2014; Imagawa et al., 2011[b]; Kobayashi et al., 2012; Matsumura et al., 2012; Sakai et al., 2012; Konishi et al, 2014), Portugal (n=4) (Cotter, 2014; Duque et al., 2012; Boal Carvalho et al., 2016; Dias de Castro et al., 2015), Belgium (n=1) (Gupta et al., 2011), and the UK (n=1) (Krystallis et al., 2011). All studies were conducted using PillCam®SB1/2 (Medtronic, Minnesota, USA) and most used experienced VCE readers, usually defined as having read >100 VCEs.

Two sets of studies were identified as coming from the same hospitals. Two studies from the Imagawa et al. group were used for two separate analyses, one for delineation (Imagawa et al., 2011[a]) and one for detection (Imagawa et al., 2011[b]). Therefore, there was no overlap in the data used in these two studies. Another three studies (Cotter, 2014; Boal Carvalho et al., 2016; Dias de Castro et al., 2015) were carried out by the same group of researchers at the same centre; these have been confirmed –by one the authors– to have used completely separate patient groups with no overlap.

Table 6. Lesion delineation with 3 FICE settings used in small-bowel VCE: summary of studies included in this meta-analysis.

First author Year [ref.]	Readers, n	Images, n	Outcomes for FICE settings (modes) 1–3								
			FICE 1			**FICE 2**			**FICE 3**		
			Improved	Similar	Worse	Improved	Similar	Worse	Improved	Similar	Worse
Angioectasias											
Krystallis 2011 [21]	2	18	14	2	2	5	3	9	1	7	10
Imagawa 2011 [13]	5	23	20	3	0	20	2	1	1	22	0
Sato 2014 [22]	5	152	VAS average (SD): 72.7 (5.2) *			VAS average (SD): 74.0 (14.9) *			VAS average (SD): 58.7 (14.9) *		
Cotter 2014 [23]	2	39	38	1	0	38	1	0	18	18	3
Ulcers/erosions											
Krystallis 2011 [21]	2	60	22	6	32	2	8	50	2	4	54
Imagawa 2011 [13]	5	47	26	19	2	12	32	3	0	34	13
Sato 2014 [22]	5	88	VAS average (SD): 72.9 (5.4) *			VAS average (SD): 67.9 (5.7) *			VAS average (SD): 53.5 (6.5) *		
Cotter 2014 [23]	2	49	31	12	6	28	10	11	12	18	19

* Outcome measure: average VAS from readers, with positive scoring for “improved” and negative scoring for “worse”; breakdown not specified.

Table 7. Lesion detection with flexible spectral imaging colour enhancement (FICE) used in small-bowel capsule endoscopy: summary of studies.

First author Year [ref.]	Readers, n	Videos, n	Study design	Lesions detected by different modes, n				
				Reference	WLE	FICE 1	FICE 2	FICE 3
Angioectasia								
Imagawa 2011 [24]	2	50	1 reader for WLE 1 for FICE	Not available	17	48	45	24
Duque 2012 [25]	4	20	1 reader for WLE 1 for FICE	Not available	32	Not available	35	Not available
Kobayashi 2012 [26]	3	24	All videos seen by all readers	Not available	Average (SD) lesions per video: 21 (2.6)	25.7 (SD 3.2)	22.0 (SD 3.0)	22.7 (SD 2.1)
Matsumura 2012 [27]	2	81	All videos and modes seen by all readers	14	Average (SD) lesions per video: 2 9 (1.5)	2 (SD 1.4)	1.3 (SD 0.5)	4 (SD 1.2)
Sakai 2012 [28]	4	12	Crossover	60	26	40	38	31
Konishi 2014 [29]	5	10	All videos seen by all readers	Not available	Average (SD) lesions per video: 0.58 (0.15)	0.92 (SD 0.2)	0.72 (SD 0.18)	0.74 (SD 0.2)
Sato 2014 [22]	3	50	Crossover	Not available	17	24	33	18
Boal Carvalho 2016 [30]	4	60	Crossover	54	26	54	Not available	Not available
Ulcers/erosions								
Imagawa 2011 [24]	2	50	1 reader for WLE 1 for FICE	Not available	32	40	54	51
Duque 2012 [25]	4	20	1 reader for WLE 1 for FICE	Not available	24	Not available	41	Not available
Kobayashi 2012 [26]	3	24	All videos seen by all readers	Not available	Average (SD) lesions per video: 14 (0.0)	19.3 (2.3)	15.3 (1.2)	11.3 (4)
Matsumura 2012 [27]	2	81	All videos seen by all readers	24	Average (SD) lesions per video: 1.9±1.9	3.3 (2.3)	3.6 (3.4)	1.9 (1.2)

Sakai, 2012 [28]	4	12	Crossover	82	38	62	60	20
Konishi 2014 [29]	5	10	All videos seen by all readers	Not available	Average (SD) lesions per video: Erosions 3.3 (4.29) Ulcers 1.66 (4.00)	Erosions 8.65 (8.55) Ulcers 4.86 (12.9)	Erosions 11.94 (15.12) Ulcers 5.6 (14.51)	Erosions 3.54 (4.03) Ulcers 2.9 (8.50)
Sato 2014 [22	3	50	Crossover	Not available	28	22	41	24
Boal Carvalho 2016 [30]	4	60	Crossover	17	15	17	Not available	Not available
Studies where Saurin score used (lesion types not specified)								
Gupta 2011 [31]	2	60	Crossover	131 P0: 15 P1: 41 P2: 75	Not available	All 3 FICE modes used together P0: 20 (reader 1), 27 (reader 2) P1: 37 (reader 1), 55 (reader 2) P2: 60 (reader 1), 72 (reader 2)		
Dias de Castro 2015 [32]	1	42	1 reader for all videos	All videos initially "negative" for cause of GI bleeding	Not available	14 remained negative: 19 P1 lesions 2 P2 lesions 7 both P1 & P2	Not available	Not available

WLE white light endoscopy; VCE, video capsule endoscopy; CE, capsule endoscope; SD, standard deviation; GI, gastrointestinal; P0, 0 probability of bleeding; P1, intermediate; P2, strong probability of bleeding, N/s: Not specified; n/a: not applicable.

Table 8. FICE settings used in SB VCE: pooled proportion of images with "improved" visualization of findings.

	FICE mode, proportion (95%CI)		
	FICE 1	**FICE 2**	**FICE 3**
Angiectasias (n=80)	0.89 (0.69-1.08)	0.43 (0.32-0.54) *	0.05 (0.04-0.07) *
Ulcers/erosions (n=156)	0.45 (0.38-0.52) *	0.04 (0.03-0.05) *	0.04 (0.03-0.04) *

FICE, flexible spectral imaging colour enhancement; SB VCE, small-bowel video capsule endoscopy; CI, confidence interval. *Denotes statistical significance.

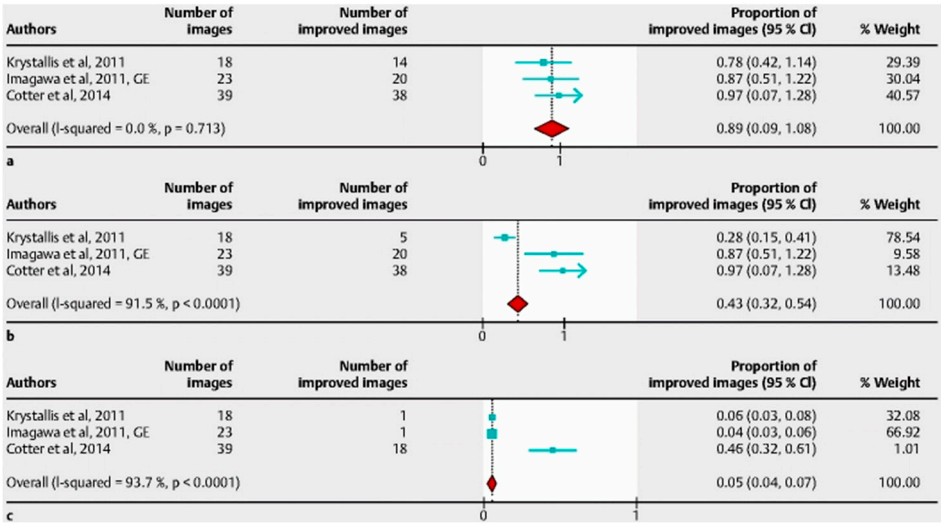

Figure 17. Pooled proportions of images of angiectasias considered to show 'improved' visualization under flexible spectral imaging colour enhancement (FICE): a FICE 1; b FICE 2; c FICE 3.

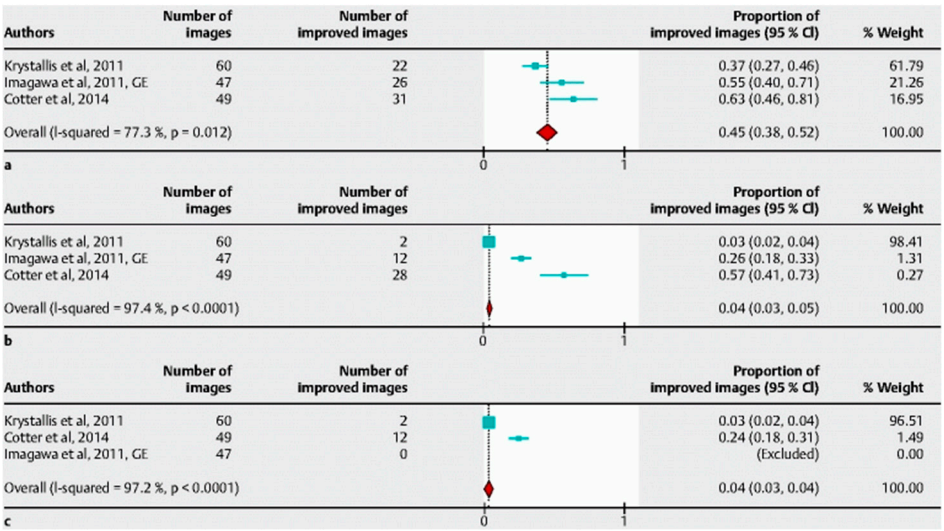

Figure 18. Pooled proportions of images of ulcers/erosions considered to show 'improved' visualization under flexible spectral imaging colour enhancement (FICE): a FICE 1; b FICE 2; c FICE 3.

Lesion delineation

Improvement in delineation of capsule endoscopy images of lesions was investigated in 4 studies (Imagawa et al, 2011[a]; Krystallis et al., 2011; Sato et al., 2014; Cotter, 2014). Of these, 1 study (Sato et al., 2014) was excluded from further analysis: the use of a visual analogue scoring system meant that the results could not be entered into the meta-analysis.

Only the use of FICE setting 1 on images of angiectasias appeared to produce a higher rate of improved delineation, with 89% of images considered improved, whereas 45% of images of ulcers/erosions were considered improved using FICE 1. FICE 2 improved delineation in 43% of images of angiectasias. For images of angiectasias in FICE 3 and images of ulcers/erosions in FICE 2 and 3, negligible proportions of images were considered to show improved delineation (Table 8, Figure 17, Figure 18). Heterogeneity of studies was high with I^2 >90 % in 4/6 analyses carried out.

Lesion detection

A total of 10 studies (Sato et al., 2014; Imagawa et al., 2011[b]; Duque et al., 2012; Kobayashi et al., 2012; Matsumura et al., 2012; Sakai et al., 2012; Konishi et al., 2014; Boal Carvalho et al., 2016; Gupta et al., 2011; Dias de Castro et al., 2015) measured improvement in detection of lesions. Of these, 3 studies (Kobayashi et al., 2012; Matsumura et al., 2012; Konishi et al., 2014) reported results as average numbers of lesions identified by multiple readers; the present study did not allow those studies to be included in analysis. Another 2 studies (Gupta et al., 2011; Dias de Castro et al., 2015) did not give results by types of lesions, instead using the Saurin score (Saurin et al., 2003); these were not analysed as the numbers of angiectasias and ulcers/ erosions remained unknown.

The remaining 5 studies were designed such that each video in each mode was viewed only once by one reader over the course of the study (Sato et al., 2014; Imagawa et al., 2011[b]; Duque et al., 2012; Sakai et al., 2012; Boal Carvalho et al., 2016). Therefore, these were entered into the analysis, and ANOVA was carried out using the average number of lesions detected per video (Table 9). The F statistic for the difference in detection of angiectasias and ulcers/erosions in the three FICE modes compared to WLE had a P value >0.05 for both types of lesions, showing that the detection of these lesions did not differ significantly between any of the FICE modes and WLE.

	Sum of squares	Degrees of freedom	Sum of squares (mean)	*F* statistic & result
Angiectasias				
Between	1.02	3	0.34	1.146
Within	20.179	16	1.261	
Error	3.559	12	0.297	
Subjects	16.62	4	4.155	
Total	21.199	19		
				Critical value: 3.4903 Result: **Do not** reject the null hypothesis. **Conclusion**: compared groups **do not** differ significantly: *F* (3,12) = 1.146, *P*>0.05.
Ulcers/erosions				
Between	3.467	3	1.156	1.723
Within	41.093	16	2.568	
Error	8.052	12	0.671	
Subjects	33.041	4	8.26	
Total	44.56	19		

Table 9. Difference in lesion detection between WLE and the 3 FICE settings: repeated-measures analysis of variance (ANOVA), for angiectasias and ulcers/erosions.
WLE, white-light endoscopy; FICE, flexible spectral imaging colour enhancement.

Quality analysis

The majority of the included studies were of high quality (Table 10). The main risk of bias identified was recall bias in studies where videos were viewed in more than one mode by the same reviewer.

Table10. FICE settings used in SB VCE. Quality of studies and risk of bias as determined by QUADAS 2 scale. + denotes low risk of bias, ? denotes unclear risk of bias.

	Item 1	**Item 2**	**Item 3**	**Item 4**	**Item 5**	**Item 6**	**Item 7**
	Risk of bias in patient selection	Representative patient spectrum	Risk of bias in conduct and/or interpretation of Index test (FICE)	Applicability of Index test to review question	Risk of bias from conduct or interpretation of RS (WLE and/or expert review)	Use of appropriate RS	Risk of bias from study flow/timing
Gupta, 2011	+	+	+	?	+	+	+
Imagawa, 2011[a]	?	+	+	+	+	+	+
Imagawa, 2011[b]	?	+	?	+	+	+	?
Krystallis, 2011	+	+	?	+	+	+	+
Duque, 2012	+	+	+	?	+	+	+
Kobayashi, 2012	?	+	?	+	+	+	+
Matsumura, 2012	?	+	?	+	+	+	+
Sakai, 2012	?	+	+	?	+	+	+
Cotter, 2014	+	+	?	+	+	+	?
Konishi, 2014	+	+	+	+	+	+	+
Sato, 2014	?	+	+	+	+	+	+
Boal Carvalho, 2015	+	+	+	+	?	+	+
Dias de Castro, 2015	?	+	+	?	+	+	+

FICE, flexible spectral imaging colour enhancement; SB VCE, small-bowel video capsule endoscopy; RS, reference standard; WLE, white light endoscopy

.

Study III

The algorithm was evaluated for the measurement of six different types of SB lesions, for each channel of CIE-Lab colour space. The lesion areas were measured in pixel units, which, in the context of VCE, is a more feasible and accurate approach. The average surface measurements closest to those performed by expert human readers were obtained by application of LRAC on the red-green scale of the CIE-Lab colour space, with a JI of 67±13%. This result complements the findings in our previous study, indicating component a as an informative source of saliency for automated lesion detection (Iakovidis et al., 2014[b]). The agreement between human readers and the algorithm per lesion type is summarized (Table 11). The most accurate measurements were obtained for lymphangiectasias, whereas this algorithm is less suitable for the measurement of ulcers.

Table 11. Agreement between reviewers and software in measuring lesion size for various types of lesions seen in CE.

Lesion type	JI, mean ±SD, %
Angiectasias	64 ±11
Aphthae	64 ±8
Chylous Cysts	70 ±14
Lymphangiectasias	81 ±6
Polypoid lesions	75 ±21
Ulcers	56 ±9

Abbreviations: CE, capsule endoscopy; JI, Jaccard Index; SD, standard deviation.

Study IV

Seventeen video frames of the checkerboard (Figure 15) were used for calibration. As the capsule was navigated through the model bowel, the number of video frames per movement ranged from 42 to 66, due to the variable frame rate of the capsule. Overall, the MAE in the estimated distance travelled by the capsule was 4.1±3.9 cm, for a camera focal length of 1.16 mm. Minimum error achieved was 1.4±0.8 cm, and the respective results per row of thumbtacks are illustrated in Table 12 and Figure 19. The 2D reconstruction of the capsule's trajectory through the model bowel is shown in Figure 20. The solid red line represents the estimated capsule movement, in comparison to the actual path shown by the straight broken line.

Table 12. Best results for travel distance estimation obtained applying the Kannala & Brandt's method.

Row of pins	Travelled distance (in cm)		
	Actual	**Estimated**	**Absolute error**
1	19.8	20.7	0.9
2	17.4	14.8	2.6
3	19.9	20.7	0.8
4	19.6	20.9	1.3

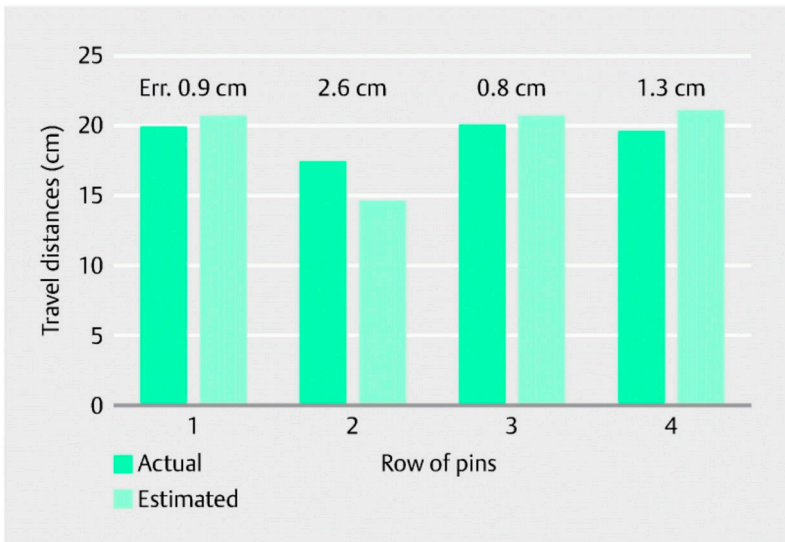

Figure 19. Best results in travel distance estimation after calibration per row of thumbtacks. The error between the actual and the estimated travel distance is presented on top of the respective bars.

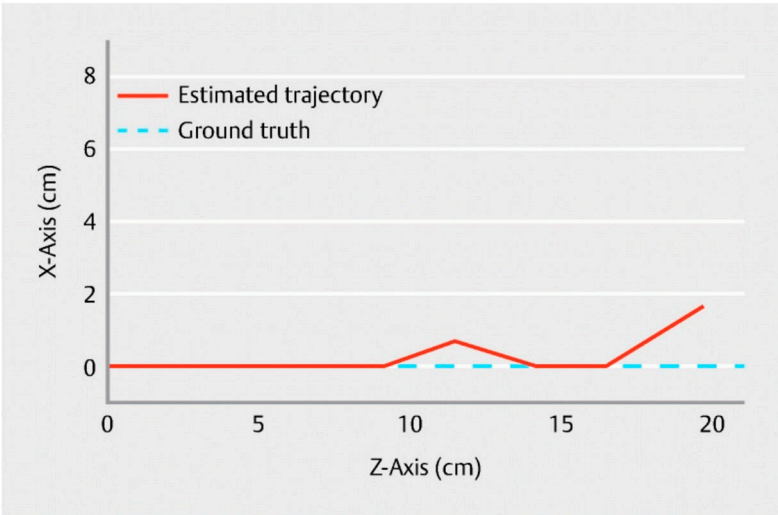

Figure 20. Graph showing the estimated *vs* the actual capsule endoscope (CE) trajectory.

3D reconstruction

Both 3D reconstruction methods detailed above were able to achieve a good, but not optimal, reconstruction of the bowel model using information from the VCE video alone. Using the modified SfS technique, the cylindrical shape of the model bowel, with details of the tissue and attached thumbtacks, was successfully reconstructed. Examples of reconstructed bowel lumen, with corresponding original images (Figure 21).

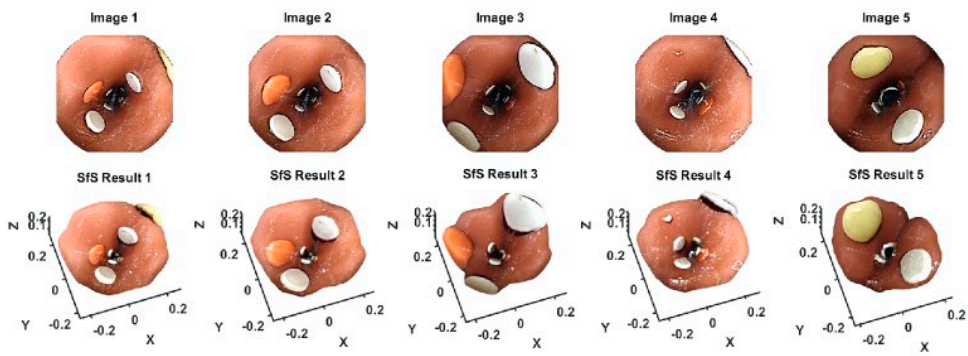

Figure 21. Reconstruction results using the modified Shape-from-shadow (SfS) technique. Selected frames from the video capsule endoscopy (VCE) clip are shown above, with the corresponding reconstructions below.

The ORB-SLAM method of 3D reconstruction produced good localisation of the capsule within the reconstructed model. Results using this method are presented in (Figure 22). The blue triangles, corresponding to the outline of the reconstructed bowel wall from each frame of the video, are positioned in a straight line, with the overall 'track' denoted by the green line passing through the triangles. This corresponds with the linear forwards-backwards movement of the capsule in the straight bowel model used.

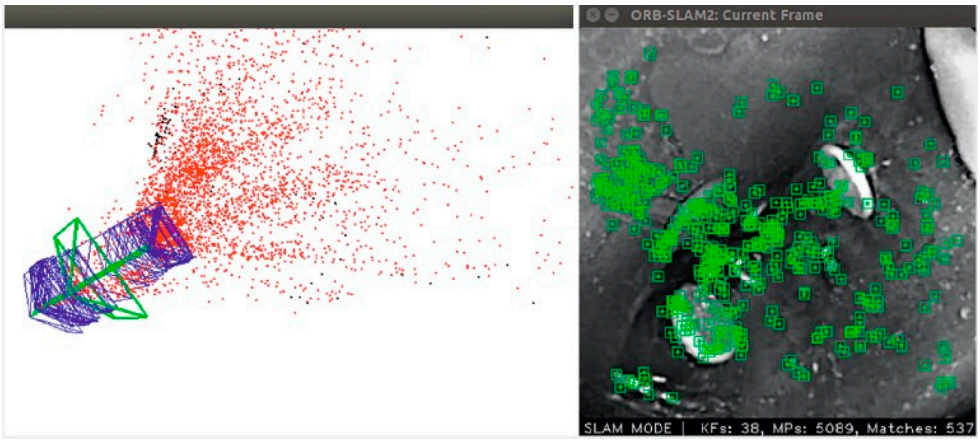

Figure 22. Results obtained using the ORB-SLAM algorithm. The location and post of the VCE camera is estimated foreach frame (current track in green rectangle; previous tracks in blue rectangles). The green line denotes the overall CE trajectory. The sparse 3D reconstruction is illustrated as a point cloud.

Discussion

VCE has been well-established as the prime investigation modality for a whole host of SB conditions such as bleeding, CD and polyps/tumours. Achieving this was not easy but –essentially– existing competitors were not offering as much as VCE has to provide. However, the manual reading process of VCE sequences is prone to diagnostic errors as a result of the natural limitation of human capabilities in concentration and findings' interpretation (Iakovidis et al., 2015). Computational methods, which are integral to the reviewing software of all VCE platforms, could contribute to the reduction of both VCE reading times and errors in human interpretation of VCE sequences. Essential progress can be achieved by knowledge and data sharing. This can only be achieved when collaboration hubs between clinicians and IT scientists are formed aiming to engagement in common scientific efforts and publications that address important clinical problems in VCE through IT backing and feedback loops.

The intention with this thesis was to increase the knowledge and critically evaluate the use of calprotectin, and FICE as adjunct(s) in clinical VCE. Moreover, I have intended to explore the use of novel experimental and software methods for image reconstruction and localisation in VCE together with the development of an internet-based digital video database of VCE for research purposes.

Capsule findings and inflammatory biomarkers

FC levels in the stool are directly proportional to neutrophils in the intestinal wall (Logan, 2010); therefore, its use as biomarker of enteric inflammation and neoplastic lesions has been proposed. One of the main indications for VCE is the direct visualization of the extent, location, and severity of SB inflammation (Kopylov et al., 2014). Others suggest that FC could discriminate between organic and functional intestinal pathology and allow selection of patients who are more likely to benefit from a colonoscopy (van Rheenen et al., 2010). Recently, we hypothesized that FC can be used as selection tool for performing VCE in patients with continuing clinical suspicion for SB IBD, despite preliminary negative diagnostic workup (Koulaouzidis et al., 2011). Currently, healthcare systems worldwide are under significant economic strain to provide high-quality care with shrivelling budgets (Bolanis et al., 2011; Sandler et al., 2002). Therefore, increasing

the DY of patient workup with inexpensive, accurate, non-invasive investigations, has multiple benefits (Logan, 2010; Dhaliwal et al., 2015).

In the present study, retrospective data on FC, monocyte count, and CRP paired with VCE findings (LS was used to quantify SB inflammation in an objective way) (Gralnek et al., 2008; Koulaouzidis et al., 2012[b]) were collected from patients with clinical suspicion of SB IBD (n=287), out of which 3% had ileitis on colonoscopy but inconclusive histology, from high-volume VCE centres (UK×2, Finland, Sweden, Canada, Israel). The remainder (n=43) had a history of known CD and were referred for SB assessment with VCE. Experienced VCE reviewers reported the VCE results at each site for the purpose of clinical care/need using WLI and/or blue mode (depending on preference per reviewer) (Cotter et al., 2015; Koulaouzidis et al., 2012[a]). In 84.8 % of cases, FC was measured using a commercially available ELISA (range 0-50 mcg/g). In these patients, CE was performed using the PillCam®SB in 46.4 % of cases; the remainder was performed with MiroCam®. Based on the CE system used, the two patient subgroups were equivalent in terms of FC levels, time interval between FC measurement and performance of CE, and procedural factors for SB VCE such as the use of a prokinetic and/or a bowel purge (or not). Therefore, we are able to confirm that the lack of an integrated calculator in the MiroCam® proprietary software (MiroView®) notwithstanding the calculated LS had the same correlation with FC levels.

Another finding of this study is low correlation of FC with monocyte count, CRP, CRP/monocyte, and LS (Table 2). The former has been previously shown in studies from our group (Sipponen et al. 2012; Koulaouzidis et al., 2015[b]). Furthermore, elevated CRP, FC, or the combination of both was poorly correlated with detectable SB inflammation (Kopylov et al., 2015[a]; Kopylov et al, 2015[b]). Nevertheless, it is worth noting that when the threshold level of significant SB inflammation, as denoted by LS was shifted from 135 to 350, the correlation of FC and LS was similar at r*s*: 0.07 (P=0.637) and 0.09 (P=0.696) for the suspected and known CD group, respectively.

Others have recently confirmed strong inter-observer agreement in determining LS in VCE (Cotter et al., 2015). In a cohort of 30 patients (Höög et al., 2014), showed that there was a significant persistent correlation between endoscopic inflammation and FC (at study inclusion and at a year's follow-up). Another group showed that the proportion of patients with findings on SB VCE increased with increasing FC (Olsen et al., 2015). Nevertheless, in their cohort, a positive FC (=>50 mg/kg) had a sensitivity, specificity, positive predictive value (PPV), and NPV of 54.2, 69.9, 43.3, and 78.2%, respectively. The correlation of FC values with presence of active SB inflammation as detected by magnetic resonance enterography (MRE) was similar to that of VCE (Kopylov et al., 2015[b]).

Limitations of this study include the lack of formal assessment of the extent of mucosal visualization. As not all patients underwent bowel preparation prior to

VCE, it is possible that LS could in part be altered by the degree of SB visualization. However, there is a lack of data on LS correlation with the quality of SB visualization. The fact that the VCEs in this study were each reviewed by a single reviewer only, despite substantial cumulative experience in VCE, could be a further limitation leading to lower DY.

This study did not establish a correlation between endoscopic severity, as measured by the LS, and FC or other biomarkers of inflammation. This is likely to reflect deficiencies of the scoring system (Koulaouzidis et al., 2015[b]) as well as the study's inherent limitations such as the cut-off level selected. FC may also be a marker of subclinical inflammation; Gisbert and McNicholl (Gisbert et al., 2009) found that FC was higher in asymptomatic first-degree relatives of patients with IBD, and FC has been seen to predict relapse in asymptomatic or quiescent CD (Mao et al., 2012). Another study has found that FC does not reliably distinguish IBD from malignancy (Summerton et al., 2002), which may -indirectly- suggest that FC is not as good at distinguishing generalized inflammation from foci of inflammation.

Furthermore, some studies show FC is a more reliable indicator of colonic than SB inflammation, i.e., usefulness of FC varies with location of inflammation within the gut, and there is difficulty in establishing correlation due to the heterogeneity of presentations in CD (Stawczyk-Eder et al., 2015; Jensen et al., 2011). Figure 16 shows how LS is generally low in patients with normal SB VCE; however, these patients have a wide range of FC. Conversely our study also had patients with low FC but high LS, which could have been indicative of a single large lesion, such as an isolated stenosis, yielding a diagnosis. Further prospective studies should be performed to investigate the difference between the equivocal results of our study and other studies which show positive correlation between LS and FC.

FICE

The technological limitations of capsule endoscopy mean that a targeted focus on SB lesions or areas of interest is not possible; any focus occurs only for time allowed by bowel movement and propulsion (Cass, 2006). Furthermore, despite substantial improvement in recent years in image quality, particularly in image resolution, the image pixelation of SB VCE remains disappointingly low (Ciuti et al., 2011; Sliker et al., 2014), especially when compared with that of conventional high definition flexible endoscopes. This often leads to suboptimal lesion imaging and therefore potentially reduces the DY of VCE (Koulaouzidis et al., 2015[a]; Hale et al., 2014). Software such as FICE, already established in conventional GI endoscopy, has been integrated into commercially available capsule endoscopy reviewing software (RAPID®; Medtronic) in order to increase visualization and detection rate for SB findings. However, clinical opinion and pooled proportion of 89% of angiectasia

images were considered “improved” (defined as improved visualization aiding lesion characterization and enhanced delineation of lesion surface and/or borders), compared with the WLE images.

For SB angiectasias viewed under FICE 2 and 3, and for mucosal ulcers/erosions viewed under all 3 FICE settings, less than 50% of the images were considered to be improved. In fact, for FICE settings 2 and 3, there was close to no improvement in ulcer/ erosion visualization compared with WLI. Therefore, FICE performs well when there is significant colour alteration of the lesion, as in angiectasias. This could be partially explained by the fact that pigmented fluids, such as blood and bile, allow the greatest contrast with SB mucosa even under WLE. FICE further enhances this contrast, leading to subjective improvement in visualization, whereas it may not perform as well with non-pigmented lesions (Imagawa et al., 2011[b], Spada et al., 2011). The most recent technical report from the American Society for Gastrointestinal Endoscopy states that there is no evidence for an optimal FICE mode for tissue diagnosis and differentiation in conventional GI endoscopy (Manfredi et al., 2015).

Spada et al. defined the clinical usefulness of chromoendoscopy in terms of the following criteria: (i) improvement in lesion detection rate; (ii) improvement in lesion delineation; and (iii) ability to identify lesions which require treatment (Spada et al., 2011). In fact, the number of lesions detected on full video reading may be a more accurate index of the clinical performance of FICE against anecdotal evidence remain divided as to the usefulness of FICE and other chromoendoscopy software for VCE review (Spada et al., 2011).

In this meta-analysis, all three FICE modes failed to show much significant improvement in visualization of SB pathology. However, only with FICE setting 1 a pooled proportion WLE because of the unambiguous binary response of pathological finding detected or not. This approach is likely to be less subjective than assessment of delineation improvement as determined by human readers. The majority of pathological findings at capsule endoscopy consist of vascular lesions and mucosal defects. Polypoid or submucosal lesions, where software tools can enhance diagnostic accuracy (Girelli et al., 2011; Rondonotti et al., 2015), are found less frequently.

Therefore, in the video studies examining detection rate for SB pathological findings, FICE did not produce any significant improvement in the detection of angiectasias or mucosal ulcers/erosions, compared to WLE video reading. Furthermore, all these studies relied on human vision and perception for detection of lesions. Psychological studies have shown that the colour red produces a stronger reaction in humans, therefore human readers may be more likely to pick up on red-coloured lesions (i.e., blood or vascular lesions) compared to the more muted green and brown tones in FICE setting 2 and 3 (Green, 1968; Hill et al., 2005; Ilie et al., 2008). By extension, narrow band imaging (NBI) is based on the penetration

properties of different wavelengths of light corresponding to the two light absorption peaks of haemoglobin, so as to increase the contrast and therefore visibility of vasculature (Manfredi et al., 2015).

The study results are similar overall to those achieved in studies on the use of virtual chromoendoscopy in conventional GI endoscopy: the value of virtual chromoendoscopy lies in aiding lesion visualization and therefore characterization, rather than in increasing detection (Manfredi et al., 2015). Although all but one of the studies included in this meta-analysis involved experienced capsule endoscopy readers, a recent study found that using FICE and Blue mode also helped beginner capsule endoscopy readers to better characterise lesions (Rimbaş et al., 2016) suggesting that this may be an area warranting further investigation.

This review and meta-analysis focused on FICE alone, although other virtual chromoendoscopy software is currently available such as Blue mode (Manfredi et al., 2015) and Augmented Live-body Image Colour-Spectrum Enhancement (ALICE) (Intromedic, Seoul, South Korea) (Ryu et al., 2013). However, the existing body of data is small and too heterogeneous for more systematic analysis. Although in this meta-analysis FICE has not performed as well as hoped, there is some evidence for the usefulness of other forms of virtual chromoendoscopy, mainly Blue mode (Krystallis et al., 2011; Koulaouzidis et al., 2012[a]; Abdelaal et al., 2015; Koulaouzidis et al., 2012[d]). Current evidence suggests that Blue mode remains a more user-friendly form of virtual chromoendoscopy which can be applied with ease to full VCE readings. However, none of the existing studies have shown a meaningful increase in diagnostic yield with Blue mode. Interestingly, Aihara and colleagues presented a study using image-enhanced CE which increased the contrast between the surrounding mucosa and lesions such as vascular or inflammatory lesions or polyps. They reported that the effects of this contrast CE are similar to those of NBI in conventional GI endoscopy (Aihara et al., 2011). The only study using ALICE, presented as an abstract, reported improved visibility of flat and depressed SB lesions (Ryu et al., 2013).

Limitations of this meta-analysis include, firstly, the heterogeneity of current published studies investigating the usefulness of FICE, as shown by the high I^2 values. These studies varied considerably in terms of study design, selected population, images and videos for analysis, and models of CE used with their subsequent effect on technical performance. For instance, differences in the LED specifications between the PillCam®SB versions could vary the image quality and interpretation between studies. The heterogeneity of study design meant that several could not be included in the meta-analysis, thus greatly limiting the sample size. None of the included studies reported whether the readers had been tested for colour blindness; it is unclear whether this could influence intra-observer agreement. The majority of the studies included in this meta-analysis also did not specify the size or clinical significance of the lesions, another factor which could influence detection rate.

KID

Human factors remain a barrier to timely and accurate CE diagnosis (Zheng et al., 2012). AI systems can improve clinical performance, patient safety, and resource utilization (Koulaouzidis et al., 2013[b]; Iakovidis et al., 2015). Open interdisciplinary exchange of information is key to technological advancement and therefore improved clinical outcomes (Iakovidis et al., 2015). New technological developments may not always meet pertinent healthcare needs due to little communication between software engineers and clinicians; furthermore, open access databases of endoscopic images are scarce, especially those specifically related to SB VCE (http://www.endoatlas.com/websites.html). This is despite growing clinical demand and use of CE as an investigative modality.

However, such interactive formats are vital for engaging a new generation of clinicians; this is currently hindered by inadequately developed software (Kilbridge et al., 2008). Therefore, KID aims to be a comprehensive and all-encompassing resource for continuous development of CAD in CE, and to encourage two-way dialog between technological developers and end-users. For example, KID compiles images from all commercial CE models and is international, thus increasing its scope.

The experiment detailed above shows that generally good agreement was achieved between expert human readers and the MLA in measuring the size of common SB lesions. This implies automated lesion measurement is feasible, and MLAs could eventually replace or drastically reduce the workload of valuable human resources. In a recent study, van der Sommen and colleagues detailed collaboration between IT engineers and clinicians to develop a CAD algorithm for diagnosis of early neoplasia in Barrett's oesophagus, with good results (Van der Sommen et al., 2016).

An advantage of the method presented in this study over previous automated measurement approaches is its suitability for a variety of lesion types. In a recent study (Koulaouzidis et al., 2016) using images of angiectasias available in KID, we showed that the interobserver agreement between CE reviewers, in terms of JI, in lesion annotation ranges between 65±15% and 67±13%, and the respective intra-observer agreement, between 69±17% and 71±13%. This dataset was similar in terms of the morphological characteristics of the displayed angiectasias, indicating that our MLA has a performance comparable to that of human readers. However, a limitation shown by the experiment is that it does not perform as well with all mucosal lesions. Further algorithm development is therefore required, showing the need for platforms such as KID.

Image reconstruction and localisation

VCE technology has progressed significantly since its introduction to routine clinical practice; however, the interpretation of a CE examination in order to reach a diagnosis remains heavily reliant on human readers (Lo, 2006). Furthermore, the long reading times required also diminish its clinical efficiency. Therefore, further technological developments should aim to reduce CE reading times and minimize variability in CE reading. An ideal way to do so is to develop methods for computer-assisted and eventually automated diagnosis.

A significant limitation of CE is the lack of accurate localisation. Lesion(s) localisation in the SB is of paramount importance in managing SB diseases as localisation info is the cornerstone in deciding the route of insertion (transoral or transanal) of any subsequent double-balloon endoscopy. Current approaches to VCE and hence lesion localisation includes: transit time estimation from anatomical landmarks, localisation in 2D or 3D space with respect to external sensors and RF triangulation, active magnetic localisation, magnetic resonance, ultrasound and positron emission imaging-based approaches (Baptista et al., 2014; Keuchel et al., 2015; Than et al., 2012). Our method provides comparable performance to methods based on external sensor arrays, without their use. Furthermore, because CE is a wireless minimally invasive system, information is mainly obtained as videos and images. 3D information could facilitate more detailed diagnostic evaluation of lesions seen (Sakata et al., 2016). Due to the difficulty in accessing the human SB, more invasive investigations or procedures such as deep enteroscopy should be optimally planned.

Typically, in CE, monocular vision provides the only information for 3D reconstruction. Therefore, our modified SfS method uses assumptions more applicable to VCE images, obtained in the confined environment of the bowel lumen, and where manual focus is impossible due to the passive nature of capsule propulsion. To determine depth, this method estimates the albedo (whiteness coefficient, or measure of reflection) by using specular highlights and the corresponding surface ‘normals’ of the reconstructed surface (Visentini-Scarzanella et al., 2012).

Our setup has inherent limitations due to currently available technology. First, the intrinsic parameters of the PillCam®SB3 are unknown; therefore, vital information such as the focal length of the lens had to be estimated via calibration. Secondly, we assumed that the CE moved at constant velocity following the centre of the bowel lumen. Finally, the SB model was linear, immobile and had an elliptical cross-section throughout; furthermore, there was no luminal content. These do not entirely reflect actual human SB structure and function, nor the usual clinical conditions under which a CE operates.

Future perspectives

In summary, the next **TIDAL** wave in the VCE 'revolution' is one that will include solution(s) in **T***herapy capability*, **I***ntegration/Intelligence*, **D***ata* (not only images) *collection*, **A***ctuation*, and **L**ocalisation.

The accuracy of VCE is heavily dependent on accurate interpretation, which is not entirely dependent on reviewer's experience (Iakovidis et al., 2015). Historically, the VCE lesion miss rates have been reported at levels between 6% and 18% (Iakovidis et al., 2015; Zheng et al., 2012). Furthermore, there is also poor agreement on decision-making such as *'indication for a following colonoscopy*' in the case of colonic VCE, and a high intra and inter-observer agreement for polyp detection among experts, as well as a moderate agreement between beginners and experts (Buijs et al., 2018). Nevertheless, errors and oversights are akin to human nature; when these are associated with erroneous diagnosis, the impact/harm for both patients and healthcare professionals who experience them may be detrimental and associated with loss, emotional hardship, and medical litigation (Koulaouzidis et al., 2020). However, the way forward seems to be capsule-paved as the fields of application will eventually expand worldwide (consider recent developments in the 'social distancing' and tele-health promotion) (Kobaek-Larsen et al., 2018); colonic VCE is not only superior to colonoscopy in polyp detection rate and per-patient sensitivity to>9 mm polyps, but patient's acceptance is also extremely high (Steffenssen et al., 2019).

The buzz of AI is not new; the very essence of VCE reading software, in fact, is one of early AI in action. Tools such as Lewis Score, QuickView, Suspected Blood Indicator are nothing more than clever snippets of AI integrated in the very early versions of proprietary reading software with main aim to assist, support and/or speed up medical decision process (Koulaouzidis et al., 2020). Soon we will be able to rely on AI to analyse VCE and simply present us with abnormal findings. In the meantime, it is certainly beneficial to have efforts and works like those the KID – with VCE images and their annotations available to the wider scientific community– to foster essential multidisciplinary cooperation and progress in this field and continue with the hard work required to continue populating the database with images and relevant annotations (Koulaouzidis et al., 2020).

Conclusions

1. In patients with strong clinical suspicion of SB CD and negative conventional bidirectional endoscopy, VCE should not be limited to patients with elevated biomarkers only. In particular, CRP and the ratio to monocytes were not associated with SB inflammation in VCE. Moreover, the correlation was moderate for FC, and if this biomarker is used to guide the decision to perform VCE, at least 40% of patients will be misdiagnosed. Nevertheless, FC =>76 mcg/g may be associated with appreciable inflammation on VCE in patients with negative prior diagnostic workup.
2. Overall, the use of the three FICE modes did not significantly improve detection rate or the quality of visualization of the most common pathological findings seen on SB VCE. FICE 1 seems to perform better for pigmented lesions such as angiectasias, in terms of lesion delineation and detection. However, the evidence is equivocal as to whether FICE 2 and 3 aid SB VCE reading.
3. KID is the only database of VCE images and videos with both graphic and semantic annotations developed specifically for MDSS research. KID provides a platform for data sharing and CAD software development. The experiments detailed are proof-of-principle studies demonstrating the potential for KID to fulfil this role.
4. Based on our experimental set-up of study IV, we present methods for both 2D and 3D localisation of a capsule using visual information alone. Such methods are feasible and have potential to be of clinical use. However, there remains a significant margin of error, indicating that much further work is required to refine these processes.

Populärvetenskaplig sammanfattning

Gastrointestinala sjukdomar, som blödning, inflammation och tumörer är ganska vanliga med betydande sjuklighet, dödlighet och försämrad livskvalitet för de drabbade. Undersökning och behandling av sådana sjukdomar involverar både primär- och specialistvård med betydande kostnader för samhället. Övre och nedre delarna av mag-tarmkanalen var lättillgängliga med traditionella endoskopiska metoder som gastroskop och koloskop, medan fram till årtusendets början var tunntarmen ganska otillgänglig för undersökningar och området nämndes som 'ingen mans land'.

Fram till år 2000, då gastroskopi och koloskopi var negativa och de diagnostiska frågorna fortfarande var obesvarade, användes radiologiska metoder (röntgenstrålningar från Barium, CT /MR-undersökningar, angiografier osv.), och ibland kirurgi för att undersöka resten av mag-tarmkanalen med begränsad information, särskilt när till exempel blödningskällan fanns i tunntarmen. Diagnosen av olika sjukdomar som inflammatorisk tarmsjukdom försenades. Flesta av de tidigare nämnda undersökningsmetoderna saknar inte bara noggrannhet utan är förknippade med obehag för patienterna och möjliga komplikationer eller joniserande strålning.

För detta ändamål ledde ett fruktbart samarbete mellan läkare och ingenjörer fram till uppfinningen av kapselendoskopi som ger möjlighet för trådlös och detaljerad avbildning av hela tunntarmens slemhinna. Kapseln har inte någon aktiv rörelsekapacitet utan beror helt enkelt på tarmens rörelse, ofrivillig sammandragning och avkoppling av tarmens muskler som skapar vågliknande rörelser som driver innehållet i tarmen framåt. Utrustningen består av tre huvuddelar: kapselendoskopet, en bärbar mottagare och ett digitalt system installerat i en vanlig stationär dator där bilder laddas ner och utvärderas.

Kapselendoskopet är stort som en vitaminkapsel (26x11 mm) och innehåller ett smart elektroniskt kamerachip samt flera ljusdioder som blinkar 2–4 gånger per sekund. Kapseln innehåller också en minikamera som tar vidvinkelbilder. Bilderna överförs - vanligtvis - via en radiosignal till antenner anordnade i ett bälte runt patientens midja. De inspelade signalerna överförs sedan till en stationär arbetsstation och de nedladdade bilderna behandlas för att skapa ett videoklipp för utvärdering. Mottagaren har kapacitet att lagra flera hundratusentals bilder. Bilderna förstoras 8 gånger och kan upptäcka slemhinneförändringar ner till 1.1 mm.

Kapselendoskopet är en biologiskt inert enhet, miljövänlig och lämnar kroppen med avföringen.

Trots sin unika karaktär och diagnostiska kapacitet av videokapselendoskopi finns det områden där det finns brist på noggrannhet och behov för klinisk och teknisk utveckling. Följaktligen var det huvudsakliga syftet med denna avhandling att studera och optimera den tekniska kliniska prestandan genom att undersöka effekten av att kombinera bildinformation som erhållits med kapsel med biokemisk information erhållen genom att mäta proteiner såsom kalprotektin i avföringen; undersöka användbarheten av digitalt bildfilter vid bildtolkning samt utveckla och utforska användningen av en bilddatabas såväl som möjliga tillvägagångssätt för lokalisering av kapselendoskop i tunntarmen.

Syftet med första delarbete var att undersöka sambandet mellan tunntarmsinflammation som ses vid kapselendoskopi (kvantifierat med ett mjukvarubaserat verktyg, nämligen Lewis-poäng) och en biokemisk parameter för inflammation (ett protein i tarmlumen och uppmätt i avföring som kallas fekal kalprotektin) i en stor grupp patienter som genomgår videokapselendoskopi för misstänkt eller känd inflammatorisk tarmsjukdom. Under en period av tre år granskades och insamlades relevant data från fem akademiska centra och ett distriktssjukhus med videokapselendoskopi i Storbritannien, Finland, Sverige, Kanada och Israel. Totalt inkluderades 333 patienter. Alla patienter hade endoskopi med tunntarmsvideokapsel och en mätning av fekal kalprotektin med högst 3 månaders mellanrum. Alla genomgick koloskopi för att utesluta betydande tjocktarmsinflammation som kunde ha stört den exakta tolkningen av resultaten. Sammantaget var korrelationen mellan fekal kalprotektin och tunntarmsinflammation, kvantifierad med användning av Lewis-poäng, svag. Vi drog slutsatsen att inflammation som observerats och rapporterats via Lewis-poäng vid kapselendoskopi tycks ha låg korrelation med uppmätt fekal kalprotektin.

Syftet med delarbete nr 2 var att undersöka värdet av en digital färgteknik (FICE) vid kapselendoskopi för att detektera, avgränsa och karakterisera slemhinneförändringar i tunntarmen. FICE är en tillgänglig mjukvara i vissa typ av kapselendoskopisystem med olika inställningsmöjligheter, men det kliniska värdet av teknologin är fortfarande oklart. Genom litteraturgenomgång analyserades data från alla tidigare publikationer och värdet av FICE-färgteknik för diagnostiken av olika tunntarmsförändringar bedömdes. Sammantaget drog vi slutsatsen att användningen av FICE-färgteknik med olika inställningar inte signifikant förbättrar avgränsningen eller detekteringen av slemhinneförändringar vid kapselendoskopi.

Syftet med delarbete nr 3 var att utveckla en ny databas, kallad KID (kapsel interaktiv databas), med syfte till att erbjuda en referens för forskning och utveckling av medicinska beslutssupportsystem för kapselendoskopi. Det är känt att beräkningsmetoder kan förbättra diagnostik utbyte av klinisk kapselendoskopi, men att integrera maskininlärningsalgoritmer i videokapselens endoskopi är svårt

eftersom en stor mängd bildanteckningar krävs för träning. Aktuella databaser saknar grafiska kommentarer av patologier och kan inte användas maskininlärning. För att utveckla denna databas användes en öppen källkodsprogramvara. Kliniker från ett samarbetsnätverk för kapselendoskopi bidragit med anonymiserade, annoterade kapselendoskopibilder och videor. Grafiska kommentarer till förändringar utfördes av ett öppet-kommentarverktyg Ratsnake. För att undersöka den praktiska användbarheten för en sådan databas genomfördes ett experiment baserat på KID-databasen för att jämföra utvärderingen av kapselfynden med expertutvärderare och en maskininlärningsalgoritm. Studiens slutsats var att vårt utvecklingsarbete visade att maskininlärningsalgoritmer kan fungera lika bra som mänskliga läsare vid utvärderingen av små slemhinneförändringar vid kapselendoskopi vilket visar potential för automatisk utvärdering av kapselendoskopiundesökningar i framtiden.

Syftet med delarbete nr 4 var att undersöka en metod för 3D-rekonstruktion av bilder och lokalisering av kapsel i tunntarmen med hjälp av visuell information från 2D-videokapselendoskopibilder. Tillgängliga kapselendoskopisystem innehåller mjukvara för lokalisation av förändringar i tunntarmen, dessa verktyg är dock opålitliga. I detta experimentella arbete användas en tarmmodell. En PillCam®SB3 kapsel kalibrerades och navigerades genom tarmlumen av en robot med hög precision. ORB-SLAM-tekniken användes för 3D-bildrekonstruktion och lokalisering av kapselendoskop inom den rekonstruerade modellen. Vi drog slutsatsen att rekonstruktionsmetoderna, som beskrivs ovan, kunde uppnå 3D-rekonstruktion av god kvalitet i tarmmodellen och lokalisering av kapselbanan med hjälp av information baserad på videofilm och bilder registrerade av kapselendoskop. Vårt arbete kan ligga till grunden för vidareutveckling av dagens kapselendoskopimodeller för bättre lokalisation och klinisk diagnostik av slemhinneförändringar i tunntarmen.

Acknowledgments

I would like to thank all those people who made this work possible. More specifically, I would like to express my deep appreciation to:

All the patients who participated in the studies.

Ervin Toth, an excellent principal supervisor, and a true friend. It has been almost a decade since a I met him first time in one of the European Gastroenterology conferences held in Stockholm, and he has been since an inspiration and guiding paradigm with his kindness, humanity and acumen. His persistence and gentle 'push' during the final stages of this second doctorate thesis cannot be overstated.

Henrik Thorlacius, a brilliant and inspirational co-supervisor. This thesis would not have been possible without his great-hearted support. Henrik was the one who accepted me in for the doctoral degree and has been inspirational with his laissez faire supervision. I hope the future holds for us a few more collaborations. And for sure I am looking forward enjoying some more discussion in one of the conferences.

All of my co-authors, especially, for their support, excellent collaboration and friendly spirit.

Artur Nemeth for his wonderful and friendly support.

Gastone Ciuti for his ideas, collaboration and dedication.

Dimitris Iakovidis, a close collaborator, ideas generator and an excellent scientist.

Andry Giannakou, for the selfless & indispensable statistics contribution for this work.

John Plevris, a mentor in the field of capsule endoscopy and a friend.

Eirini Koulaouzidou, my loving and supporting mother.

George Koulaouzidis, my loving brother.

Maria, for her introduction to spirituality and mindfulness.

This work was partially supported by the European Commission within the framework of the endoscopic versatile robotic guidance, diagnosis and therapy of magnetic- driven soft-tethered endoluminal robots Project-H2020-ICT- 24-2015 (EU Project-G.A. number: 688592).

References

Abdelaal UM, Morita E, Nouda S, Abdelaal UM, Morita E, Nouda S, et al. (2015). Blue mode imaging may improve the detection and visualization of small-bowel lesions: A capsule endoscopy study. Saudi J Gastroenterol. 21(6):418-422.

Aihara H, Ikeda K, Tajiri H (2011). Image-enhanced capsule endoscopy based on the diagnosis of vascularity when using a new type of capsule. Gastrointest Endosc. 73(6):1274-1279.

ASGE Technology Committee; Manfredi MA, Abu Dayyeh BK, Bhat YM, Chauhan SS, Gottlieb KT, Hwang JH, et al. (2015). Electronic chromoendoscopy. Gastrointest Endosc. 81(2):249-61.

ASGE Technology Committee; Wang A, Banerjee S, Barth BA, ASGE Technology Committee; Wang A, Banerjee S, Barth BA, et al. (2013). Wireless capsule endoscopy. et al. Wireless capsule endoscopy. Gastrointest Endosc. 78(6):805-815.

Baptista V, Marya N, Singh A, Rupawala A, Gondal B, Cave D (2014). Continuing challenges in the diagnosis and management of obscure gastrointestinal bleeding. World J Gastrointest Pathophysiol. 5(4):523-533.

Bartzis L, Koulaouzidis A (2014). String-mounted double-headed capsule and Z-line detection: is string really the thing? Eur J Gastroenterol Hepatol. 26(6):685-6.

Boal Carvalho P, Magalhães J, Dias de Castro F, Gonçalves TC, Rosa B, Moreira MJ, et al. (2016). Virtual chromoendoscopy improves the diagnostic yield of small bowel capsule endoscopy in obscure gastrointestinal bleeding. Dig Liver Dis 2016; 48(2):172-175.

Bolanis P, Stauropoulou E (2011). The ratio of monocytes to CRP correlates to symptoms induction time of the acute phase. 37 Annual Panhellenic Medical congress.

Buijs MM, Kroijer R, Kobaek-Larsen M, Spada C, Fernandez-Urien I, et al. (2018). Intra and inter-observer agreement on polyp detection in colon capsule endoscopy evaluations. United European Gastroenterol J. 6(10):1563-1568.

Calafat M, Cabré E, Mañosa M, Lobatón T, Marín L, Domènech E (2015). High within-day variability of fecal calprotectin levels in patients with active ulcerative colitis: what is the best timing for stool sampling? Inflamm Bowel Dis. 21(5):1072-1076.

Calonder M, Lepetit V, Strecha C, Fua P (2010) Brief: Binary robust independent elementary features. Computer Vision–ECCV 2010. 778-792.

Cass OW (2006). Is half-knowledge worse than ignorance? Gastrointest Endosc. 64(4):542-543.

Chong AKH, Chin BWK, Meredith CG (2006). Clinically significant small-bowel pathology identified by double-balloon enteroscopy but missed by capsule endoscopy. Gastrointest Endosc. 64(3):445-449.

Ciuti G, Menciassi A, Dario P (2011). Capsule endoscopy: From current achievements to open challenges. IEEE Rev Biomed Eng. 4:59-72.

Ciuti G, Visentini-Scarzanella M, Dore A, Menciassi A, Dario P, Yang GZ (2012). Intra-operative monocular 3D reconstruction for image-guided navigation in active locomotion capsule endoscopy. In: 2012 4th IEEE RAS & EMBS International Conference on Biomedical Robotics and Biomechatronics (BioRob). 768-774.

Cong Y, Wang S, Liu J, Cao J, Yunsheng Y, Luo J (2015). Deep sparse feature selection for computer aided endoscopy diagnosis. Pattern Recognit. 48(3):907-917.

Cool S, Pieters JG, Mertens KC Mora S, Cointault F, Dubois J, et al (2015). Development of a high irradiance LED configuration for small field of view motion estimation of fertilizer particles. Sensors. 15(11):28627-28645.

Cotter J (2014). Virtual chromoendoscopy in small bowel capsule endoscopy: New light or a cast of shadow? World J Gastrointest Endosc. 6(8):359-365.

Cotter J, Dias de Castro F, Magalhães J, Moreira MJ, Rosa B (2015). Validation of the Lewis score for the evaluation of small-bowel Crohn's disease activity. Endoscopy. 47(4):330-335.

Cummins G, Cox BF, Ciuti G, Anbarasan T, Desmulliez MPY, Cochran S, et al. (2019). Gastrointestinal diagnosis using non-white light imaging capsule endoscopy. Nat Rev Gastroenterol Hepatol. 16(7):429-447.

Dhaliwal A, Zeino Z, Tomkins C, Cheung M, Nwokolo C, Smith S, et al. (2015). Utility of faecal calprotectin in inflammatory bowel disease (IBD): what cut-offs should we apply? Frontline Gastroenterol. 6(1):14-19.

Dias de Castro F, Magalhães J, Boal Carvalho P, Cúrdia Gonçalves T, Rosa B, Moreira MJ, et al. (2015). Improving diagnostic yield in obscure gastrointestinal bleeding – how virtual chromoendoscopy may be the answer. Eur J Gastroenterol Hepatol. 27(6):735-740.

Eliakim R (2017). Where do I see minimally invasive endoscopy in 2020: clock is ticking. Ann Transl Med. 5(9):202.

Fagerhol MK, Dale I, Andersson T (1980). Release and quantitation of a leukocyte derived protein (L1). Scand J Haematol. 24:393-398.

Freitas F, Schulz S, Moraes E (2009). Survey of current terminologies and ontologies in biology and medicine. RECIIS Electron J Commun Inf Innov Health. 3(1):7-18.

Gal E, Geller A, Fraser G, Levi Z, Niv Y (2008). Assessment and validation of the new capsule endoscopy Crohn's disease activity index (CECDAI). Dig Dis Sci. 53(7):1933-1937.

Girelli CM, Porta P, Colombo E, Lesinigo E, Bernasconi G (2011). Development of a novel index to discriminate bulge from mass on small-bowel capsule endoscopy. Gastrointest Endosc. 74(5):1067-1074.

Gisbert JP, McNicholl AG (2009). Questions and answers on the role of faecal calprotectin as a biological marker in inflammatory bowel disease. Dig Liver Dis. 41(1):56-66.

Gralnek IM, Defranchis R, Seidman E, Leighton JA, Legnani P, Lewis BS (2008). Development of a capsule endoscopy scoring index for small bowel mucosal inflammatory change. Aliment Pharmacol Ther. 27(2):146-154.

Green DG (1968). The contrast sensitivity of the colour mechanisms of the human eye. J Physiol. 196(2):415-429.

Grove PM (2013). The Psychophysics of binocular vision. In: 3D-TV System with Depth-Image-Based Rendering. New York, NY: Springer New York 2013.347-373.

Gupta T, Ibrahim M, Deviere J, van Gossum A (2011). Evaluation of Fujinon intelligent chromo endoscopy-assisted capsule endoscopy in patients with obscure gastroenterology bleeding. World J Gastroenterol. 17(41):4590-4595.

Gurudu SR, Leighton JA (2012). Correlation of two capsule endoscopy scoring systems with fecal calprotectin: does it really matter? Dig Dis Sci. 57(4):827-829.

Hale M, McAlindon ME (2014). Capsule endoscopy as a panenteric diagnostic tool. Br J Surg. 101(3):148-149.

Higgins JPT, Thompson SG (2002). Quantifying heterogeneity in a meta-analysis. Stat Med. 21(11):1539-1558.

Hill RA, Barton RA (2005). Psychology: red enhances human performance in contests. Nature. 435:293.

Höög CM, Bark LÅ, Broström O, Sjöqvist U (2014). Capsule endoscopic findings correlate with fecal calprotectin and C-reactive protein in patients with suspected small-bowel Crohn's disease. Scand J Gastroenterol. 49(9):1084-1090.

http://www.endoatlas.com/websites.html; Selected websites recommended by the Atlas of Gastrointestinal Endoscopy.

http://www.statstutor.ac.uk/resources/uploaded/spearmans.pdf.

Iakovidis DK, Goudas T, Smailis C, Maglogiannis I (2014[a]). Ratsnake: A versatile image annotation tool with application to computer-aided diagnosis. Sci World J. 286856.

Iakovidis DK, Koulaouzidis A (2014[b]). Automatic lesion detection in capsule endoscopy based on color saliency: Closer to an essential adjunct for reviewing software. Gastrointest Endosc. 80(5): 877-883.

Iakovidis DK, Koulaouzidis A (2015). Software for enhanced video capsule endoscopy: challenges for essential progress. Nat Rev Gastroenterol Hepatol. 12(3):172-186.

Iddan G, Meron G, Glukhovsky A, Swain P (2000). Wireless Capsule Endoscopy. Nature. 405(6785):417.

Ilie A, Ioan S, Zagrean L, Moldovan M (2008). Better to be red than blue in virtual competition. Cyber Psychol Behav. 11(3):375-377.

Imagawa H, Oka S, Tanaka S, Noda I, Higashiyama M, Sanomura Y, et al. (2011[a]). Improved visibility of lesions of the small intestine via capsule endoscopy with computed virtual chromoendoscopy. Gastrointest Endosc. 73(2):299-306.

Imagawa H, Oka S, Tanaka S, Noda I, Higashiyama M, Sanomura Y, et al. (2011[b]). Improved detectability of small-bowel lesions via capsule endoscopy with computed virtual chromoendoscopy: A pilot study. Scand J Gastroenterol; 46(9):1133-1137.

Jensen MD, Kjeldsen J, Nathan T (2011). Fecal calprotectin is equally sensitive in Crohn's disease affecting the small bowel and colon. Scand J Gastroenterol. 46(6):694-700.

Kannala J, Brandt SS (2006). A generic camera model and calibration method for conventional, wide-angle, and fish-eye lenses. IEEE Trans Pattern Anal Mach Intell. 28(8):1335-1340.

Keuchel M, Kurniawan N, Baltes P, Bandorski D, Koulaouzidis A (2015). Quantitative measurements in capsule endoscopy. Comput Biol Med.65:333-347.

Kilbridge PM, Classen DC, (2008). The informatics opportunities at the intersection of patient safety and clinical informatics. J Am Med Inform Assoc. 15(4): 397-407.

Kobaek-Larsen M, Kroijer R, Dyrvig AK, Buijs MM, Steele RJC, Qvist N, et al. (2018). Back-to-back colon capsule endoscopy and optical colonoscopy in colorectalcancer screening individuals. Colorectal Dis.20(6):479-485.

Kobayashi Y, Watabe H, Yamada A, Hirata Y, Yamaji Y, Yoshida H, et al. (2012). Efficacy of flexible spectral imaging color enhancement on the detection of small intestinal diseases by capsule endoscopy. J Dig Dis. 13(12):614-620.

Konishi M, Shibuya T, Mori H, Kurashita E, Takeda T, Nomura O, et al (2014). Usefulness of flexible spectral imaging color enhancement for the detection and diagnosis of small intestinal lesions found by capsule endoscopy. Scand J Gastroenterol. 49(4):501-505.

Kopylov U, Seidman EG (2014). Role of capsule endoscopy in inflammatory bowel disease. World J Gastroenterol. 20(5):1155-1164.

Kopylov U, Nemeth A, Koulaouzidis A, Makins R, Wild G, Afif W, et al (2015[a]). Small bowel capsule endoscopy in the management of established Crohn's disease: clinical impact, safety, and correlation with inflammatory biomarkers. Inflamm Bowel Dis. 21(1):93-100.

Kopylov U, Yablecovitch D, Lahat A, Neuman S, Levhar N, Greener T, et al. (2015[b]). Detection of small bowel mucosal healing and deep remission in patients with known small bowel Crohn's disease using biomarkers, capsule endoscopy and imaging. Am J Gastroenterol. 110(9):1316-1323.

Korman LY, Delvaux M, Gay G, Hagenmuller F, Keuchel M, Friedman S, et al. (2005). Capsule Endoscopy Structured Terminology (CEST): Proposal of a standardized and structured terminology for reporting capsule endoscopy procedures. Endoscopy. 37(10):951-959.

Koulaouzidis A, Douglas S, Rogers MA, Arnott ID, Plevris JN (2011). Fecal calprotectin: a selection tool for small bowel capsule endoscopy in suspected IBD with prior negative bi-directional endoscopy. Scand J Gastroenterol. 46(5):561-566.

Koulaouzidis A (2012). Upper oesophageal images and Z-line detection with 2 different small-bowel capsule systems. World J Gastroenterol. 18(41):6003-6004.

Koulaouzidis A, Douglas S, Plevris JN (2012[a]). Blue mode does not offer any benefit over white light when calculating Lewis score in small-bowel capsule endoscopy. World J Gastrointest Endosc. 4(2):33-37.

Koulaouzidis A, Douglas S, Plevris JN (2012[b]). Lewis score correlates more closely with fecal calprotectin than Capsule Endoscopy Crohn's Disease Activity Index. Dig Dis Sci. 57(4):987-993.

Koulaouzidis A, Smirnidis A, Douglas S, Plevris JN (2012[c]). QuickView in small-bowel capsule endoscopy is useful in certain clinical settings, but QuickView with Blue Mode is of no additional benefit. Eur J Gastroenterol Hepatol. 24(9):1099-1104.

Koulaouzidis A, Plevris JN (2012[d]). Detection of the ampulla of Vater in small bowel capsule endoscopy: experience with two different systems. J Dig Dis. 13(12):621-627.

Koulaouzidis A, Dabos KJ (2013[a]). Looking forwards: not necessarily the best in capsule endoscopy? Ann Gastroenterol. 26(4): 365-367.

Koulaouzidis A, Rondonotti E, Karargyris A (2013[b]). Small-bowel capsule endoscopy: A ten-point contemporary review. World J Gastroenterol. 19(24):3726-3746.

Koulaouzidis A, Giannakou A, Yung DE, Dabos KJ, Plevris JN (2013[c]). Do prokinetics influence the completion rate in small-bowel capsule endoscopy? A systematic review and meta-analysis. Curr Med Res Opin. 29(9):1171-1185.

Koulaouzidis A, Iakovidis DK, Karargyris A, Plevris JN (2015[a]). Optimizing lesion detection in small-bowel capsule endoscopy: from present problems to future solutions. Expert Rec Gastroenterol Hepatol. 9(2):217-235.

Koulaouzidis A, Nemeth A, Johansson GW, Toth E (2015[b]). Dissecting Lewis score under the light of fecal calprotectin; an analysis of correlation of score components with calprotectin levels in capsule endoscopy. Ann Gastroenterol. 28(2): 259-264.

Koulaouzidis A, Iakovidis DK, Karargyris A, Rondonotti E (2015[c]). Wireless endoscopy in 2020: Will it still be a capsule? World J Gastroenterol. 21(17):5119-5130.

Koulaouzidis A, Yung D, Rondonotti E, Voulgarakis D, Iakovidis DK (2016). Chromoendoscopy for angiectasias in capsule endoscopy; blue or just white? Gut. 65:A52-A53.

Koulaouzidis A, Toth E (2020). Image database, AI and capsule endoscopy; the bets are on. Endosc Int Open. 8(3):E421-E422.

Krystallis C, Koulaouzidis A, Douglas S, Plevris JN (2011). Chromoendoscopy in small bowel capsule endoscopy: Blue mode or Fuji Intelligent Colour Enhancement? Dig Liver Dis. 43(12):953-957.

Lankton S, Tannenbaum A (2008). Localizing region-based active contours. IEEE Trans Image Process. 17(11):2029-2039.

Lasson A, Stotzer PO, Öhman L, Isaksson S, Sapnara M, Strid H (2015). The intra-individual variability of faecal calprotectin: a prospective study in patients with active ulcerative colitis. J Crohns Colitis. 9(1):26-32.

Lo SK (2006). How Should We Do Capsule Reading? Tech Gastrointest Endosc. 8(4):146-148.

Logan R (2010). Faecal calprotectin for the diagnosis of inflammatory bowel disease. BMJ. 341:c3636.

MacKay RS, Jacobson B (1957). Endoradiosonde. Nature;179(4572):1239-40

Maeda M, Hiraishi H (2014). Efficacy of video capsule endoscopy with flexible spectral imaging color enhancement at setting 3 for differential diagnosis of red spots in the small bowel. Dig Endosc. 26(2):228-231.

Mao R, Xiao YL, Gao X, Chen BL, He Y, Yang L, et al. (2012). Fecal calprotectin in predicting relapse of inflammatory bowel diseases: A meta-analysis of prospective studies. Inflamm Bowel Dis. 18(100:1894-1899.

Matsumura T, Arai M, Sato T, Nakagawa T, Maruoka D, Tsuboi M, et al. (2012). Efficacy of computed image modification of capsule endoscopy in patients with obscure gastrointestinal bleeding. World J Gastrointest Endosc. 4(9):421-428.

Metzger YC, Adler SN, Bar-Gil Shitrit A, Koslowsky B, Bjarnason I (2009). Comparison of a new PillCam™ SB2 video capsule versus the standard PillCam™ SB for detection of small bowel disease. Reports in Medical Imaging. 2:7-11.

Misangyi VF, LePine JA, Algina J, Goeddeke F (2006). The adequacy of repeated-measures regression for multilevel research: comparisons with repeated-measures ANOVA, multivariate repeated-measures ANOVA, and multilevel modeling across various multilevel research designs. Organ Res Methods. 9(1):5-28.

Mishkin DS, Chuttani R, Croffie J, Disario J, Liu J, Shah R, et al. (2006). ASGE Technology Status Evaluation Report: Wireless capsule endoscopy. Gastrointest Endosc. 63(4):539-545.

Mur-Artal R, Montiel JM, Tardos JD (2015). ORB-SLAM: a versatile and accurate monocular SLAM system. IEEE Transactions on Robotics. 31: 1147-1163.

Neumann H, Fry LC, Bellutti M, Malfertheiner P, Mönkemüller K (2009). Double-balloon enteroscopy-assisted virtual chromoendoscopy for small-bowel disorders: a case series. Endoscopy. 41(5):468-471.

Niv Y, Ilani S, Levi Z, Hershkowitz M, Niv E, Fireman Z, et al. (2012). Validation of the Capsule Endoscopy Crohn's Disease Activity Index (CECDAI or Niv score): a multicenter prospective study. Endoscopy. 44(1):21-26.

Olsen PA, Fossmark R, Qvigstad G (2015). Fecal calprotectin in patients with suspected small bowel disease–a selection tool for small bowel capsule endoscopy? Scand J Gastroenterol. 50(3):272-277.

Omori T, Hara T, Sakasai S, Kambayashi H, Murasugi S, Ito A, et al. Does the PillCam SB3 capsule endoscopy system improve image reading efficiency irrespective of experience? A pilot study. Endosc Int Open. 6(6):E669-E675.

Pennazio M, Spada C, Eliakim R Keuchel M, May A, Mulder CJ, et al. (2015). Small-bowel capsule endoscopy and device-assisted enteroscopy for diagnosis and treatment of small-bowel disorders: European Society of Gastrointestinal Endoscopy (ESGE) Clinical Guideline. Endoscopy. 47(4):352-376.

Pohl J, Aschmoneit I, Schuhmann S, Ell C (2010). Computed image modification for enhancement of small-bowel surface structures at video capsule endoscopy. Endoscopy. 42(6):490-492.

Pont-Tuset J, Marques F (2016). Supervised evaluation of image segmentation and object proposal techniques. IEEE Trans Pattern Anal Mach Intell. 38(7): 1465-1478.

Postgate A, Despott E, Burling D, Gupta A, Phillips R, O'Beirne J, et al. (2008). Significant small-bowel lesions detected by alternative diagnostic modalities after negative capsule endoscopy. Gastrointest Endosc. 68(6):1209-1214.

Rimbaș M, Negreanu L, Ciobanu L, Benguș A, Spada C, Băicuș CR (2015). Is virtual chromoendoscopy useful in the evaluation of subtle ulcerative small-bowel lesions detected by video capsule endoscopy? Endosc Int Open. 3(6):E615-20.

Rimbaș M, Zahiu DCM, Voiosu AM, Voiosu TA, Zlate AA, Dinu R, et al. (2016). Usefulness of virtual chromoendoscopy in the evaluation of subtle small bowel ulcerative lesions by endoscopists with no experience in videocapsule. Endosc Int Open. 4(5):E508-514.

Rondonotti E, Herrerias JM, Pennazio M, Caunedo A, Mascarenhas-Saraiva M, deFranchis R, et al. (2005). Complications, limitations, and failures of capsule endoscopy: A review of 733 cases. Gastrointest Endosc. 62(5):712-716.

Rondonotti E, Koulaouzidis A, Karargyris A, Giannakou A, Fini L, Soncini M, et al (2015). Utility of 3-dimensional image reconstruction in the diagnosis of small-bowel masses in capsule endoscopy (with video). Gastrointest Endosc. 80(4):642-651.

Rondonotti E, Spada C, Adler S, May A, Despott EJ, Koulaouzidis A, et al. (2018). Small-bowel capsule endoscopy and device-assisted enteroscopy for diagnosis and treatment of small-bowel disorders: European Society of Gastrointestinal Endoscopy (ESGE) Technical Review. Endoscopy. 50(4):423-446.

Rosa B, Moreira MJ, Rebelo A, Cotter J (2012). Lewis Score: a useful clinical tool for patients with suspected Crohn's Disease submitted to capsule endoscopy. J Crohns Colitis. 6(6):692-697.

Røseth AG (2003). Determination of faecal calprotectin, a novel marker of organic gastrointestinal disorders. Dig Liver Dis. 35(9):607-609.

Rosten E, Drummond T (2006). Machine learning for high-speed corner detection. Computer Vision–ECCV 2006. 430-443.

Ryu CB, Song J-Y, Lee MS, Shim CS (2013). Mo1670 Does capsule endoscopy with alice improves visibility of small bowel lesions? Gastrointest Endosc. 77:AB466.

Sakai E, Endo H, Kato S, Matsuura T, Tomeno W, Taniguchi L, et al (2012). Capsule endoscopy with flexible spectral imaging color enhancement reduces the bile pigment effect and improves the detectability of small bowel lesions. BMC Gastroenterol 2012. 12:83.

Sakata S, Grove PM, Stevenson ARL, Hewett DG (2016). The impact of three-dimensional imaging on polyp detection during colonoscopy: a proof of concept study. Gut. 65(5):730-731.

Sato Y, Sagawa T, Hirakawa M, Ohnuma H, Osuga T, Okagawa Y, et al. (2014). Clinical utility of capsule endoscopy with flexible spectral imaging color enhacement for diagnosis of small bowel lesions. Endosc Int Open. 2(2):E80-87.

Sandler RS, Everhart JE, Donowitz M, Adams E, Cronin K, Goodman C, et al. (2002). The burden of selected digestive diseases in the United States. Gastroenterology. 122(5):1500-1511.

Saurin JC, Delvaux M, Gaudin JL, Fassler I, Villarejo J, Vahedi K, et al. (2003). Diagnostic value of endoscopic capsule in patients with obscure digestive bleeding: Blinded comparison with video push-enteroscopy. Endoscopy. 35(7):576-584.

Selby WS, Prakoso E (2011). The inability to visualize the ampulla of Vater is an inherent limitation of capsule endoscopy. Eur J Gastroenterol Hepatol. 23(1):101-103.

Sipponen T, Haapamäki J, Savilahti E, Alfthan H, Hämäläinen E, Rautiainen H, et al. (2012). Fecal calprotectin and S100A12 have low utility in prediction of small bowel Crohn's disease detected by wireless capsule endoscopy. Scand J Gastroenterol. 47(7):778-784.

Sipponen T (2013). Diagnostics and prognostics of inflammatory bowel disease with fecal neutrophil-derived biomarkers calprotectin and lactoferrin. Dig Dis. 31(3-4):336-344.

Sipponen T, Kolho KL (2015). Fecal calprotectin in diagnosis and clinical assessment of inflammatory bowel disease. Scand J Gastroenterol. 50(1):74-80.

Sliker LJ, Ciuti G (2014). Flexible and capsule endoscopy for screening, diagnosis and treatment. Expert Rev Med Devices. 11(6):649-666.

Spada C, Hassan C, Costamagna G (2011). Virtual chromoendoscopy: Will it play a role in capsule endoscopy? Dig Liver Dis. 43(12):927-928.

Spyrou E, Iakovidis DK (2014). Video-based Measurements for Wireless Capsule Endoscope Tracking. Meas Sci Technol. 25(1):14.

Spyrou E, Iakovidis DK, Niafas S, Koulaouzidis A (2015). Comparative assessment of feature extraction methods for visual odometry in wireless capsule endoscopy. Comput Biol Med. 65:297-307.

Stawczyk-Eder K, Eder P, Lykowska-Szuber L, Krela-Kazmierczak I, Klimczak K, Szymczak A, et al. (2015). Is faecal calprotectin equally useful in all Crohn's disease locations? A prospective, comparative study. Arch Med Sci. 11(2):353-361.

Steffenssen MW, Al-Najami I, Baatrup G (2019). Patient-reported minor adverse events after colonoscopy: a systematic review. Acta Oncol. 58(sup1):S22-S28.

Summerton CB, Longlands MG, Wiener K, Shreeve DR (2002). Faecal calprotectin: a marker of inflammation throughout the intestinal tract. Eur J Gastroenterol Hepatol. 14(8):841-845.

Than TD, Alici G, Zhou H, Li W (2012). A review of localization systems for robotic endoscopic capsules. IEEE Trans Biomed Eng. 59(9): 2387-2399.

Van der Sommen F, Zinger S, Curvers WL, Bisschops R, Pech O, Weusten BL, et al. (2016). Computer-aided detection of early neoplastic lesions in Barrett's esophagus. Endoscopy 2016; 48(7):617-624.

van Rheenen PF, Van de Vijver E, Fidler V (2010). Faecal calprotectin for screening of patients with suspected inflammatory bowel disease: diagnostic meta-analysis. BMJ. 341:c3369.

Van Rijn JC, Reitsma JB, Stoker J, Bossuyt PM, van Deventer SJ, Dekker E (2006). Polyp miss rate determined by tandem colonoscopy: A systematic review. Am J Gastroenterol. 101(2): 343-350.

Vasilakakis M, Koulaouzidis A, Yung DE, Plevris JN, Toth E, Iakovidis DK (2019). Follow-up on: optimizing lesion detection in small bowel capsule endoscopy and beyond: from present problems to future solutions. Expert Rev Gastroenterol Hepatol. 13(2):129-141.

Vasilakakis MD, Koulaouzidis A, Marlicz W, Iakovidis DK (2020). The future of capsule endoscopy in clinical practice: from diagnostic to therapeutic experimental prototype capsules. doi: https://doi.org/10.5114/pg.2019.87528. [Epub ahead of print] date: 2019-09-04.

Visentini-Scarzanella M, Stoyanov D, Yang G-Z (2012). Metric depth recovery from monocular images using Shape-from-Shading and specularities. In: 2012 19th IEEE International Conference on Image Processing 2012. 25-28.

Whiting PF, Rutjes AWS, Westwood ME, Mallett S, Deeks JJ, Reitsma JB (2011). Quadas-2: a revised tool for the quality assessment of diagnostic accuracy studies. Ann Intern Med. 155(8): 529-536.

Yung DE, Sykes C, Koulaouzidis A (2017). The validity of suspected blood indicator software in capsule endoscopy: a systematic review and meta-analysis. Expert Rev Gastroenterol Hepatol. 11(1):43-51.

Zagorowicz ES, Pietrzak AM, Wronska E Pachlewski J, Rutkowski P, Kraszewska E, et al. (2013). Small bowel tumors detected and missed during capsule endoscopy: Single center experience. World J Gastroenterol. 19(47):9043-9048.

Zheng Y, Hawkins L, Wolff J, Goloubeva O, Goldberg E (2012). Detection of lesions during capsule endoscopy: physician performance is disappointing. Am J Gastroenterol.107(4):554-560.

Paper I

Dig Dis Sci (2016) 61:2033–2040
DOI 10.1007/s10620-016-4104-7

ORIGINAL ARTICLE

Association Between Fecal Calprotectin Levels and Small-bowel Inflammation Score in Capsule Endoscopy: A Multicenter Retrospective Study

Anastasios Koulaouzidis[1] · Taina Sipponen[2] · Artur Nemeth[3] · Richard Makins[4] · Uri Kopylov[5] · Moshe Nadler[6] · Andry Giannakou[7] · Diana E. Yung[1] · Gabriele Wurm Johansson[3] · Leonidas Bartzis[1] · Henrik Thorlacius[8] · Ernest G. Seidman[5] · Rami Eliakim[6] · John N. Plevris[1] · Ervin Toth[3]

Received: 2 November 2015 / Accepted: 28 February 2016 / Published online: 23 March 2016

Abstract
Background Accurate inflammation reporting in capsule endoscopy (CE) is important for diagnosis and monitoring of treatment of inflammatory bowel disease (IBD). Fecal calprotectin (FC) is a highly specific biomarker of gut inflammation. Lewis score (LS) was developed to standardize quantification of inflammation in small-bowel (SB) CE images.
Goals Multicenter retrospective study aiming to investigate correlation between LS and FC in a large group of patients undergoing CE for suspected or known small-bowel IBD, and to develop a model for prediction of CE results (LS) based on FC levels.
Study Five academic centers and a district general hospital offering CE in UK, Finland, Sweden, Canada, and Israel. In total, 333 patients were recruited. They had small-bowel CE and FC done within 3 months.
Results Overall, correlation between FC and LS was weak (r_s: 0.232, $P < 0.001$). When two clinically significant FC thresholds (100 and 250 μg/g) were examined, the r_s between FC and LS was 0.247 (weak) and 0.337 (moderate), respectively ($P = 0.307$). For clinically significant ($LS \geq 135$) or negative ($LS < 135$) for SB inflammation, ROC curves gave an optimum cutoff point of FC 76 μg/g with sensitivity 0.59 and specificity 0.41.
Limitations: Retrospective design.
Conclusions LS appears to show low correlation with FC as well as other serology markers of inflammation. FC does not appear to be a reliable biomarker for significant small-bowel inflammation. Nevertheless, FC level ≥ 76 μg/g may be associated with appreciable visual inflammation on small-bowel CE in patients with negative prior diagnostic workup.

Keywords Capsule endoscopy · Fecal calprotectin · Lewis score · Small-bowel inflammation · Monocyte count · C-reactive protein · Multicenter study

✉ Diana E. Yung
diana.e.yung@gmail.com

[1] Endoscopy Unit, Centre for Liver and Digestive Disorders, The Royal Infirmary of Edinburgh, 51 Little France Crescent, Edinburgh, UK

[2] Department of Gastroenterology, University of Helsinki and Helsinki University Hospital, Helsinki, Finland

[3] Department of Gastroenterology, Skåne University Hospital, Lund University, Malmö, Sweden

[4] Department of Gastroenterology, Gloucestershire Hospitals NHS Foundation Trust, Cheltenham, UK

[5] Division of Gastroenterology, McGill University Health Center, Montreal, QC, Canada

[6] Department of Gastroenterology, Sheba Medical Center, Sackler School of Medicine, Tel-Aviv University, Tel-Aviv, Israel

[7] Faculty of Economics and Management, Open University of Cyprus, Nicosia, Cyprus

[8] Department of Surgery, Skåne University Hospital, Lund University, Malmö, Sweden

Introduction

Capsule endoscopy (CE) is the prime modality for accurate, non-invasive, and pain-free investigation of the small bowel [1]. In order to standardize reporting of small-bowel inflammation using CE, two scoring indices have been developed: the Lewis score (LS) and the Capsule Endoscopy Crohn's Disease Activity Index (CECDAI) [2–4]. Both scores are based on parameters and descriptors of

inflammatory change and have been externally validated in several reports [5–8]. However, they are of limited discriminatory ability, and it is still unclear how accurately they measure the degree of mucosal inflammation [6, 9].

Calprotectin was first isolated from human granulocyte cells by Fagerhol et al. [10]. Calprotectin is a major component of the cytosol of neutrophils and, to a lesser extent, monocytes and activated macrophages, released in feces upon leukocyte and epithelial activation [11–13]. In the presence of calcium, calprotectin is resistant to degradation and stable in feces at room temperature for up to 7 days [11, 14]. Fecal calprotectin (FC) 'leaks' into the gut lumen through inflamed mucosa therefore reflecting the amount of leukocyte cell activation, migration, and death [15]. Although FC is not disease specific, a recent meta-analysis showed an excellent correlation of FC with the severity of mucosal inflammation. At a cutoff level of 100 μg/g, FC can distinguish inflammatory bowel disease (IBD) from non-inflammatory conditions [16]. Therefore, many experts consider FC a reliable and highly specific biomarker of inflammation [9, 11]. There are conflicting reports suggesting that the correlation between FC and mucosal inflammation may be weaker in small-bowel inflammation in comparison with the colon. Monoclonal, polyclonal, and combination ELISA (quantitative), and bedside immune-chromatographic (semiquantitative) methods have been developed (and validated) for FC measurement [12].

Recently, we showed that measurement of FC levels prior to referral for CE is a useful tool to select patients with possible small-bowel IBD [17]. In this single-center study, FC > 100 μg/g is good predictor of positive small-bowel CE findings, while FC > 200 μg/g was associated with higher CE diagnostic yield (65 %) and confirmed small-bowel inflammation in 50 % of cases. Hence, it is reasonable to consider that strong correlation should exist between FC levels and LS [7–9]. However, in a separate cohort of patients with suspected, isolated small-bowel disease, LS showed strong correlation with FC at levels <100 μg/g [8]. The overall correlation between FC and LS is moderate at best [18]. This is certainly consistent with the high-negative predictive value (NPV) of FC [9]. Nonetheless, in individuals with higher FC levels, LS does not correlate well, and this can have impact on both patient selection for CE as well as with final outcomes.

The primary aim of this multicenter, retrospective study was to investigate the correlation between LS and FC in a larger group of patients who underwent CE for suspected or known small-bowel IBD.

Our secondary aim was to develop a model for prediction of CE results (LS) based on FC levels.

Materials and Methods

Patients and CE Procedure

This was a retrospective, multicenter study. The study cohort included all consecutive patients who underwent small-bowel CE in five academic referral centers (UK, Finland, Sweden, Canada, and Israel) and a large district general hospital (UK), from January 2010 to December 2013, with clinical suspicion of IBD or for IBD reassessment. Patients having normal ileocolonoscopy, without histological confirmation of Crohn's Disease (CD) on any biopsy material examined, were also eligible. A FC measurement within 3 months from the time of CE was considered necessary for inclusion. The absence of a bidirectional digestive endoscopy in the preceding period (up to a year before CE) was considered an exclusion criterion. Other causes of raised CRP or monocytes were excluded following review of patient case notes. Clinical and demographic data on age, gender, and CE indications were extracted from the patients' files and/or electronic hospital records. A small part of the UK and Swedish data may have been used in a previous publication [25].

The CE was performed with PillCam®SB2/SB3 (Given® Imaging Ltd, Yokneam, Israel) and MiroCam® (IntroMedic Co, Seoul, South Korea), according to local hospital protocols. Technical characteristics of these systems can be found elsewhere in the literature [19, 20]. Bowel preparation, where used, was polyethylene glycol (PEG) 2 or 4 lt. Prokinetics, where used, was in the form of domperidone (5–10 mg orally) and/or metoclopramide (10 mg intramuscularly) [21].

Fecal Calprotectin, C-Reactive Protein, and Monocyte Count

FC was measured with monoclonal/polyclonal ELISA (CALPRO AS, Lysaker, Norway; reference range 0–50 μg/g) or immune-chromatographic assay (Buhlmann's Quantum Blue, Basel, Switzerland; reference range: normal < 50 μg/g; "gray zone" 51–99 μg/g; positive > 100 μg/g) [11]. For the purpose of further statistical analysis, where FC < 20 μg/g, i.e., undetectable, the value 0 was used; for the semi-quantitative assays, for values >300 μg/g, the 300 μg/g was used. The C-reactive protein (CRP) and monocyte count were normal across sites if levels were <5 and <0.8 ng/l, respectively.

Lewis Score Calculation

All videos were reviewed by experienced CE readers (AK, TS, AN, ET, RM, GW, ES and RE). LS was calculated using the integrated LS Calculator (*RAPID*®, Given® Imaging Ltd, Yokneam, Israel) under white light or blue mode review [22]; where the calculator was not available

(MiroView®, IntroMedic Co, Seoul, South Korea), the calculation was performed manually. LS is based on the number and distribution of intestinal segments with villous edema, ulceration, and stenosis. To calculate the LS, the small bowel is first divided into equal transit thirds (tertiles). The final LS represents the highest tertile or the score with stenosis, if demonstrated [23]. Eventually, the LS allows small-bowel inflammatory activity to be classified into three grades: (1) normal or clinically insignificant mucosal inflammatory change (LS $<$ 135); (2) mild disease (135 $\leq$ LS $<$ 790); and (3) moderate-to-severe disease (LS $\geq$ 790) [2, 5, 6]. The CE date, FC measurement date, and time difference in days between the two was also calculated [8].

Statistical Analysis

Baseline quantitative data are presented as median and inter-quartiles range (IQR). For nominal variables, the Chi-square test or Fisher's exact test were used as appropriate. Student's t test was used for quantitative variables with normal distribution. Spearman's rank correlation coefficient (rho; r_s) was used to assess the correlation between LS and FC. The strength of correlation was defined as follows: r_s values $\leq$0.1 were considered to denote no correlation; 0.1–0.3 weak to modest; 0.3–0.49 moderate; 0.5–0.79 strong; and, $\geq$0.8 very strong correlation [24].

In order to detect the association between FS and LS adjusted for other factors, a multivariate linear regression analysis was used. The initial model contained age and monocyte count as adjustment factors of time lag between FC measurement and small-bowel CE. The model was subjected to a backwards elimination procedure using a multivariate linear regression analysis using the likelihood ratio test. A two-tailed probability (P) value $<$ 0.05 was considered to be statistically significant. In addition, a receiver operating characteristic (ROC) analysis was conducted in order to determine the optimum cutoff point of FC results using the dichotomization of LS as explained in the previous paragraph. Statistical analyses were carried out in R statistical package.

Ethics Consideration

This study was conducted in accordance with local research ethics guidelines. After review by the local ethics committee(s), further specific ethical review and approval was not required, as the study was considered a service evaluation/clinical audit based on previously collected clinical data, with no additional patient intervention, obtained as part of regular clinical care.

Results

Patients and Capsule Endoscopy Data

In the aforementioned period, 333 (119M/214F; median age: 41 years; IQR: 25) patients who fulfilled the study inclusion criteria were referred for CE due to clinical suspicion of small-bowel IBD (n = 287; 98M/189F; median age: 41 years; IQR: 26) or suspicion of small-bowel inflammation reactivation in patients with known CD (n = 46; 21M/25F; median age: 34.5 years; IQR: 24). Two different small-bowel CE systems were used (PillCam®SB: 150/MiroCam®: 183); in three patients the capsule endoscope (2 PillCamSB®, 1 MiroCam®) was retained in the stomach for the entire period of the recording, hence no LS data were available. These cases were excluded from further analysis. Symptoms were mainly diarrhea, anemia, weight loss, and/or abdominal pain, Table 1.

Fecal Calprotectin

Clinically Important FC Thresholds

FC measurements were performed with a quantitative ELISA in 280 patients and with semiquantitative assays in the remainder (n = 50). Overall, for the entire dataset (n = 330), correlation between FC and LS was weak (r_s: 0.232, P $<$ 0.001). When the two clinically significant FC thresholds of 100 and 250 μg/g were examined [11, 17], irrespective of the FC assay used, the r_s between FC and LS for the two threshold levels was 0.247 (weak) and 0.337 (moderate), respectively (P = 0.307). The median values (with range; IQR) for FC, LS and the time interval between FC measurement and small-bowel CE were 90 (15,255; 240) μg/g, and 0 (0,337.5; 337.5) and 0 (0,62.75; 62.75) days, respectively. Furthermore, no LS/FC correlation difference was recorded between the two small-bowel CE systems, (P = 0.118).

In the quantitative FC (ELISA) subgroup (n = 280), the correlation between FC and LS was moderate (r_s: 0.385, P: 0.0), as previously shown [8, 25]. The median values (with range; IQR) for FC, LS, and the time interval between FC measurement and small-bowel CE were 28 μg/g (9,220; 211), and 0 (0,339.75; 339.75) and 14.5 days (0,46.75; 46.75), respectively. In this subgroup, 150 CE were performed with MiroCam® and the remainder (n = 130) with PillCam®SB. No statistical difference between FC levels (100.37 ± 191.24 vs 90.71 μg/g; P = 0.649), time interval between FC/CE (28.4 ± 39.4 vs 20.63 ± 29.5 days; P = 0.059), prokinetic use (P = 0.547), or bowel prep use (P = 0.717) between the two CE subgroups was noted, Table 2a, b.

Table 1 Indications for referral for CE

Indication	Number of patients (% of total)
Diarrhea	112 (33.6)
Abdominal pain	104 (31.2)
Iron deficiency anemia	62 (18.6)
Raised FC	26 (7.8)
Weight loss	23 (6.9)
OGIB	19 (5.7)
Abnormal radiological investigations	11 (3.3)
Background of celiac disease, autoimmune disease or IBD	11 (3.3)
Nutritional deficiencies/malabsorption, e.g., B12/folate, albumin	9 (2.7)
Family history of IBD	6 (1.8)
Perianal fistula	6 (1.8)

Please note that numbers do not add up to study size of 333 as many patients had more than one indication for referral

FC fecal calprotectin, *IBD* inflammatory bowel disease

Table 2 Breakdown of results by subgroup

(a) Comparison of subgroups

	Quantitative FC	Semiquantitative FC
N	280	50
Median FC (μg/g) (range IQR)	28 (9–220; 211)	145 (105.75–300; 194.25)
Median LS (range IQR)	0 (0–339.75; 339.75)	135 (0–287; 287)
Median time from FC to CE (days) (range IQR)	14.5 (0–46.75; 46.75)	25 (0–474; 474)

(b) Comparison of MiroCam® vs. PillCam® SB2 subgroups in the quantitative FC group

	MiroCam®	PillCam®SB2	*P* value
N	150	130	
Median FC (μg/g, SD)	100.37 ± 191.24	90.71 ± 166.1	0.547
Time from FC to SBCE (days, SD)	28.4 ± 39.4	20.63 ± 29.5	0.059
Prokinetic use	55	42	0.547
Bowel prep used	54	42	0.717

FC fecal calprotectin, *IQR* inter-quartile range, *LS* Lewis score, *SD* standard deviation, *SBCE* small-bowel capsule endoscopy

In the subgroup of semiquantitative FC ($n = 50$), there was no correlation between FC and LS (r_s: −0.130, *P*: 0.377). In this subgroup, the median values (with range and IQR) for FC and LS were 145 μg/g (105.75,300; 194.25), 135 (0,287; 287), respectively. PillCam®SB was used in 18 and MiroCam® in 32 patients. Furthermore, the median interval between small-bowel CE and FC was 25 days (0–474; 474) (i.e., not significantly different from the quantitative FC group; $P = 0.07$).

Monocytes and CRP

The median (range; IQR) monocyte and CRP counts were 0.535 (0.41, 0.72; 0.31) and 7 (3,15; 12), respectively. The correlation between monocyte count and LS was weakly negative (r_s: −0.019, *P*: 0.732), while the relevant value for CRP was r_s: −0.095, *P*: 0.086. It has been reported that the CRP/monocyte ratio represents the acute phase of inflammation [26]. There were 73 complete datasets (ratio, FC and LS) with measurements obtained ±7 days around the CE (median: 0 days, IQR: 0 days). The median value of the ratio was 12 (5.21, 24.47; 24.25), and the correlation of the ratio with FC and LS was r_s: 0.14 (*P*: 0.235) and r_s: 0.02 (*P*: 0.865), respectively.

Model Creation

In order to investigate the potential association between LS and FC, both variables were log-transformed. The final model for the association of LS and FC was found to be:

$$\log(\mathrm{LS}+1) = -1.05 - 0.0087 \times \text{time lag simplistic} + 1.0471 \times \log(\mathrm{FC}+1)$$

Other predictors such as age ($P = 0.902$) and monocyte count ($P = 0.805$) were eliminated from the initial model during the backwards elimination procedure. The results of the final model are provided in Table 3, where the intercept ($P = 0.269$) was kept as it was found that the normality of the residuals was violated when this was removed. Furthermore, the model is interpreted as an increase of 1 point in FC gives an increase of 1.0471 in log(LS + 1) (95 % CI: 0.679; 1.415). The latter translates to a 0.389 points increase in LS (95 % CI: 0.159; 0.832) for a constant FC/CE time lag simplicity of zero. Also an increase of 1 point in FC/CE time lag gives a decrease of −0.0087 (95 % CI: −0.016; −0.001) in log(LS + 1).

Optimum Cutoff Point of FC

The analysis using ROC curves gave that the dichotomization of LS at 135 for clinically significant (LS ≥ 135) or negative (LS < 135) for SB inflammation gave an optimum cutoff point of FC 76 at μg/g with sensitivity 0.59 and specificity 0.41.

Discussion

FC level in the stool is directly proportional to neutrophils in the intestinal lumen; therefore, its use as biomarker of enteric inflammation and neoplastic lesions has been proposed. One of the main indications for CE is the direct visualization of the extent, location, and severity of small-bowel inflammation [23]. Others suggest that FC could discriminate between organic and functional intestinal pathology and allow selection of patients who are more likely to benefit from a colonoscopy [16]. Recently, we hypothesized that FC can be used as selection tool for performing CE in patients with continuing clinical suspicion for small-bowel IBD, despite preliminary negative diagnostic workup [17]. Currently, healthcare systems worldwide are under significant economic strain to provide high-quality care with shrivelling budgets [26, 27]. Therefore, increasing the diagnostic yield of patient workup with inexpensive, accurate, non-invasive investigations, has multiple benefits [13, 28].

In the present study, retrospective data on FC, monocyte count, and CRP paired with CE findings (LS was used to quantify small-bowel inflammation in an objective way) [2, 8] were collected from patients with clinical suspicion of small-bowel IBD ($n = 287$), out of which 3% had ileitis on colonoscopy but inconclusive histology, from high-volume CE centers (UKx2, Finland, Sweden, Canada, Israel). The remainder ($n = 43$) had a history of known CD and were referred for small-bowel assessment with CE. Experienced CE reviewers reported the CE results at each site for the purpose of clinical care/need using white light and/or blue mode (depending on preference per reviewer) [6, 22]. In 84.8 % of cases, FC was measured using a commercially available ELISA (range 0–50 μg/g). In these patients, CE was performed using the PillCam®SB in 46.4 % of cases; the remainder was performed with MiroCam®. Based on the CE system used, the two patient subgroups were equivalent in terms of FC levels, time interval between FC measurement and performance of CE, and procedural factors for small-bowel CE such as the use of a prokinetic and/or a bowel purge (or not). Therefore, we are able to confirm that the lack of an integrated calculator in the MiroCam® proprietary software (MiroView®) notwithstanding the calculated LS had the same correlation with FC levels.

Another finding of this study is low correlation of FC with monocyte count, CRP, CRP/monocyte, and LS, Table 2. The former has been previously shown in studies from our group [15, 25]. Furthermore, elevated CRP, FC, or the combination of both was poorly correlated with detectable small-bowel inflammation [18, 29]. Nevertheless, it is worth noting that when the threshold level of significant SB inflammation, as denoted by LS was shifted from 135 to 350, the correlation of FC and LS was similar at r_s: 0.07 (P: 0.637) and 0.09 (P: 0.696) for the suspected and known CD group, respectively.

Others have recently confirmed strong inter-observer agreement in determining LS in CE [6]. Höög et al. [7], in a cohort of 30 patients, showed that there was a significant persistent correlation between endoscopic inflammation and FC (at study inclusion and at a year's follow-up). More recently, Olsen et al showed that the proportion of patients with findings on small-bowel CE increased with increasing FC [30]. Nevertheless, in their cohort, a positive FC (≥50 mg/kg) had a sensitivity, specificity, positive predictive value (PPV), and negative predictive value (NPV)

Table 3 Model for the association of FC and LS

Model	Coefficients	SE	*t* value	Pr(> |t|)	95 % CI
Intercept	−1.0513	0.9466	−1.11	0.269	−2.907; 0.804
Time lag FC/CE	−0.0087	0.0039	−2.24	0.027	−0.016; −0.001
Log (FC + 1)	1.0471	0.1876	5.58	<0.001	0.679; 1.415

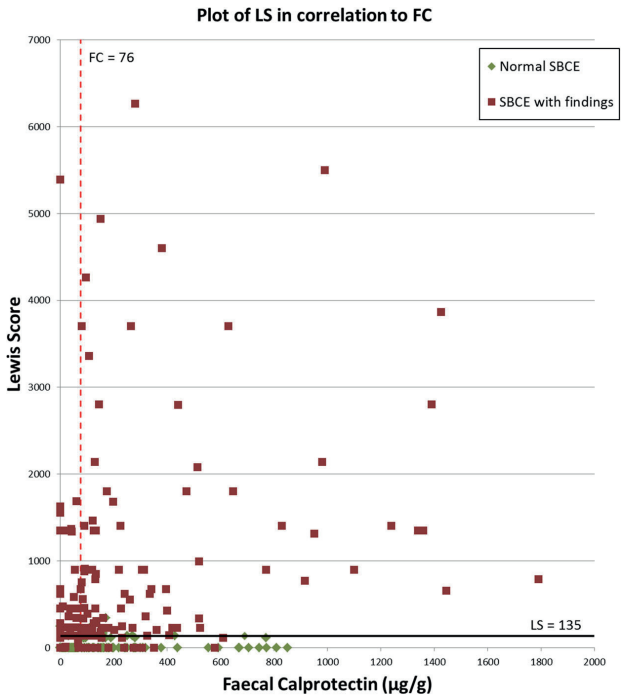

Fig. 1 Plot of LS in correlation to FC

of 54.2, 69.9, 43.3, and 78.2 %, respectively. The correlation of FC values with presence of active small-bowel inflammation as detected by magnetic resonance enterography (MRE) was similar to that of CE [29].

Limitations of this study include the lack of formal assessment of the extent of mucosal visualization. As not all patients underwent bowel preparation prior to CE, it is possible that LS could in part be altered by the degree of small-bowel visualization. However, there is a lack of data on LS correlation with the quality of SB visualization. The fact that the CEs in this study were each reviewed by a single reviewer only, despite substantial cumulative experience in CE, could be a further limitation leading to lower diagnostic yield.

This study did not establish a correlation between endoscopic severity, as measured by the LS, and FC or other biomarkers of inflammation. This is likely to reflect deficiencies of the scoring system [25] as well as the study's inherent limitations such as the cutoff level selected. FC may also be a marker of subclinical inflammation; Gisbert and McNicholl [31] found that FC was higher in asymptomatic first-degree relatives of patients with IBD, and FC has been seen to predict relapse in asymptomatic or quiescent CD [32]. Another study has found that FC does not reliably distinguish IBD from malignancy [33], which may—indirectly—suggest that FC is not as good at distinguishing generalized inflammation from foci of inflammation. Furthermore, some studies show FC is a more reliable indicator of colonic than SB inflammation, i.e., usefulness of FC varies with location of inflammation within the gut, and there is difficulty in establishing correlation due to the heterogeneity of presentations in CD [34, 35]. Figure 1 shows how LS is generally low in patients with normal SBCE; however these patients have a wide range of FC. Conversely our study also had patients with low FC but high LS, which could have been indicative of a single large lesion, such as an isolated stenosis, yielding a diagnosis. Further prospective studies should be performed to investigate the difference between the equivocal results of our study and other studies which show positive correlation between LS and FC.

Our findings suggest that in patients with strong clinical suspicion of small-bowel CD and negative bidirectional endoscopy, CE should not be limited to patients with elevated biomarkers only. Especially, CRP and the ratio in particular were not associated with SB inflammation on CE. Moreover, the correlation was moderate for FC, and if this biomarker was used to guide the decision to perform

CE, at least 40 % of patients will be misdiagnosed. However, the use of single FC measurement per patient for the purpose of this study [36, 37], its retrospective nature and the use of different laboratories and FC kits should be considered as additional limitations of this study. Nevertheless, FC $\geq$ 76 μg/g may be associated with appreciable inflammation on CE in patients with negative prior diagnostic workup.

Acknowledgments The authors thank Pirkko Tuukkala and Virpi Pelkonen (both with Helsinki University Central Hospital, Finland) for their invaluable help with the data collection.

Authors' contributions All authors contributed to data collection. Dr. A Koulaouzidis created the first draft. All authors critically reviewed the document and provided changes. All authors approved the final version of the article, including the authorship list.

Compliance with ethical standards

Conflict of interest Dr. Koulaouzidis received an Given Imaging Ltd/ESGE Ltd research Grant in 2011. He has also accepted material support for research from SynMedUK Ltd. Dr. Seidman has received in-kind research support from Given Imaging/Medtronic Inc., 2011–2015. Rami Eliakim received consultation fees from Given Imaging. The rest of the authors have no disclosure to make.

Competing interests None.

Patient consent None.

Ethics approval Clinical Audit Department at the Royal Infirmary of Edinburgh.

References

1. Koulaouzidis A, Iakovidis DK, Karargyris A, Rondonotti E. Wireless endoscopy in 2020: Will it still be a capsule? *World J Gastroenterol*. 2015;21:5119–5130. doi:10.3748/wjg.v21.i17.5119.
2. Gralnek IM, Defranchis R, Seidman E, Leighton JA, Legnani P, Lewis BS. Development of a capsule endoscopy scoring index for small bowel mucosal inflammatory change. *Aliment Pharmacol Ther*. 2008;27:146–154.
3. Gal E, Geller A, Fraser G, Levi Z, Niv Y. Assessment and validation of the new capsule endoscopy Crohn's disease activity index (CECDAI). *Dig Dis Sci*. 2008;53:1933–1937.
4. Niv Y, Ilani S, Levi Z, et al. Validation of the Capsule Endoscopy Crohn's Disease Activity Index (CECDAI or Niv score): a multicenter prospective study. *Endoscopy*. 2012;44:21–26. doi:10.1055/s-0031-1291385.
5. Rosa B, Moreira MJ, Rebelo A, Cotter J. Lewis Score: a useful clinical tool for patients with suspected Crohn's Disease submitted to capsule endoscopy. *J Crohns Colitis*. 2012;6:692–697. doi:10.1016/j.crohns.2011.12.002.
6. Cotter J. Dias de Castro F, Magalhães J, Moreira MJ, Rosa B. Validation of the Lewis score for the evaluation of small-bowel Crohn's disease activity. *Endoscopy*. 2015;47:330–335. doi:10.1055/s-0034-1390894.
7. Höög CM, Bark LÅ, Broström O, Sjöqvist U. Capsule endoscopic findings correlate with fecal calprotectin and C-reactive protein in patients with suspected small-bowel Crohn's disease. *Scand J Gastroenterol*. 2014;49:1084–1090. doi:10.3109/00365521.2014.920915.
8. Koulaouzidis A, Douglas S, Plevris JN. Lewis score correlates more closely with fecal calprotectin than Capsule Endoscopy Crohn's Disease Activity Index. *Dig Dis Sci*. 2012;57:987–993. doi:10.1007/s10620-011-1956-8.
9. Gurudu SR, Leighton JA. Correlation of two capsule endoscopy scoring systems with fecal calprotectin: does it really matter? *Dig Dis Sci*. 2012;57:827–829. doi:10.1007/s10620-012-2079-6.
10. Fagerhol MK, Dale I, Andersson T. Release and quantitation of a leukocyte derived protein (L1). *Scand J Haematol*. 1980;24:393–398.
11. Sipponen T. Diagnostics and prognostics of inflammatory bowel disease with fecal neutrophil-derived biomarkers calprotectin and lactoferrin. *Dig Dis*. 2013;31:336–344. doi:10.1159/000354689.
12. Sipponen T, Kolho KL. Fecal calprotectin in diagnosis and clinical assessment of inflammatory bowel disease. *Scand J Gastroenterol*. 2015;50:74–80. doi:10.3109/00365521.2014.987809.
13. Logan R. Faecal calprotectin for the diagnosis of inflammatory bowel disease. *BMJ*. 2010;341:c3636. doi:10.1136/bmj.c3636.
14. Røseth AG. Determination of faecal calprotectin, a novel marker of organic gastrointestinal disorders. *Dig Liver Dis*. 2003;35:607–609.
15. Sipponen T, Haapamäki J, Savilahti E, et al. Fecal calprotectin and S100A12 have low utility in prediction of small bowel Crohn's disease detected by wireless capsule endoscopy. *Scand J Gastroenterol*. 2012;47:778–784. doi:10.3109/00365521.2012.677953.
16. van Rheenen PF, Van de Vijver E, Fidler V. Faecal calprotectin for screening of patients with suspected inflammatory bowel disease: diagnostic meta-analysis. *BMJ*. 2010;341:c3369. doi:10.1136/bmj.c3369.
17. Koulaouzidis A, Douglas S, Rogers MA, Arnott ID, Plevris JN. Fecal calprotectin: a selection tool for small bowel capsule endoscopy in suspected IBD with prior negative bi-directional endoscopy. *Scand J Gastroenterol*. 2011;46:561–566. doi:10.3109/00365521.2011.551835.
18. Kopylov U, Nemeth A, Koulaouzidis A, et al. Small bowel capsule endoscopy in the management of established Crohn's disease: clinical impact, safety, and correlation with inflammatory biomarkers. *Inflamm Bowel Dis*. 2015;21:93–100. doi:10.1097/MIB.0000000000000255.
19. Sliker LJ, Ciuti G. Flexible and capsule endoscopy for screening, diagnosis and treatment. *Expert Rev Med Devices*. 2014;11:649–666. doi:10.1586/17434440.2014.941809.
20. Koulaouzidis A, Iakovidis DK, Karargyris A, Plevris JN. Optimizing lesion detection in small-bowel capsule endoscopy: from present problems to future solutions. *Expert Rev Gastroenterol Hepatol*. 2015;9:217–235. doi:10.1586/17474124.2014.952281.
21. Koulaouzidis A, Giannakou A, Yung DE, Dabos KJ, Plevris JN. Do prokinetics influence the completion rate in small-bowel capsule endoscopy? A systematic review and meta-analysis. *Curr Med Res Opin*. 2013;29:1171–1185. doi:10.1185/03007995.2013.818532.
22. Koulaouzidis A, Douglas S, Plevris JN. Blue mode does not offer any benefit over white light when calculating Lewis score in small-bowel capsule endoscopy. *World J Gastrointest Endosc*. 2012;4:33–37. doi:10.4253/wjge.v4.i2.33.
23. Kopylov U, Seidman EG. Role of capsule endoscopy in inflammatory bowel disease. *World J Gastroenterol*. 2014;20:1155–1164. doi:10.3748/wjg.v20.i5.1155.
24. http://www.statstutor.ac.uk/resources/uploaded/spearmans.pdf.
25. Koulaouzidis A, Nemeth A, Johansson GW, Toth E. Dissecting Lewis score under the light of fecal calprotectin; an analysis of correlation of score components with calprotectin levels in capsule endoscopy. *Ann Gastroenterol*. 2015;28:259–264.

26. Bolanis P, Stauropoulou E. The ratio of monocytes to CRP correlates to symptoms induction time of the acute phase. 37 Annual Panhellenic Medical congress, May 2011.
27. Sandler RS, Everhart JE, Donowitz M, et al. The burden of selected digestive diseases in the United States. *Gastroenterology*. 2002;122:1500–1511.
28. Dhaliwal A, Zeino Z, Tomkins C, et al. Utility of faecal calprotectin in inflammatory bowel disease (IBD): what cut-offs should we apply? *Frontline Gastroenterol*. 2015;6:14–19.
29. Kopylov U, Yablecovitch D, Lahat A, et al. Detection of small bowel mucosal healing and deep remission in patients with known small bowel Crohn's disease using biomarkers, capsule endoscopy and imaging. *Am J Gastroenterol*. 2015;110:1316–1323.
30. Olsen PA, Fossmark R, Qvigstad G. Fecal calprotectin in patients with suspected small bowel disease–a selection tool for small bowel capsule endoscopy? *Scand J Gastroenterol*. 2015;50:272–277. doi:10.3109/00365521.2014.1003395.
31. Gisbert JP, McNicholl AG. Questions and answers on the role of faecal calprotectin as a biological marker in inflammatory bowel disease. *Dig Liver Dis*. 2009;41:56–66.
32. Mao R, Xiao YL, Gao X, et al. Fecal calprotectin in predicting relapse of inflammatory bowel diseases: A meta-analysis of prospective studies. *Inflamm Bowel Dis*. 2012;18:1894–1899.
33. Summerton CB, Longlands MG, Wiener K, et al. Faecal calprotectin: a marker of inflammation throughout the intestinal tract. *Eur J Gastroenterol Hepatol*. 2002;14:841–845.
34. Stawczyk-Eder K, Eder P, Lykowska-Szuber L, et al. Is faecal calprotectin equally useful in all Crohn's disease locations? A prospective, comparative study. *AMS*. 2015;1:353–361.
35. Jensen MD, Kjeldsen J, Nathan T. Fecal calprotectin is equally sensitive in Crohn's disease affecting the small bowel and colon. *Scand J Gastroenterol*. 2011;46:694–700.
36. Lasson A, Stotzer PO, Öhman L, Isaksson S, Sapnara M, Strid H. The intra-individual variability of faecal calprotectin: a prospective study in patients with active ulcerative colitis. *J Crohns Colitis*. 2015;9:26–32. doi:10.1016/j.crohns.2014.06.002.
37. Calafat M, Cabré E, Mañosa M, Lobatón T, Marín L, Domènech E. High within-day variability of fecal calprotectin levels in patients with active ulcerative colitis: what is the best timing for stool sampling? *Inflamm Bowel Dis*. 2015;21:1072–1076. doi:10.1097/MIB.0000000000000349.

Paper II

Thieme

Clinical validity of flexible spectral imaging color enhancement (FICE) in small-bowel capsule endoscopy: a systematic review and meta-analysis

Authors

Diana E. Yung[1], Pedro Boal Carvalho[2], Andry Giannakou[3], Uri Kopylov[4], Bruno Rosa[2], Emanuele Rondonotti[5], Ervin Toth[6], John N. Plevris[1], Anastasios Koulaouzidis[1]

Institutions

1 Centre for Liver and Digestive Disorders, Royal Infirmary of Edinburgh, Edinburgh, United Kingdom
2 Gastroenterology Department, Hospital Senhora da Oliveira, Guimarães, Portugal
3 Faculty of Economics and Management, Open University of Cyprus, Nicosia, Cyprus
4 Department of Gastroenterology, Sheba Medical Center, Tel Hashomer, and Sackler School of Medicine, Tel Aviv University, Israel
5 Gastroenterology Unit, Valduce Hospital, Como, Italy
6 Department of Gastroenterology, Skåne University Hospital, Lund University, Malmö, Sweden

Bibliography

DOI http://dx.doi.org/10.1055/s-0042-122015
Published online: 25.1.2017 | Endoscopy 2017; 49: 258–269

ISSN 0013-726X

Corresponding author

Diana E. Yung, MD, Royal Infirmary of Edinburgh, Endoscopy Unit, 51 Little France Crescent, Edinburgh EH16 4SA, United Kingdom
diana.e.yung@gmail.com

ABSTRACT

Patients and methods A comprehensive literature search was conducted. We measured pooled rate of lesion visualization improvement and improvement in lesion detection comparing FICE settings 1 – 3 and WLE, for angioectasias and ulcers/erosions. Pooled results were derived using the random-effects model because of high heterogeneity as measured by I^2. Repeated-measures analysis of variance (ANOVA) was used to measure differences in lesion detection between WLE and the three FICE modes.

Results 13 studies were analyzed. All studies used the PillCam SB 1 and/or SB 2 devices. Most used experienced readers. Improvement in delineation had been investigated in 4 studies; in the 3 studies entered into the meta-analysis, using FICE setting 1, 89 % of angioectasias and 45 % of ulcer/erosions were considered to show improved delineation. For FICE settings 2 and 3, small proportions of images showed improved delineation. Heterogeneity of studies was high with $I^2 > 90$ % in 4/6 analyses. Lesion detection had been investigated in 10 studies; meta-analysis included 5 studies. Lesion detection did not differ significantly between any of the FICE modes and WLE.

Conclusions Overall, the use of the three FICE modes did not significantly improve delineation or detection rate in SBCE. In pigmented lesions, FICE setting 1 performed better in lesion delineation and detection.

Introduction

Capsule endoscopy has been proven to have a positive impact on diagnosis and management in patients with small-bowel disorders [1, 2]. The diagnostic yield of small-bowel capsule endoscopy (SBCE) has been shown to be superior to that of other diagnostic modalities [1]. However, the overall positive diagnostic yield of capsule endoscopy for small-bowel disease remains at about 60 % [3]. Furthermore, because of its inherent technological limitations capsule endoscopy continues to miss lesions such as ulcers and submucosal tumors and/or other small-bowel malignancies [4 – 7]. Current capsule endoscopy devices are passively propelled by gut peristalsis. Consequently, visualization of the entire length of the small bowel is achieved in 80 % – 90 % of patients [2, 8], while the uncontrollability of the movement of the capsule leads to up to 30 % of discrete lesions being missed, especially when there is increased gut motility and/or an image of a lesion is captured in only one frame [9, 10]. Developments in software for image and video processing might help to increase the diagnostic yield of SBCE.

Flexible spectral imaging color enhancement (FICE; also Fujinon Intelligent Chromo Endoscopy; Fujinon, Saitama, Japan) is a digital processing algorithm which takes white-light endoscopy (WLE) images and mathematically processes the image by emphasizing certain ranges of wavelengths. Three single-wavelength images can be selected and assigned to red, green, and blue (RGB) monitor inputs to display a composite color-enhanced image (▶ **Table 1**, ▶ **Fig. 1**) [11]. FICE virtual chromoendoscopy is hypothesized to thereby enhance surface patterns, improving visualization and detection of mucosal lesions [12]. FICE has been applied to endoscopy of the upper and lower gastrointestinal (GI) tract, as well as in double-balloon enteroscopy [13, 14], with the aim of increasing detection of neoplastic lesions. However, there remains a lack of conclusive evidence for its clinical effectiveness in enhancing lesion visualization and detection in SBCE [1].

▶ **Table 1** Flexible spectral imaging color enhancement (FICE) settings 1 – 3 used in small-bowel capsule endoscopy: wavelengths in nanometers (nm) for the red, green, and blue channels.

	Red	Green	Blue
Mode			
FICE 1	595	540	535
FICE 2	420	520	530
FICE 3	595	570	415

This review and meta-analysis aims to consolidate existing clinical data on the utility of FICE in improving delineation (i. e., visibility of lesion surface and/or lesion borders which would aid more accurate characterization of the lesion) and detection rate for small-bowel pathological findings in capsule endoscopy as compared to conventional WLE reading.

Methods

A comprehensive literature search was conducted using the PubMed and Embase databases (January 2000 to November 2015). The search was performed on December 12 2015. In order to capture as many full-text articles and abstracts as possible, a broad search strategy was employed, using the terms "capsule endoscopy," "small-bowel," "FICE," and "chromoendoscopy" in various combinations. The initial search was performed with no limitations. Primary selection was based on titles and abstracts; further selection involved reading the full texts of any relevant publications (▶ **Fig. 2**).

For a study to be included in this meta-analysis, the following criteria were considered necessary: (a) complete articles published in English; (b) articles where capsule endoscopy was used to investigate small-bowel pathology only; and (c) articles where one or more of the three FICE modes was used on capsule endoscopy images and/or videos. Lastly, we included studies that investigated: (i) changes in image delineation or (ii) changes in lesion detection, using FICE.

Data extraction and quality control were performed independently by two reviewers (D. Y., P. B. C.). A third reviewer (A. K.), expert in capsule endoscopy and the content material, was involved if there was any uncertainty about the data. When additional data were required, primary (first and/or senior) authors of the specific manuscript(s) were contacted by email with relevant questions.

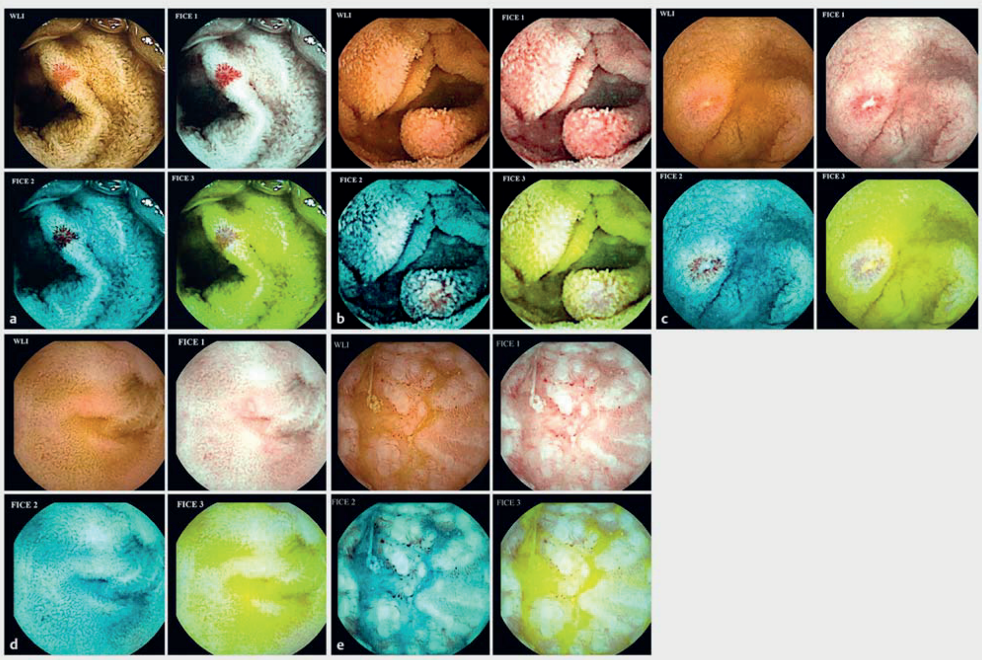

▶ **Fig. 1** Small-bowel pathological findings seen at capsule endoscopy, as visualized with white-light imaging (WLI) and flexible spectral imaging color enhancement (FICE) settings 1 to 3: **a** angioectasia; **b** polyp; **c** ulcer; **d** mucosal erosions; **e** nodular lymphoid hyperplasia. (PillCam SB 2 used for part **b** images; SB 3 for all other images.)

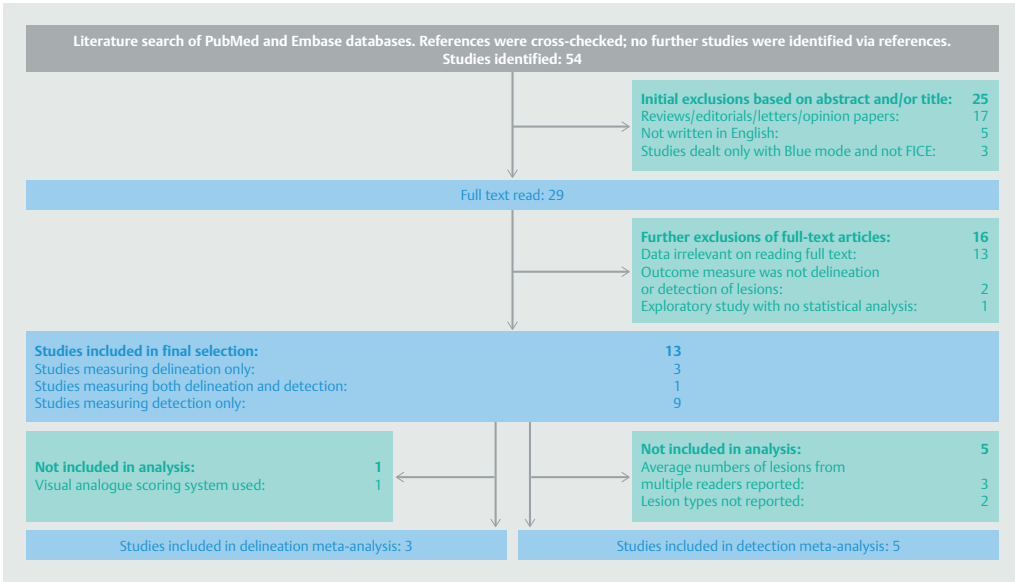

▶ **Fig. 2** Flexible spectral imaging color enhancement (FICE) and improvement of delineation and detection of pathological findings in small-bowel capsule endoscopy: selection of studies for inclusion in meta-analysis.

Outcome measures

Lesion delineation

The outcome measure was the pooled rate of improvement in lesion visualization based on reader rating (individual or average), as measured against the original WLE image for: (a) each of the FICE modes, and (b) the two main pathological findings consistently presented across all studies: angioectasias and small-bowel mucosal ulcers/erosions.

Images where visualization was deemed similar to or worse than with WLE were grouped together as "lack of improvement."

Lesion detection

We analyzed studies where each video was viewed only once by one reader. The outcome measure was whether there was any significant difference between the average number of lesions detected across the three FICE modes and the white-light mode, for angioectasias and mucosal ulcers/erosions.

Statistical analysis

Data on the diagnostic yield of SBCE were extracted, pooled, and analyzed. Pooled results with corresponding 95 % confidence interval (95 %CI) were derived using the fixed-effects model (Mantel – Haenszel method) unless significant heterogeneity was detected, in which case, a random-effects model (DerSimonian – Laird) was used. We used the Q statistic of χ^2 test and I^2 to estimate the heterogeneity of individual studies contributing to the pooled estimate. I^2 values were used to evaluate whether the differences across the studies were greater than could be expected by chance alone. A P value < 0.05 suggests the presence of heterogeneity beyond what could be expected by chance alone. I^2 values of 20 % – 50 % or of > 50 % suggest moderate and high heterogeneity, respectively. Forest plots were constructed for visual display of individual study and pooled results [15].

Repeated-measures analysis of variance (ANOVA) was used to measure the difference in lesion detection between WLE and the three FICE modes based on the findings from the videos in WLE mode and using FICE settings 1 – 3. The F statistic was used to determine significance in repeated-measures ANOVA. P < 0.05 for the F-statistic was considered statistically significant [16]. Statistical analysis was performed by using the Metan package of STATA version 12.1 (StataCorp, College Station, Texas, US).

Assessment of study bias

Methodological quality and potential bias of the included studies was evaluated by using the Quality Assessment of Diagnostic Accuracy Studies (QUADAS) 2 scale [17]. The use of FICE was the "index test" and capsule endoscopy imaging or video review under WLE was taken to be the "reference standard."

Results

The initial search yielded 54 publications (▶ **Fig. 2**) of which 39 were excluded for the following reasons: articles were reviews/editorials/letters/opinion papers (n = 17); data found to be irre-

▶ **Table 2** Lesion delineation with flexible spectral imaging color enhancement (FICE) used in small-bowel capsule endoscopy: summary of studies.

First author Year [ref.]	Country	Capsule endoscopy device	Readers, n	Readers' experience	Images, n	Outcomes for FICE settings (modes) 1 – 3								
						FICE 1			FICE 2			FICE 3		
						Improved	Similar	Worse	Improved	Similar	Worse	Improved	Similar	Worse
Angioectasias														
Krystallis 2011 [21]	UK	PillCam SB1/2	2	1 moderate (>50 VCEs) 1 experienced (>500 VCEs)	18	14	2	2	5	3	9	1	7	10
Imagawa 2011 [13]	Japan	PillCam SB1	5	Not specified	23	20	3	0	20	2	1	1	22	0
Sato 2014 [22]	Japan	PillCam SB1/2	5	Experienced (>100 VCEs)	152	VAS average (SD): 72.7 (5.2)[1]			VAS average (SD): 74.0 (14.9)[1]			VAS average (SD): 58.7 (14.9)[1]		
Cotter 2014 [23]	Portugal	PillCam SB2	2	Experienced (>200 VCEs)	39	38	1	0	38	1	0	18	18	3
Ulcers/erosions														
Krystallis 2011 [21]	UK	PillCam SB1/2	2	1 moderate (>50 VCEs) 1 experienced (>500 VCEs)	60	22	6	32	2	8	50	2	4	54
Imagawa 2011 [13]	Japan	PillCam SB1	5	Not specified	47	26	19	2	12	32	3	0	34	13
Sato 2014 [22]	Japan	PillCam SB1/2	5	Experienced (>100 VCEs)	88	VAS average (SD): 72.9 (5.4)[1]			VAS average (SD): 67.9 (5.7)[1]			VAS average (SD): 53.5 (6.5)[1]		
Cotter 2014 [23]	Portugal	PillCam SB2	2	Experienced (>200 VCEs)	49	31	12	6	28	10	11	12	18	19

VCE, video capsule endoscopy; SD, standard deviation; VAS, visual analogue score.
[1] Outcome measure: average VAS from readers, with positive scoring for "improved" and negative scoring for "worse"; breakdown not specified.

▶ **Table 3** Lesion detection with flexible spectral imaging color enhancement (FICE) used in small-bowel capsule endoscopy: summary of studies.

First author Year [ref.]	Country	Capsule endoscopy device	Readers, n	Readers' experience	Videos, n	Study design	Lesions detected by different modes, n				
							Reference	WLE	FICE 1	FICE 2	FICE 3
Angioectasia											
Imagawa 2011 [24]	Japan	PillCam SB2	2	Experienced (>50 VCEs)	50	1 reader for WLE 1 for FICE	Not available	17	48	45	24
Duque 2012 [25]	Portugal	PillCam SB2	4	Experienced	20	1 reader for WLE 1 for FICE	Not available	32	Not available	35	Not available
Kobayashi 2012 [26]	Japan	PillCam (Not specified)	3	Not specified	24	All videos and modes seen by all readers	Not available	Average (SD) lesions per video: 21 (2.6)	25.7 (SD 3.2)	22.0 (SD 3.0)	22.7 (SD 2.1)
Matsumura 2012 [27]	Japan	PillCam SB1/2	2	Experienced	81	All videos and modes seen by all readers	14	Average (SD) lesions per video: 2 9 (1.5)	2 (SD 1.4)	1.3 (SD 0.5)	4 (SD 1.2)
Sakai 2012 [28]	Japan	PillCam SB2	4	No previous VCE experience	12	Crossover[1]; each video in each mode read once only	60	26	40	38	31
Konishi 2014 [29]	Japan	PillCam SB2	5	Experienced	10	All videos and modes seen by all readers	Not available	Average (SD) lesions per video: 0.58 (0.15)	0.92 (SD 0.2)	0.72 (SD 0.18)	0.74 (SD 0.2)
Sato 2014 [22]	Japan	PillCam SB1/2	3	Experienced (>100 VCEs)	50	Crossover	Not available	17	24	33	18
Boal Carvalho 2016 [30]	Portugal	Not specified	4	Experienced (>100 VCEs)	60	Crossover	54	26	54	Not available	Not available
Ulcers/erosions											
Imagawa 2011 [24]	Japan	PillCam SB2	2	Experienced (>50 VCEs)	50	1 reader for WLE 1 for FICE	Not available	32	40	54	51
Duque 2012 [25]	Portugal	PillCam SB2	4	Experienced	20	1 reader for WLE 1 for FICE	Not available	24	Not available	41	Not available
Kobayashi 2012 [26]	Japan	PillCam (Not specified)	3	(Not specified)	24	All videos and modes seen by all readers	Not available	Average (SD) lesions per video: 14 (0.0)	19.3 (2.3)	15.3 (1.2)	11.3 (4)
Matsumura 2012 [27]	Japan	PillCam SB1/2	2	Experienced	81	All videos and modes seen by all readers	24	Average (SD) lesions per video: 1.9±1.9	3.3 (2.3)	3.6 (3.4)	1.9 (1.2)

▶ **Table 3** (Continuation)

First author Year [ref.]	Country	Capsule endoscopy device	Readers, n	Readers' experience	Videos, n	Study design	Lesions detected by different modes, n				
							Reference	WLE	FICE 1	FICE 2	FICE 3
Sakai, 2012 [28]	Japan	PillCam SB2	4	No previous VCE experience	12	Crossover[1]; each video in each mode read once only	82	38	62	60	20
Konishi 2014 [29]	Japan	PillCam SB2	5	Experienced	10	All videos and modes seen by all readers	Not available	Average (SD) lesions per video: Erosions 3.3 (4.29) Ulcers 1.66 (4.00)	Erosions 8.65 (8.55) Ulcers 4.86 (12.9)	Erosions 11.94 (15.12) Ulcers 5.6 (14.51)	Erosions 3.54 (4.03) Ulcers 2.9 (8.50)
Sato 2014 [22]	Japan	PillCam SB1/2	3	Experienced (>100 VCEs)	50	Crossover	Not available	28	22	41	24
Boal Carvalho 2016 [30]	Portugal	Not specified	4	Experienced (>100 VCEs)	60	Crossover	17	15	17	Not available	Not available
Studies where Saurin score used (lesion types not specified)											
Gupta 2011 [31]	Belgium	PillCam SB2	2	Moderate experience (about 70 VCEs)	60	Crossover	131 P0[2]: 15 P1: 41 P2: 75	Not available	All 3 FICE modes used together P0[2]: 20 (reader 1), 27 (reader 2) P1: 37 (reader 1), 55 (reader 2) P2: 60 (reader 1), 72 (reader 2)		
Dias de Castro 2015 [32]	Portugal	PillCam SB1/2	1	Experienced (>200 VCEs)	42	1 reader for all videos	All videos initially "negative" for cause of GI bleeding	Not available	14 remained negative: 19 P1[2] lesions 2 P2 lesions 7 both P1 & P2	Not available	Not available

WLE white light endoscopy; VCE, video capsule endoscopy; SD, standard deviation; GI, gastrointestinal.

[1] Example of "crossover" study: Reader 1 viewed group A of videos under WLE only, then group B under FICE 1. Reader 2 viewed group A under FICE 1 only and group B under WLE only. Therefore each video is seen by only 1 reader for each mode.

[2] P0, P1, P2: Saurin score [33].

▶ **Table 4** Flexible spectral imaging color enhancement (FICE) used in small-bowel capsule endoscopy: pooled proportion of images with "improved" visualization of pathological findings.

	FICE mode, proportion (95 %CI)		
	FICE 1	FICE 2	FICE 3
Angioectasias (n = 80)	0.89 (0.69 – 1.08)	0.43 (0.32 – 0.54)[1]	0.05 (0.04 – 0.07)[1]
Ulcers/erosions (n = 156)	0.45 (0.38 – 0.52)[1]	0.04 (0.03 – 0.05)[1]	0.04 (0.03 – 0.04)[1]

CI, confidence interval
[1] Denotes statistically significant heterogeneity.

levant on reading of full text (n = 13); not in English language (n = 5); studies dealt exclusively with other chromoendoscopy techniques (e. g. Blue mode) and not FICE (n = 3); outcome measure not delineation or detection of lesions (n = 2) [18, 19]; study was exploratory with no statistical analysis (n = 1) [20].

Eventually, 13 studies were included in the final review, with 8 then included in meta-analyses (▶ **Table 2** and ▶ **Table 3**) [13, 21 – 32]. The countries of origin for the studies were: Japan (n = 7) [13, 22, 24, 26 – 29], Portugal (n = 4) [23, 25, 30, 32], Belgium (n = 1) [31], and the United Kingdom (n = 1) [21]. All studies were conducted using PillCam SB 1 and/or 2 (Medtronic, Minnesota, USA) and most used experienced readers, usually defined as having read > 100 capsule endoscopies.

Two sets of studies were identified as coming from the same hospitals. Two studies from the Imagawa et al. group were used for two separate analyses, one for delineation [13] and one for detection [24]. Therefore there was no overlap in the data used in these two studies. Another three studies [23, 30, 32] were carried out by the same group of researchers at the same center; these have been confirmed by present study author P. B. C. to have used completely separate patient groups with no overlap.

Lesion delineation

Improvement in delineation of capsule endoscopy images of lesions was investigated in 4 studies [13, 21 – 23]. Of these, 1 study [22] was excluded from further analysis: the use of a visual analogue scoring system meant that the results could not be entered into the meta-analysis.

Only the use of FICE setting 1 on images of angioectasias appeared to produce a higher rate of improved delineation, with 89 % of images considered improved, whereas 45 % of images

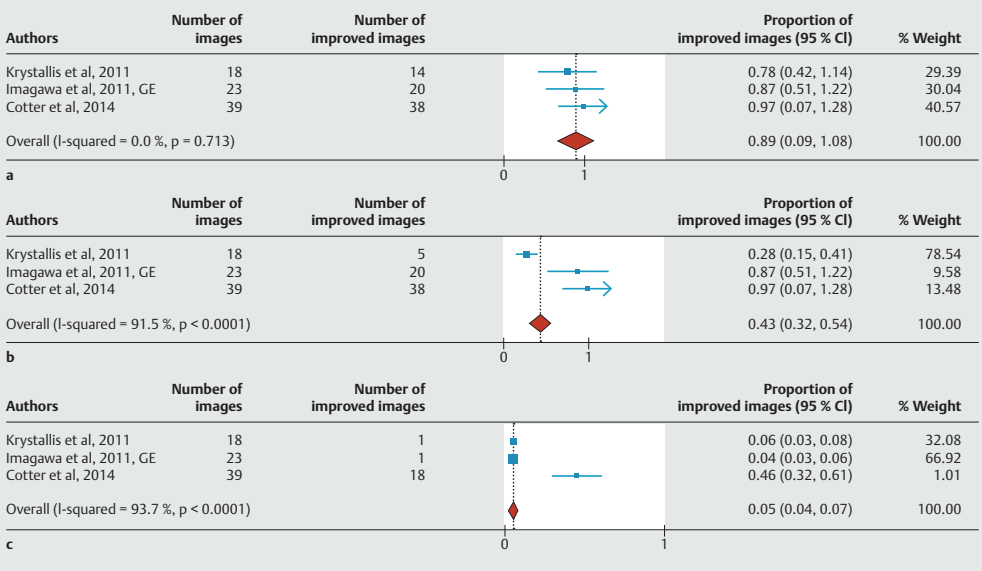

▶ **Fig. 3** Pooled proportions of images of angioectasias considered to show "improved" visualization under flexible spectral imaging color enhancement (FICE): **a** FICE 1; **b** FICE 2; **c** FICE 3.

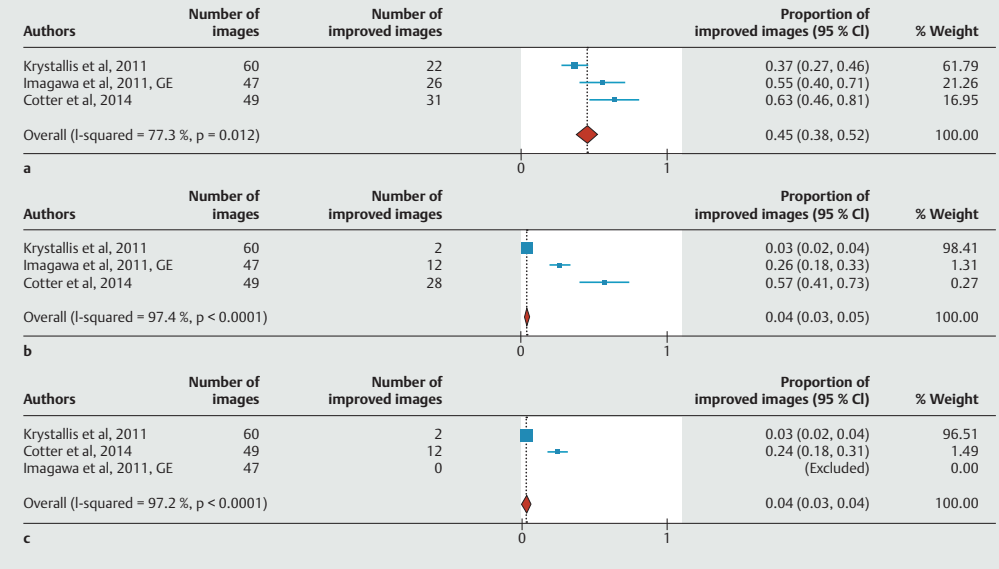

▶ **Fig. 4** Pooled proportions of images of ulcers/erosions considered to show "improved" visualization under flexible spectral imaging color enhancement (FICE): **a** FICE 1; **b** FICE 2; **c** FICE 3.

of ulcers/erosions were considered improved using FICE 1. FICE 2 improved delineation in 43 % of images of angioectasias. For images of angioectasias in FICE 3 and images of ulcers/erosions in FICE 2 and 3, negligible proportions of images were considered to show improved delineation (▶ **Table 4**, ▶ **Fig. 3** and ▶ **Fig. 4**).

Heterogeneity of studies was high with $I^2 > 90$ % in 4/6 analyses carried out.

Lesion detection

A total of 10 studies [22, 24 – 32] measured improvement in detection of lesions. Of these, 3 studies [26, 27, 29] reported results as average numbers of lesions identified by multiple readers; the present study did not allow those studies to be included in analysis. Another 2 studies [31, 32] did not give results by types of lesions, instead using the Saurin score [33]; these were not analyzed as the numbers of angioectasias and ulcers/erosions remained unknown.

The remaining 5 studies were designed such that each video in each mode was viewed only once by one reader over the course of the study [22, 24, 25, 28, 30]. Therefore these were entered into the analysis, and ANOVA was carried out using the average number of lesions detected per video (▶ **Table 5**). The *F* statistic for the difference in detection of angioectasias and ulcers/erosions in the three FICE modes compared to WLE had a *P* value > 0.05 for both types of lesions, showing that the detection of these lesions did not differ significantly between any of the FICE modes and WLE.

Quality analysis

The majority of the included studies were of high quality (▶ **Table 6**). The main risk of bias identified was recall bias in studies where videos were viewed in more than one mode by the same reviewer.

Discussion

The technological limitations of capsule endoscopy mean that a targeted focus on small-bowel lesions or areas of interest is not possible; any focus occurs only for the amount of time allowed by bowel movement and propulsion [34]. Furthermore, despite substantial improvement in recent years in image quality, particularly in image resolution, the image pixelation of SBCE remains disappointingly low [35, 36], especially when compared with that of conventional high definition flexible endoscopes. This often leads to suboptimal lesion imaging and therefore potentially reduces the diagnostic yield of capsule endoscopy [10, 37]. Software such as FICE, already established in conventional GI endoscopy, has been integrated into commercially available capsule endoscopy reviewing software (RAPID; Medtronic) in order to increase visualization and detection rate for small-bowel findings. However, clinical opinion and anecdotal evidence remain divided as to the usefulness of FICE and other chromoendoscopy software for capsule endoscopy review [38].

In this meta-analysis, all three FICE modes failed to show much significant improvement in visualization of small-bowel pathology. However, only with FICE setting 1 a pooled propor-

▶ **Table 5** Difference in lesion detection between white-light endoscopy (WLE) and the three flexible spectral imaging color enhancement (FICE) modes: repeated-measures analysis of variance (ANOVA), for angioectasias and ulcers/erosions.

	Sum of squares	Degrees of freedom	Mean sum of squares	*F* statistic and result
Angioectasias				
Between	1.02	3	0.34	1.146
Within	20.179	16	1.261	
▪ Error	3.559	12	0.297	
▪ Subjects	16.62	4	4.155	
Total	21.199	19		
				Critical value: 3.4903 Result: Do not reject the null hypothesis. Conclusion: The compared groups do not differ significantly: $F(3,12) = 1.146$, $P > 0.05$.
Ulcers/erosions				
Between	3.467	3	1.156	1.723
Within	41.093	16	2.568	
▪ Error	8.052	12	0.671	
▪ Subjects	33.041	4	8.26	
Total	44.56	19		
				Critical value: 3.4903 Result: Do not reject the null hypothesis. Conclusion: The compared groups do not differ significantly: $F(3,12) = 1.723$, $P > 0.05$.

tion of 89 % of angioectasia images were considered "improved" (defined as improved visualization aiding lesion characterization and enhanced delineation of lesion surface and/or borders), compared with the WLE images. For small-bowel angioectasias viewed under FICE 2 and 3, and for mucosal ulcers/erosions viewed under all three FICE modes, less than 50 % of the images were considered to be improved. In fact, for FICE modes 2 and 3, there was close to no improvement in ulcer/erosion visualization compared with WLE imaging. Therefore, FICE performs well when there is significant color alteration of the lesion, as in angioectasias. This could be partially explained by the fact that pigmented fluids, such as blood and bile, allow the greatest contrast with small-bowel mucosa even under WLE. FICE further enhances this contrast, leading to subjective improvement in visualization, whereas it may not perform as well with nonpigmented lesions [24, 38]. The most recent technical report from the American Society for Gastrointestinal Endoscopy (ASGE) states that there is no evidence for an optimal FICE mode for tissue diagnosis and differentiation in conventional GI endoscopy [11].

Spada et al. defined the clinical usefulness of chromoendoscopy in terms of the following criteria: (i) improvement in lesion detection rate; (ii) improvement in lesion delineation; and (iii) ability to identify lesions which require treatment [38]. In fact, the number of lesions detected on full video reading may be a more accurate index of the clinical performance of FICE against WLE because of the unambiguous binary response of pathological finding detected or not. This approach is likely to be less subjective than assessment of delineation improvement as determined by human readers. The majority of pathological findings at capsule endoscopy consist of vascular lesions and mucosal defects. Polypoid or submucosal lesions, where software tools can enhance diagnostic accuracy [39, 40], are found less frequently.

Therefore, in the video studies examining detection rate for small-bowel pathological findings, FICE did not produce any significant improvement in the detection of angioectasias or mucosal ulcers/erosions, compared to WLE video reading. Furthermore, all these studies relied on human vision and perception for detection of lesions. Psychological studies have shown that the color red produces a stronger reaction in humans, therefore human readers may be more likely to pick up on red-colored lesions (i. e., blood or vascular lesions) compared to the more muted green and brown tones in FICE modes 2 and 3 [41 – 43]. By extension, narrow band imaging (NBI) is based on the penetration properties of different wavelengths of light corresponding to the two light absorption peaks of hemoglobin, so as to increase the contrast and therefore visibility of vasculature [11]. Our results are similar overall to those achieved in studies on the use of virtual chromoendoscopy in conventional GI endoscopy: the value of virtual chromoendoscopy lies in aiding lesion visualization and therefore characterization, rather

▶ **Table 6** Flexible spectral imaging color enhancement (FICE) used in small-bowel capsule endoscopy. Quality of studies and risk of bias as determined by Quality Assessment of Diagnostic Accuracy Studies (QUADAS) 2 scale; + denotes low risk of bias, ? denotes unclear risk of bias.

First author year [ref.]	Item						
	1: Risk of bias in patient selection?	2: Representative patient spectrum?	3: Risk of bias in conduct or interpretation of index test (use of FICE)?	4: Applicability of index test to review question?	5: Risk of bias from conduct or interpretation of reference standard (WLE and/or expert review)?	6: Is the use of the reference standard appropriate?	7: Risk of bias from flow/timing of study?
Gupta 2011 [31]	+	+	+	?	+	+	+
Imagawa 2011 [13]	?	+	+	+	+	+	+
Imagawa 2011 [24]	?	+	?	+	+	+	?
Krystallis 2011 [21]	+	+	?	+	+	+	+
Duque 2012 [25]	+	+	+	?	+	+	+
Kobayashi 2012 [26]	?	+	?	+	+	+	+
Matsumura 2012 [27]	?	+	?	+	+	+	+
Sakai 2012 [28]	?	+	+	?	+	+	+
Cotter 2014 [23]	+	+	?	+	+	+	?
Konishi 2014 [29]	+	+	+	+	+	+	+
Sato 2014 [22]	?	+	+	+	+	+	+
Boal Carvalho 2015 [30]	+	+	+	+	?	+	+
Dias de Castro 2015 [32]	?	+	+	?	+	+	+

WLE, white-light endoscopy.

than in increasing detection [11]. Although all but one of the studies included in this meta-analysis involved experienced capsule endoscopy readers, a recent study found that using FICE and Blue mode also helped beginner capsule endoscopy readers to better characterize lesions [44], suggesting that this may be an area warranting further investigation.

This review and meta-analysis has focused on FICE alone, although other virtual chromoendoscopy software is currently available such as Blue mode [11] and Augmented Live-body Image Color-Spectrum Enhancement (ALICE) (Intromedic, Seoul, South Korea) [45]. However, the existing body of data is small and too heterogeneous for more systematic analysis. Although in this meta-analysis FICE has not performed as well as hoped, there is some evidence for the usefulness of other forms of virtual chromoendoscopy, mainly Blue mode [21, 46 – 48]. Current evidence suggests that Blue mode remains a more user-friendly form of virtual chromoendoscopy which can be applied with ease to full video readings. However, none of the existing studies have shown a meaningful increase in diagnostic yield with Blue mode. Interestingly, Aihara et al. presented a study using image-enhanced capsule endoscopy which increased the contrast between the surrounding mucosa and lesions such as vascular or inflammatory lesions or polyps. They reported that the effects of this contrast capsule are similar to those of NBI in conventional GI endoscopy [49]. The only study using ALICE, presented as an abstract, reported improved visibility of flat and depressed small-bowel lesions [45].

Limitations of this meta-analysis include, firstly, the heterogeneity of current published studies investigating the usefulness of FICE, as shown by the high I^2 values. These studies varied considerably in terms of study design, selected population, images and videos for analysis, and models of capsule endoscope used with their subsequent effect on technical performance. For instance, differences in the LED specifications between the PillCam versions could vary the image quality and interpretation between studies. The heterogeneity of study design meant that several could not be included in the meta-analysis, thus greatly limiting the sample size. None of the included studies reported whether the readers had been tested for color blindness; it is unclear whether this could influence intraobserver agreement. The majority of the studies included in this meta-analysis also did not specify the size or clinical significance of the lesions, another factor which could influence detection rate.

In conclusion, FICE 1 seems to perform better for pigmented lesions such as angioectasias, both in lesion delineation and detection. However, the evidence is equivocal as to whether FICE 2 and 3 aid SBCE reading. Overall, the use of the three FICE modes did not significantly improve detection rate or the quality of visualization of the most common pathological findings seen on SBCE.

Competing interests

Dr. Koulaouzidis has received an European Society of Gastrointestinal Endoscopy (ESGE) Given Imaging grant and material support for research from SynMed UK. Dr. Toth has received lecture fees from Given Imaging/Medtronic. No other conflict of interest exists for all authors.

References

[1] Koulaouzidis A, Rondonotti E, Karargyris A. Small-bowel capsule endoscopy: A ten-point contemporary review. World J Gastroenterol 2013; 19: 3726 – 3746

[2] Pennazio M, Spada C, Eliakim R et al. Small-bowel capsule endoscopy and device-assisted enteroscopy for diagnosis and treatment of small-bowel disorders: European Society of Gastrointestinal Endoscopy (ESGE) Clinical Guideline. Endoscopy 2015; 47: 352 – 376

[3] Zheng Y, Hawkins L, Wolff J et al. Detection of lesions during capsule endoscopy: physician performance is disappointing. Am J Gastroenterol 2012; 107: 554 – 560

[4] Rondonotti E, Herrerias JM, Pennazio M et al. Complications, limitations, and failures of capsule endoscopy: A review of 733 cases. Gastrointest Endosc 2005; 62: 712 – 716

[5] Chong AKH, Chin BWK, Meredith CG. Clinically significant small-bowel pathology identified by double-balloon enteroscopy but missed by capsule endoscopy. Gastrointest Endosc 2006; 64: 445 – 449

[6] Postgate A, Despott E, Burling D et al. Significant small-bowel lesions detected by alternative diagnostic modalities after negative capsule endoscopy. Gastrointest Endosc 2008; 68: 1209 – 1214

[7] Zagorowicz ES, Pietrzak AM, Wronska E et al. Small bowel tumors detected and missed during capsule endoscopy: Single center experience. World J Gastroenterol 2013; 19: 9043 – 9048

[8] ASGE Technology Committee Wang A, Banerjee S, Barth BA et al. Wireless capsule endoscopy. Gastrointest Endosc; 2013; 78: 805 – 815

[9] Selby WS, Prakoso E. The inability to visualize the ampulla of Vater is an inherent limitation of capsule endoscopy. Eur J Gastroenterol Hepatol 2011; 23: 101 – 103

[10] Koulaouzidis A, Iakovidis DK, Karargyris A et al. Optimizing lesion detection in small-bowel capsule endoscopy: from present problems to future solutions. Expert Rec Gastroenterol Hepatol 2015; 9: 217 – 235

[11] Manfredi MA, Abu Dayyeh BK, Bhat YM et al. Electronic chromoendoscopy. Gastrointest Endosc 2015; 81: 249 – 261

[12] Mishkin DS, Chuttani R, Croffie J et al. ASGE Technology Status Evaluation Report: Wireless capsule endoscopy. Gastrointest Endosc 2006; 63: 539 – 545

[13] Imagawa H, Oka S, Tanaka S et al. Improved visibility of lesions of the small intestine via capsule endoscopy with computed virtual chromoendoscopy. Gastrointest Endosc 2011; 73: 299 – 306

[14] Neumann H, Fry LC, Bellutti M et al. Double-balloon enteroscopy-assisted virtual chromoendoscopy for small-bowel disorders: a case series. Endoscopy 2009; 41: 468 – 471

[15] Higgins JPT, Thompson SG. Quantifying heterogeneity in a meta-analysis. Stat Med 2002; 21: 1539 – 1558

[16] Misangyi VF, LePine JA, Algina J et al. The adequacy of repeated-measures regression for multilevel research: comparisons with repeated-measures ANOVA, multivariate repeated-measures ANOVA, and multilevel modeling across various multilevel research designs. Organ Res Methods 2006; 9: 5 – 28

[17] Whiting PF, Rutjes AWS, Westwood ME et al. Quadas-2: A revised tool for the quality assessment of diagnostic accuracy studies. Ann Intern Med 2011; 155: 529 – 536

[18] Rimbaş M, Negreanu L, Ciobanu L et al. Is virtual chromoendoscopy useful in the evaluation of subtle ulcerative small-bowel lesions detected by video capsule endoscopy? Endosc Int Open 2015; 3: E615 – 620

[19] Maeda M, Hiraishi H. Efficacy of video capsule endoscopy with flexible spectral imaging color enhancement at setting 3 for differential diagnosis of red spots in the small bowel. Dig Endosc 2014; 26: 228 – 231

[20] Pohl J, Aschmoneit I, Schuhmann S et al. Computed image modification for enhancement of small-bowel surface structures at video capsule endoscopy. Endoscopy 2010; 42: 490 – 492

[21] Krystallis C, Koulaouzidis A, Douglas S et al. Chromoendoscopy in small bowel capsule endoscopy: Blue mode or Fuji Intelligent Colour Enhancement? Dig Liver Dis 2011; 43: 953 – 957

[22] Sato Y, Sagawa T, Hirakawa M et al. Clinical utility of capsule endoscopy with flexible spectral imaging color enhacement for diagnosis of small bowel lesions. Endosc Int Open 2014; 2: E80 – 87

[23] Cotter J. Virtual chromoendoscopy in small bowel capsule endoscopy: New light or a cast of shadow? World J Gastrointest Endosc 2014; 6: 359 – 365

[24] Imagawa H, Oka S, Tanaka S et al. Improved detectability of small-bowel lesions via capsule endoscopy with computed virtual chromoendoscopy: A pilot study. Scand J Gastroenterol 2011; 46: 1133 – 1137

[25] Duque G, Almeida N, Figueiredo P et al. Virtual chromoendoscopy can be a useful software tool in capsule endoscopy. Rev Esp Enfermedades Dig 2012; 104: 231 – 236

[26] Kobayashi Y, Watabe H, Yamada A et al. Efficacy of flexible spectral imaging color enhancement on the detection of small intestinal diseases by capsule endoscopy. J Dig Dis 2012; 13: 614 – 620

[27] Matsumura T, Arai M, Sato T et al. Efficacy of computed image modification of capsule endoscopy in patients with obscure gastrointestinal bleeding. World J Gastrointest Endosc 2012; 4: 421 – 428

[28] Sakai E, Endo H, Kato S et al. Capsule endoscopy with flexible spectral imaging color enhancement reduces the bile pigment effect and improves the detectability of small bowel lesions. BMC Gastroenterol 2012; 12: 83

[29] Konishi M, Shibuya T, Mori H et al. Usefulness of flexible spectral imaging color enhancement for the detection and diagnosis of small intestinal lesions found by capsule endoscopy. Scand J Gastroenterol 2014; 49: 501 – 505

[30] Boal Carvalho P, Magalhães J, Dias de Castro F et al. Virtual chromoendoscopy improves the diagnostic yield of small bowel capsule endoscopy in obscure gastrointestinal bleeding. Dig Liver Dis 2016; 48: 172 – 175

[31] Gupta T, Ibrahim M, Deviere J et al. Evaluation of Fujinon intelligent chromo endoscopy-assisted capsule endoscopy in patients with obscure gastroenterology bleeding. World J Gastroenterol 2011; 17: 4590 – 4595

[32] Dias de Castro F, Magalhães J, Boal Carvalho P et al. Improving diagnostic yield in obscure gastrointestinal bleeding – how virtual chromoendoscopy may be the answer. Eur J Gastroenterol Hepatol 2015; 27: 735 – 740

[33] Saurin JC, Delvaux M, Gaudin JL et al. Diagnostic value of endoscopic capsule in patients with obscure digestive bleeding: Blinded comparison with video push-enteroscopy. Endoscopy 2003; 35: 576 – 584

[34] Cass OW. Is half-knowledge worse than ignorance? Gastrointest Endosc 2006; 64: 542 – 543

[35] Ciuti G, Menciassi A, Dario P. Capsule endoscopy: From current achievements to open challenges. IEEE Rev Biomed Eng 2011; 4: 59 – 72

[36] Sliker LJ, Ciuti G. Flexible and capsule endoscopy for screening, diagnosis and treatment. Expert Rev Med Devices 2014; 11: 649 – 666

[37] Hale M, McAlindon ME. Capsule endoscopy as a panenteric diagnostic tool. Br J Surg 2014; 101: 148 – 149

[38] Spada C, Hassan C, Costamagna G. Virtual chromoendoscopy: Will it play a role in capsule endoscopy? Dig Liver Dis 2011; 43: 927 – 928

[39] Girelli CM, Porta P, Colombo E et al. Development of a novel index to discriminate bulge from mass on small-bowel capsule endoscopy. Gastrointest Endosc 2011; 74: 1067 – 1074

[40] Rondonotti E, Koulaouzidis A, Karargyris A et al. Utility of 3-dimensional image reconstruction in the diagnosis of small-bowel masses in capsule endoscopy (with video). Gastrointest Endosc 2015; 80: 642 – 651

[41] Green DG. The contrast sensitivity of the colour mechanisms of the human eye. J Physiol 1968; 196: 415 – 429

[42] Hill RA, Barton RA. Psychology: red enhances human performance in contests. Nature 2005; 435: 293

[43] Ilie A, Ioan S, Zagrean L et al. Better to be red than blue in virtual competition. Cyber Psychol Behav 2008; 11: 375 – 377

[44] Rimbaş M, Zahiu DCM, Voiosu AM et al. Usefulness of virtual chromoendoscopy in the evaluation of subtle small bowel ulcerative lesions by endoscopists with no experience in videocapsule. Endosc Int Open 2016; 4: E508 – 514

[45] Ryu CB, Song J-Y, Lee MS et al. Mo1670 Does capsule endoscopy with alice improves visibility of small bowel lesions? Gastrointest Endosc 2013; 77: AB466

[46] Koulaouzidis A, Smirnidis A, Douglas S et al. QuickView in small-bowel capsule endoscopy is useful in certain clinical settings, but QuickView with Blue Mode is of no additional benefit. Eur J Gastroenterol Hepatol 2012; 24: 1099 – 1104

[47] Abdelaal UM, Morita E, Nouda S et al. Blue mode imaging may improve the detection and visualization of small-bowel lesions: A capsule endoscopy study. Saudi J Gastroenterol 2015; 21: 418 – 422

[48] Koulaouzidis A, Douglas S, Plevris JN. Blue mode does not offer any benefit over white light when calculating Lewis score in small-bowel capsule endoscopy. World J Gastrointest Endosc 2012; 4: 33 – 37

[49] Aihara H, Ikeda K, Tajiri H. Image-enhanced capsule endoscopy based on the diagnosis of vascularity when using a new type of capsule. Gastrointest Endosc 2011; 73: 1274 – 1279

Paper III

KID Project: an internet-based digital video atlas of capsule endoscopy for research purposes

OPEN ACCESS

Authors
Anastasios Koulaouzidis[1], Dimitris K. Iakovidis[2], Diana E. Yung[1], Emanuele Rondonotti[3], Uri Kopylov[4], John N. Plevris[1], Ervin Toth[5], Abraham Eliakim[4,*], Gabrielle Wurm Johansson[5,*], Wojciech Marlicz[6,*], Georgios Mavrogenis[7,*], Artur Nemeth[5,*], Henrik Thorlacius[8,*], Gian Eugenio Tontini[9,*]

Institutions
1 Centre for Liver and Digestive Disorders, The Royal Infirmary of Edinburgh, Edinburgh, UK
2 University of Thessaly, Department of Computer Science and Biomedical Informatics, Volos, Thessaly, Greece
3 Gastroenterology Unit, Valduce Hospital, Como, Italy
4 Department of Gastroenterology, Sheba Medical Center, Tel Hashomer, and Sackler School of Medicine, Tel Aviv University, Tel-Aviv, Israel
5 Department of Gastroenterology, Skåne University Hospital, Lund University, Malmö, Sweden
6 Department of Gastroenterology, Pomeranian Medical University, Szezecin, Poland
7 Gastroenterology and Endoscopy Center of Mytilene, Mytilene, Lesvos, Greece
8 Department of Clinical Sciences, Lund University, Malmö, Sweden
9 Gastroenterology and Digestive Endoscopy Unit, IRCCS Policlinico San Donato, Milan, Italy
* KID working group

submitted 7.9.2016
accepted after revision 6.2.2017

Bibliography
DOI https://doi.org/10.1055/s-0043-105488 |
Endoscopy International Open 2017; 05: E477–E483

ISSN 2364-3722

Corresponding author
Anastasios Koulaouzidis, MD, FECG, FACG, FASGE, The Royal Infirmary of Edinburgh, Endoscopy Unit, 51 Little France Crescent, Edinburgh EH16 4SA, UK
akoulaouzidis@hotmail.com

ABSTRACT

Background and aims Capsule endoscopy (CE) has revolutionized small-bowel (SB) investigation. Computational methods can enhance diagnostic yield (DY); however, incorporating machine learning algorithms (MLAs) into CE reading is difficult as large amounts of image annotations are required for training. Current databases lack graphic annotations of pathologies and cannot be used. A novel database, KID, aims to provide a reference for research and development of medical decision support systems (MDSS) for CE.

Methods Open-source software was used for the KID database. Clinicians contribute anonymized, annotated CE images and videos. Graphic annotations are supported by an open-access annotation tool (Ratsnake). We detail an experiment based on the KID database, examining differences in SB lesion measurement between human readers and a MLA. The Jaccard Index (JI) was used to evaluate similarity between annotations by the MLA and human readers.

Results The MLA performed best in measuring lymphangiectasias with a JI of 81 ± 6 %. The other lesion types were: angioectasias (JI 64 ± 11 %), aphthae (JI 64 ± 8 %), chylous cysts (JI 70 ± 14 %), polypoid lesions (JI 75 ± 21 %), and ulcers (JI 56 ± 9 %).

Conclusion MLA can perform as well as human readers in the measurement of SB angioectasias in white light (WL). Automated lesion measurement is therefore feasible. KID is currently the only open-source CE database developed specifically to aid development of MDSS. Our experiment demonstrates this potential.

Introduction

Capsule endoscopy (CE) has changed the field of small-bowel (SB) investigation [1] with the potential to become a panenteric diagnostic tool [2]. Computational methods incorporated into CE reading software can enhance diagnostic yield (DY) [3]. Several information technology (IT) groups have proposed software for detection of SB lesions/bleeding, reducing reading time, lesion localization, motility assessment, video enhancement and/or data management [1, 3]. Reducing reading time is beneficial, especially in high volume centers. Previous work has shown that readers' experience does not improve detection

of lesions in CE [4]. Therefore, computer-aided detection/diagnosis (CAD) can improve DY.

Despite prolific IT research, incorporating artificial intelligence (AI) systems into CE reading remains difficult [3]. The backbone of AI system development is based on machine learning algorithms (MLAs) for automatic detection, localization, and recognition of pathology in CE images and videos. A large amount of data, in the form of annotations, is required to train MLAs. Semantic annotations describe the content of CE videos and images, whereas graphic annotations are pixel-level labels indicating regions of interest (ROIs) (▶ **Fig.1**). Although there are some online databases [5], these usually include the necessary semantic annotations, but lack graphic annotations of ROIs. Therefore, such material cannot be directly used by IT scientists for intelligent systems' training or as a reference for their evaluation.

A limited number of datasets composed of images with graphic annotations have become available in the context of IT studies [3, 6]. A novel database, KID (κάψουλα interactive database; based on Greek for "capsule") (http://is-innovation.eu/kid/) was developed to fill this gap. It is available online, upon free registration, aiming to provide a reference for research on the development of medical decision support systems (MDSS) for CE, including the study of the performance of human observers in comparison to others and CAD.

Methods

Database

Open-source database (Oracle MySQL; https://www.mysql.com/) and web-gallery development software (Coppermine; http://coppermine-gallery.net/) were used. Software tools for video manipulation and image annotation were added to the KID website. To date, six centers (the KID working group) have contributed anonymized, annotated CE images/videos from various CE models; more than 2500 annotated CE images and 47 videos have been uploaded. These include images of (a) normal CE; (b) vascular lesions including angioectasias and/or bleeding; (c) inflammatory lesions, including mucosal aphthae and ulcers, erythema, cobblestoning, and luminal stenosis; (d) lymphangiectasias; and (e) polypoid lesions (▶ **Fig. 2**).

Image and video standards

Lesion categorization is based on the CE Structured Terminology (CEST) [7]. Contributions are of high quality (original resolution), not distorted by additional compression. For images, the recommended standard is ISO/IEC 15948 PNG (Portable Network Graphics), a popular platform-independent format with lossless compression. Other acceptable standards include: ISO/IEC, 14496-10, MPEG-4, AVC (Advanced Video Coding) and H.264. Supported formats for videos include F4V & FLV (Flash video).

Image annotation

The usefulness of KID relies on image annotations. Semantic and graphic annotations are supported by an open access, platform-independent annotation tool (Ratsnake) [8]. The graphic annotation process is shown in ▶ **Fig. 3** and ▶ **Video 1**. Semantic annotation is done through textual labels, and using standard web ontology language description logics (OWL DL) [9]. The quality of data and annotations submitted to KID are scrutinized by an international scientific committee (http://is-innovation.eu/kid/committee.php); contributions not meeting the aforementioned standards are rejected.

An experiment using the KID database: Computer-aided lesion size measurements based on color image segmentation

A total of 64 images of gastrointestinal lesions taken with MiroCam® (IntroMedic Co., Seoul, Korea) were used. The lesions were: angioectasias (n = 27), lymphangiectasias (n = 9), ulcers (n = 9), chylous cysts (n = 8), polypoid lesions (n = 6), and small-bowel aphthae (n = 5). Graphic annotations made by expert readers (AK, ER, ET; > 2000 CE readings each) were used as lesion surface size reference standards. The images were automatically segmented into two regions: a ROI, i. e. the lesion in question, and the rest of the image. This was performed using the Localized Region-based Active Contour (LRAC) [10] algorithm, which is capable of segmenting regions characterized by heterogeneity in grayscale images; see ▶ **Fig. 4** for a stepwise graphic presentation. The reader initializes the LRAC by defining a circular contour roughly on or around the lesion, starting at a random point in the image. The lesion did not need to be fully included in the initial contour. The algorithm calculates contours based on intensity histogram information (i. e. information on image brightness and intensity) from the regions inside and outside the contour. The calculations are performed locally, around each point along the contour. The algorithm continues to run until the overall similarity of the histograms inside and outside the contour is minimized. In this experiment, we extended the algorithm to the three components of the Commission internationale de l'éclairage-Lab (CIE-Lab) color space representation (instead of the standard RGB) [11]. Components of this space represent lightness (L), which is approximately equivalent to the respective grayscale image, quantity of red ($a > 0$) or quantity of green ($-a > 0$), quantity of yellow ($b > 0$) or quantity of blue ($-b > 0$) of a pixel (▶ **Fig. 5**). ▶ **Fig. 6** shows the results of image segmentation using this algorithm applied to the a component of CIE-Lab, compared to in RGB. The Jaccard Index (JI) [12] was used to assess the similarity of the ROI obtained with the aid of LRAC compared to the graphically annotated ROI obtained by the expert readers (gold standard) per image, i. e. the agreement between the expert human readers and the algorithm. The JI is considered to be the most suitable and popular measure for the assessment of image segmentation algorithms [12]. It quantifies the overlap between two ROIs as the ratio of their intersection to their union with respect to the human readers. Therefore, it is independent from the measurement unit, e. g. pixels^2 or mm^2, used to quantify the measured area. An illustrative example is provided in ▶ **Fig. 7**.

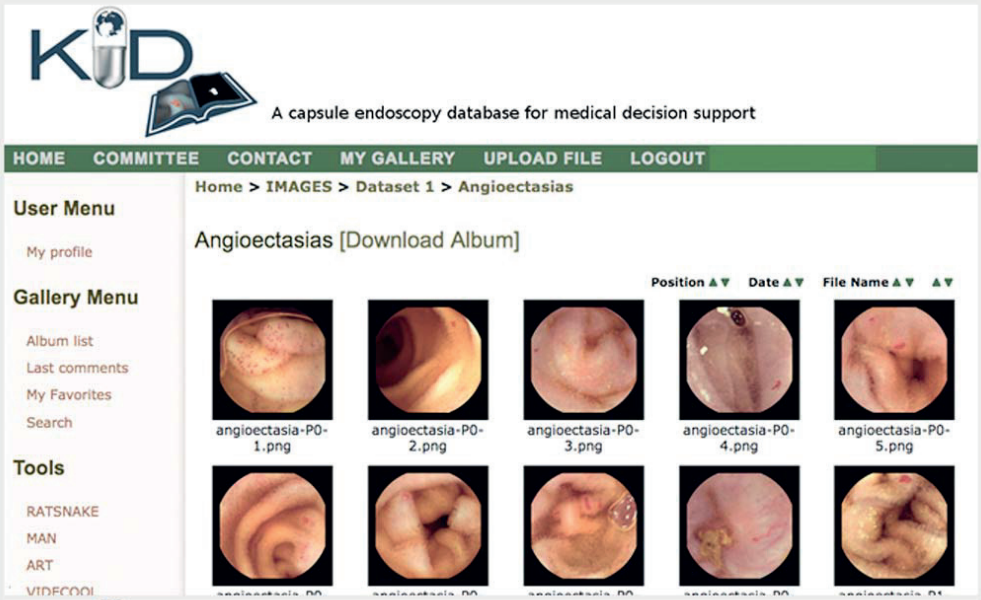

▶ **Fig. 1** Dataset of angioectasia images and their corresponding graphic annotations, seen within the KID website interface.

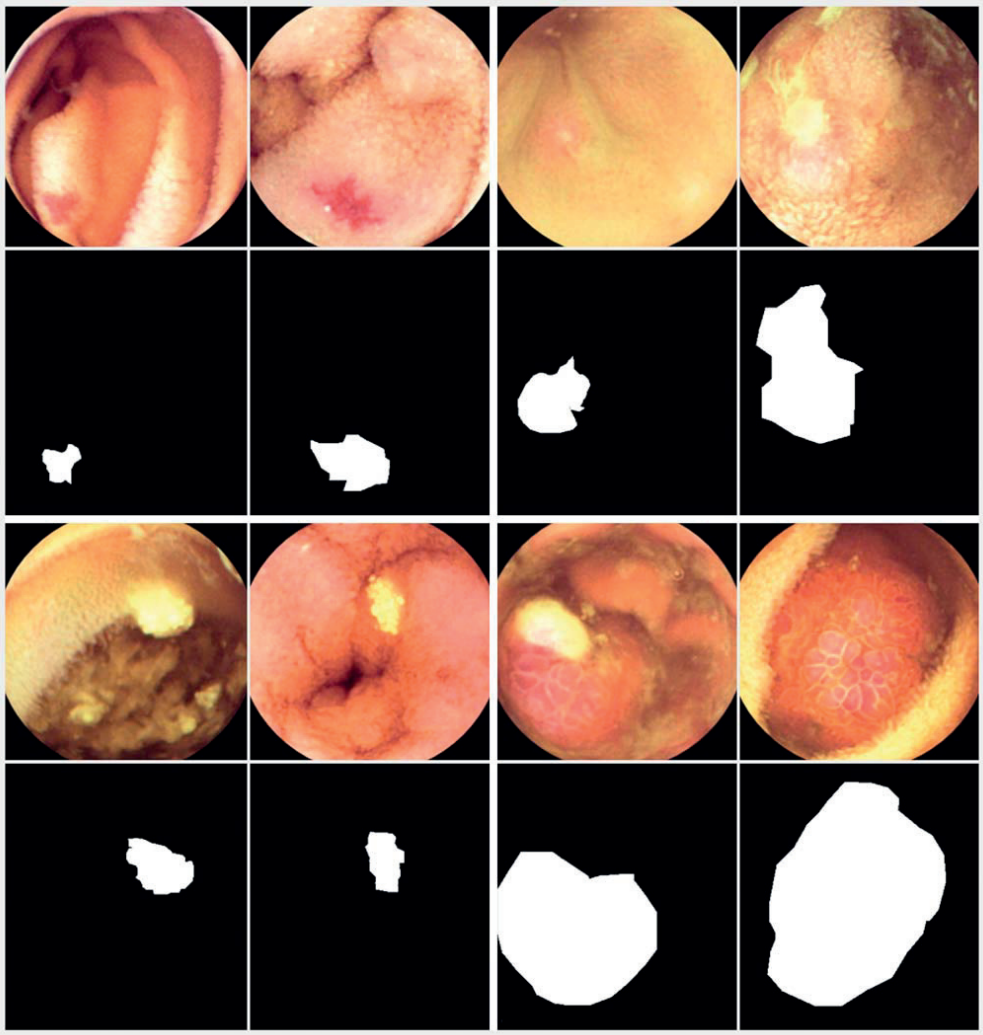

▶ **Fig. 2** Top row, from left: P1 and P2 angioectasias, aphthae and ulcer, with corresponding graphic annotations made using Ratsnake beneath each image, showing the position, size and shape of the lesions in the images. Bottom row, from left: two images of nodular lymphangiectasias and two images of polypoid lesions, with graphic annotations below each image.

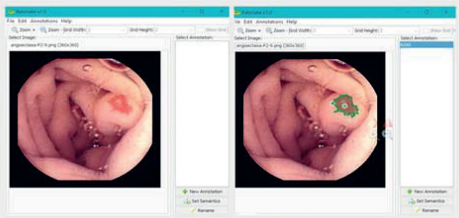

▶ **Fig. 3** Use of the Ratsnake annotation tool to perform graphical annotation of an angioectasia on capsule endoscopy (CE). Left: original image. Right: graphic annotation of the angioectasia.

VIDEO 1

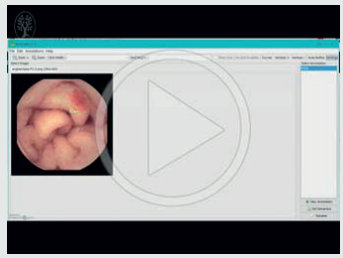

▶ Video 1: Video showing annotation process using Ratsnake software.

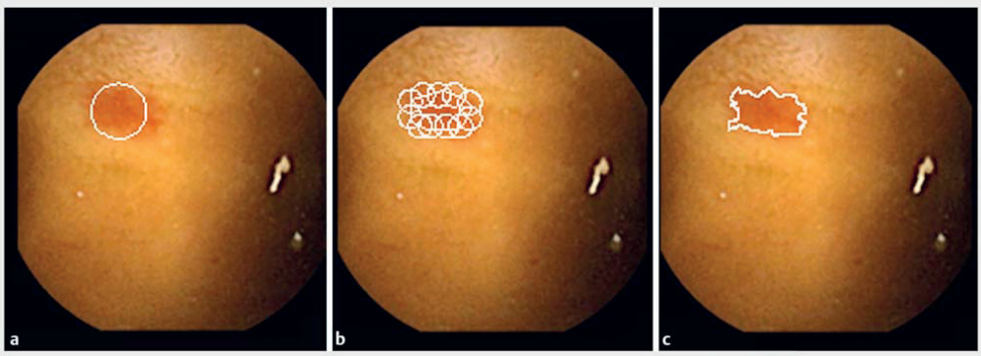

▶ **Fig. 4** Segmentation of image using the Localized Region-based Active Contour (LRAC) algorithm. **a** User-defined initial contour. **b** Contour deformation/morphing based on local histogram information on brightness and intensity in the various circular neighborhoods at each point on the contour. **c** Segmented image obtained.

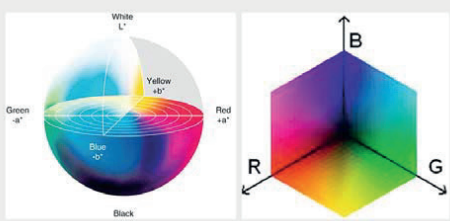

▶ **Fig. 5** CIE-Lab color wheel (left) compared to the RGB color wheel (right).

Results

The algorithm was evaluated for the measurement of six different types of small-bowel lesions, for each channel of CIE-Lab color space. The lesion areas were measured in pixel units, which, in the context of CE, is a more feasible and accurate approach. The average surface measurements closest to those performed by expert human readers were obtained by application of LRAC on the red-green scale of the CIE-Lab color space, with a JI of 67 ± 13 %. This result complements the findings in our previous study, indicating component *a* as an informative source of saliency for automated lesion detection [11]. The agreement between human readers and the algorithm per lesion type is summarized in ▶ **Table 1**. The most accurate measurements were obtained for lymphangiectasias, whereas this algorithm is less suitable for the measurement of ulcers.

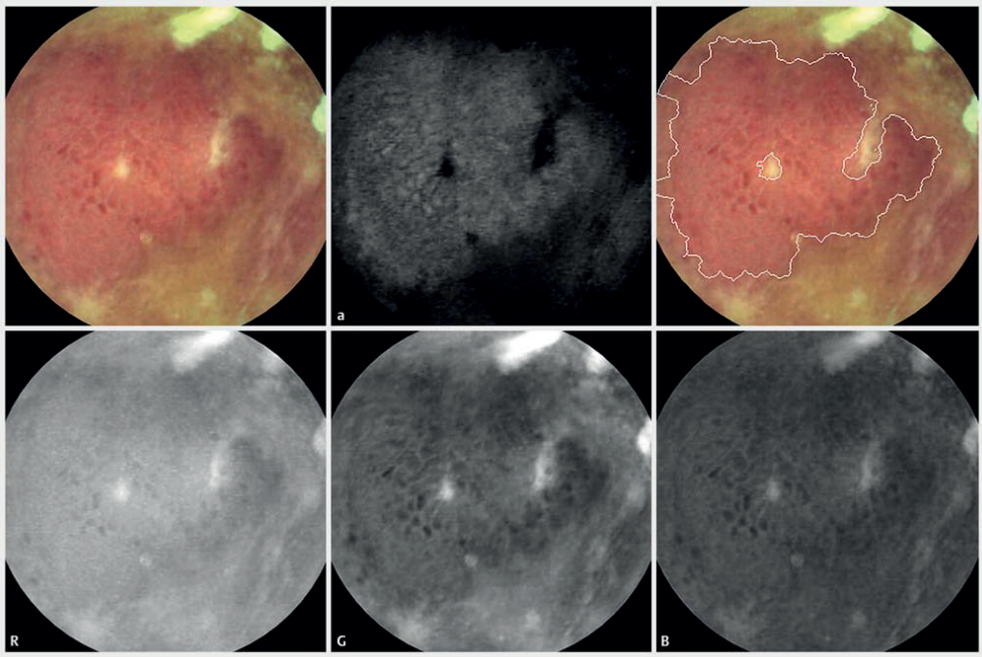

▶ **Fig. 6** Image segmentation by Localized Region-based Active Contour (LRAC) algorithm. Top row, from left: original image of mucosal break with surrounding erythema; image segmentation using the *a* component of CIE-Lab; the final result of image segmentation where the contours have been defined and marked. Bottom row: the image when broken down into red (R), green (G) and blue (B) channels under the traditional RGB system.

Discussion

Human factors remain a barrier to timely and accurate CE diagnosis [4]. AI systems can improve clinical performance, patient safety, and resource utilization [1, 3]. Open interdisciplinary exchange of information is key to technological advancement and therefore improved clinical outcomes [3]. New technological developments may not always meet pertinent healthcare needs due to little communication between software engineers and clinicians; furthermore, open access databases of endoscopic images are scarce, especially those specifically related to small-bowel CE [5]. This is despite growing clinical demand and use of CE as an investigative modality. However, such interactive formats are vital for engaging a new generation of clinicians; this is currently hindered by inadequately developed software [13]. Therefore, KID aims to be a comprehensive and all-encompassing resource for continuous development of CAD in CE, and to encourage two-way dialog between technological developers and end-users. For example, KID compiles images from all commercial CE models and is international, thus increasing its scope.

The experiment detailed above shows that generally good agreement was achieved between expert human readers and the MLA in measuring the size of common small-bowel lesions. This implies automated lesion measurement is feasible, and MLAs could eventually replace or drastically reduce the workload of valuable human resources. In a recent study, van der Sommen et al. [14] detailed collaboration between IT engineers and clinicians to develop a CAD algorithm for diagnosis of early neoplasia in Barrett's esophagus, with good results. An advantage of the method presented in this study over previous automated measurement approaches is its suitability for a variety of lesion types. In a recent study [15] using images of angiectasias available in KID, we showed that the interobserver agreement between CE reviewers, in terms of JI, in lesion annotation ranges between 65 ± 15 % and 67 ± 13 %, and the respective intraobserver agreement, between 69 ± 17 % and 71 ± 13 %. This dataset was similar in terms of the morphological characteristics of the displayed angiectasias, indicating that our MLA has a performance comparable to that of human readers. However, a limitation shown by the experiment is that it does not perform as well with all mucosal lesions. Further algorithm de-

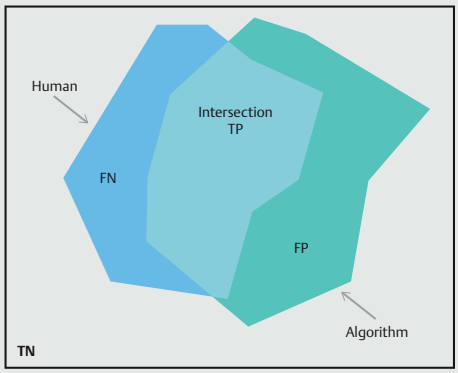

$$JI = \frac{\text{Intersection}}{\text{Union}} = \frac{TP}{TP + FP + FN}$$

▶ **Fig. 7** Agreement between a human reader and the algorithm as quantified by the Jaccard Index (JI). Given a region annotated by a human expert (left) and a region annotated by the algorithm (right), the intersection of the two regions corresponds to the True Positive (TP) pixels, i. e. those actually belonging to the abnormality. The union of the two regions corresponds to the sum of the False Negative (FN), the False Positive (FP) and the TP. Thus, if the two regions perfectly coincide, FN = 0, FP = 0 and their intersection (TP) becomes equal to their union, resulting in JI = 100 %. If there is no match between the two regions, then TP = 0 and JI = 0.

▶ **Table 1** Agreement between reviewers and software in measuring lesion size for various types of lesion seen on capsule endoscopy (CE).

Lesion	JI, mean ± SD, %
Angioectasias	64 ± 11
Aphthae	64 ± 8
Chylous cysts	70 ± 14
Lymphangiectasias	81 ± 6
Polypoid lesions	75 ± 21
Ulcers	56 ± 9

Abbreviations: JI, Jaccard Index; SD, standard deviation.

velopment is therefore required, showing the need for platforms such as KID.

In conclusion, KID is, to our knowledge, the only database of CE images and videos with both graphic and semantic annotations, developed specifically for MDSS research. It provides a platform for data sharing and CAD software development. The experiments detailed are proof-of-principle studies demonstrating the potential for KID to fulfill this role.

Competing interests

None

References

[1] Koulaouzidis A, Rondonotti E, Karargyris A. Small-bowel capsule endoscopy: A ten-point contemporary review. World J Gastroenterol 2013; 19: 3726 – 3746

[2] Hale M, McAlindon ME. Capsule endoscopy as a panenteric diagnostic tool. Br J Surg 2014; 101: 148 – 149

[3] Iakovidis DK, Koulaouzidis A. Software for enhanced video capsule endoscopy: challenges for essential progress. Nat Rev Gastroenterol Hepatol 2015; 12: 172 – 186

[4] Zheng Y, Hawkins L, Wolff J et al. Detection of lesions during capsule endoscopy: physician performance is disappointing. Am J Gastroenterol 2012; 107: 554 – 560

[5] Selected websites recommended by the Atlas of Gastrointestinal Endoscopy. Available at: http://www.endoatlas.com/websites.html

[6] Cong Y, Wang S, Liu J et al. Deep sparse feature selection for computer aided endoscopy diagnosis. Pattern Recognit 2015; 48: 907 – 917

[7] Korman LY, Delvaux M, Gay G et al. Capsule Endoscopy Structured Terminology (CEST): Proposal of a standardized and structured terminology for reporting capsule endoscopy procedures. Endoscopy 2005; 37: 951 – 959

[8] Iakovidis DK, Goudas T, Smailis C etal. Ratsnake: A versatile image annotation tool with application to computer-aideddiagnosis. Sci World J 2014: 286856

[9] Freitas F, Schulz S, Moraes E. Survey of current terminologies and ontologies in biology and medicine. RECIIS Electron J Commun Inf Innov Health 2009; 3: 7 – 18

[10] Lankton S, Tannenbaum A. Localizing region-based active contours. IEEE Trans Image Process 2008; 17: 2029 – 2039

[11] Iakovidis DK, Koulaouzidis A. Automatic lesion detection in capsule endoscopy based on color saliency: Closer to an essential adjunct for reviewing software. Gastrointest Endosc 2014; 80: 877 – 883

[12] Pont-Tuset J, Marques F. Supervised evaluation of image segmentation and object proposal techniques. IEEE Trans Pattern Anal Mach Intell 2016; 38: 1465 – 1478

[13] Kilbridge PM, Classen DC, Kohn L et al. The informatics opportunities at the intersection of patient safety and clinical informatics. J Am Med Inform Assoc 2008; 15: 397 – 407

[14] Van der Sommen F, Zinger S, Curvers WL et al. Computer-aided detection of early neoplastic lesions in Barrett's esophagus. Endoscopy 2016; 48: 617 – 624

[15] Koulaouzidis A, Yung D, Rondonotti E et al. Chromoendoscopy for angiectasias in capsule endoscopy; blue or just white? Gut 2016; 65: A52 – A53

Paper IV

Novel experimental and software methods for image reconstruction and localization in capsule endoscopy

OPEN ACCESS

Authors
Anastasios Koulaouzidis[1], Dimitris K. Iakovidis[2], Diana E. Yung[1], Evangelos Mazomenos[3], Federico Bianchi[4], Alexandros Karagyris[5], George Dimas[2], Danail Stoyanov[3], Henrik Thorlacius[6], Ervin Toth[7], Gastone Ciuti[4]

Institutions
1 Centre for Liver & Digestive Disorders, The Royal Infirmary of Edinburgh, Edinburgh, UK
2 University of Thessaly, Department of Computer Science and Biomedical Informatics, Lamia, Greece
3 Centre of Medical Image Computing and Department of Computer Science, University College London, London, UK
4 The BioRobotics Institute, Scuola Superiore Sant'Anna, Pisa, Italy
5 IBM Research, Almaden California, United States
6 Department of Clinical Sciences, Lund University, Malmö, Sweden
7 Department of Gastroenterology, Skåne University Hospital, Malmö, Sweden

submitted 16.6.2017
accepted after revision 9.10.2017

Bibliography
DOI https://doi.org/10.1055/s-0043-121882 |
Endoscopy International Open 2018; 06: E205–E210

ISSN 2364-3722

Corresponding author
Dr Anastasios Koulaouzidis, Endoscopy Unit, The Royal Infirmary of Edinburgh, 51 Little France Crescent, Edinburgh EH16 4SA, United Kingdom
Fax: +077-89-588-408
akoulaouzidis@hotmail.com

ABSTRACT

Background and study aims Capsule endoscopy (CE) is invaluable for minimally invasive endoscopy of the gastrointestinal tract; however, several technological limitations remain including lack of reliable lesion localization. We present an approach to 3D reconstruction and localization using visual information from 2D CE images.

Patients and methods Colored thumbtacks were secured in rows to the internal wall of a LifeLike bowel model. A PillCam SB3 was calibrated and navigated linearly through the lumen by a high-precision robotic arm. The motion estimation algorithm used data (light falling on the object, fraction of reflected light and surface geometry) from 2D CE images in the video sequence to achieve 3D reconstruction of the bowel model at various frames. The ORB-SLAM technique was used for 3D reconstruction and CE localization within the reconstructed model. This algorithm compared pairs of points between images for reconstruction and localization.

Results As the capsule moved through the model bowel 42 to 66 video frames were obtained per pass. Mean absolute error in the estimated distance travelled by the CE was 4.1 ± 3.9 cm. Our algorithm was able to reconstruct the cylindrical shape of the model bowel with details of the attached thumbtacks. ORB-SLAM successfully reconstructed the bowel wall from simultaneous frames of the CE video. The "track" in the reconstruction corresponded well with the linear forwards-backwards movement of the capsule through the model lumen.

Conclusion The reconstruction methods, detailed above, were able to achieve good quality reconstruction of the bowel model and localization of the capsule trajectory using information from the CE video and images alone.

Introduction

Capsule endoscopy (CE) is a key technology for minimally invasive small-bowel investigation, with good sensitivity for major pathology. Nevertheless, CE continues to face several technological limitations including lack of reliable lesion localization capability [1] and the 2-dimensional (2D) nature of CE images which hampers lesion characterisation [2, 3]. Consequently, it is difficult to determine the precise location of lesions detected within the body. This information is vital to establish prognosis and for treatment planning, e. g. deciding the appropriate route for device-assisted enteroscopy.

We present an approach to localization using visual information derived from CE images, without additional external or in-

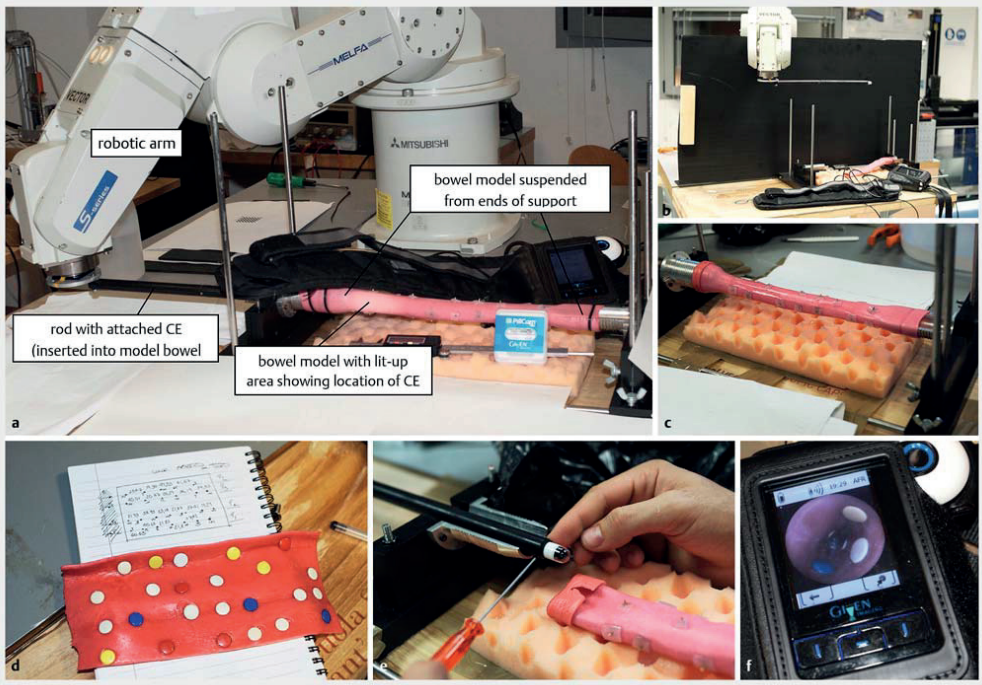

▶ **Fig. 1** Experimental set-up. **a** Overview of set-up before opaque covering was placed over model bowel. **b** View of set-up showing length of rod with attached CE compared to bowel model. **c** Detail of assembled bowel model suspended from supports. **d** Bowel model opened after test, showing coloured thumbtacks fixed in rows. **e** PillCam SB3 capsule fixed to end of straight plastic rod to enable movement through model bowel lumen. **f** Assembled bowel model with thumbtacks seen through real time CE viewer.

ternal sensory devices. Earlier such approaches include topographic video segmentation, i. e. division of video frames into a number of consecutive segments corresponding to different parts of the gastrointestinal (GI) tract [4]. Later approaches were based on motion estimation to localise the CE with respect to anatomical landmarks [1]. We propose a CE localization system based on landmark or feature extraction and tracking in consecutive video frames [5]. This system implements visual odometry to provide estimations of relative movement of the CE during its passage through the GI tract [6]; this information can also be used to achieve 3-dimensional (3D) reconstruction of the bowel lumen.

Patients and methods

Experimental procedure

The experiment was performed in a controlled setting using a commercially available capsule fixed to a robotic arm which was used to move the capsule through an in vitro bowel phantom. The setup modules are detailed below (▶ **Fig. 1**):

- High-precision robotic arm (RV-3SB robot, Mitsubishi, Tokyo, Japan): able to move the capsule forwards and backwards through the bowel phantom at programmed velocities.
- Straight plastic rod attached to the robotic arm, with the capsule fixed to one end; the rod was longer than the total length of the model to allow the capsule to traverse the entire lumen. The capsule was aligned to the center of the lumen.
- Pillcam SB3 (Medtronic, Minneapolis, USA) capsule with camera resolution 320 × 320 pixels, variable frame rate of 2 to 6 frames per second (fps), and 156° field of view.
- 30-cm lifelike bowel model (LifeLike Biotissue Inc, Ontario, Canada); the model was fixed and suspended in a custom-made support. The internal diameter was about 23 mm, consistent with that of adult humans.

The setup was covered with an opaque plastic box to minimize external illumination, similar to in vivo conditions. The real-time viewer used to show the images captured by the Pillcam SB3 capsule. Colored thumbtacks (diameter 0.95 mm) were se-

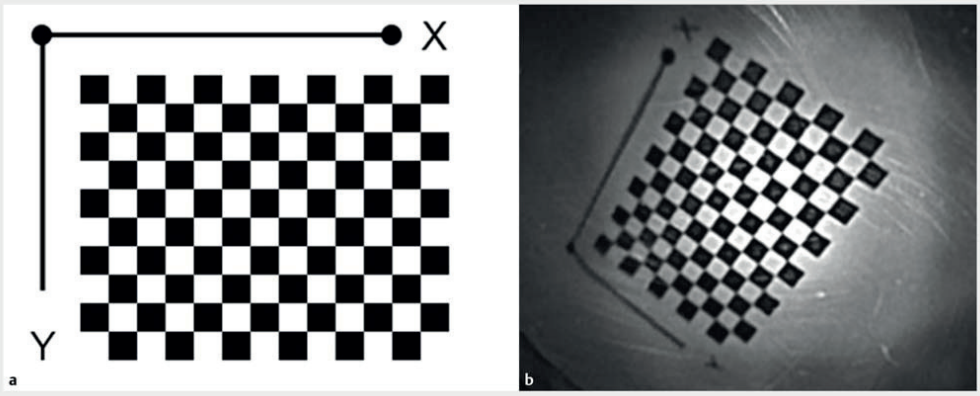

▶ **Fig. 2** Checkerboard pattern used for initial CE calibration. **a** The CE calibration pattern as printed. **b** The CE calibration pattern as viewed from the CE.

cured in four rows along the lumen and the appearance and location of each marker from the rim of the model were carefully documented. Normal gut peristalsis was not simulated at this stage to ensure accurate measurements of distances and therefore the reproducibility of results in this preliminary experiment.

Calibration and estimation of 2D trajectory

Camera calibration is a fundamental process for determining the unknown intrinsic parameters of a camera, such as its focal length. It is used by the 3D reconstruction software to produce estimates of camera position in real-world units (meters). Calibration is usually performed only once, during system development, for a given camera model. Following activation of the PillCam SB3, calibration was performed before beginning the experiment, to correct for lens distortion and calculate the unspecified intrinsic parameters of the camera including focal length. The set-up used images of a chessboard with 3-mm squares arranged in a 10×13 configuration, ▶ **Fig. 2**. The capsule was mounted on the plastic rod and robotically navigated into the model lumen. It was moved forwards and backwards in a straight line through the length of the model. Several passes were made at different constant velocities of 0.5 to 8 mm/second.

Calibration was performed using Kannala and Brandt's method, best suited for the calibration of conventional, wide-angle and fish-eye lenses [7]. The motion estimation algorithm detects corresponding points of interest (POI) in consecutive video frames; represented by the drawing pins lining the bowel wall. Relative distances between the POI and camera lens were used to estimate actual distances travelled by the capsule. The mean absolute error (MAE) of localization was used to quantify accuracy, calculated as the mean of the absolute difference between estimated and actual travel distances of the capsule.

3D reconstruction

The 2D images obtained from the capsule were then processed to achieve 3D reconstruction of the bowel model. A modified Shape-from-Shading (SfS) technique was used to reconstruct a 3D surface from 2D images. SfS refers to a computer vision technique that recovers 3D shape and depth information from 2D digital images by investigating the variation of illumination across the image. The major assumption that this technique is based on is that the amount of reflected light is dependent on the orientation (shape) of the scene that is imaged. The majority of SfS approaches assume a light source either coinciding with the optical center or infinitely far away from the scene. However, these conditions are unrealistic for endoscopic recordings. Despite the small distance between camera and light source, the observed tissue is also very close to the camera and images are therefore affected by small illumination changes. To overcome this limitation, the method used approximates the position of the light source at the tip of the endoscope and uses the position directly in the algorithm. Given the small size and the density of the circular LED array of the capsule, its overall illumination can be considered equivalent to that of such a single light source following an approximately uniform illumination aggregation model [8]. Traditional SfS can recover depth up to an unknown scale factor, using the albedo of the imaged surface [9]. Albedo is a physical measure of reflectance or brightness of a surface. For a given surface, albedo is defined as the ratio of the reflected irradiance to the incident irradiance and it is dimensionless. Irradiance is a physical measure defined as the radiant flux (power) received by a surface per unit area. Furthermore, in our technique, because we consider the camera and light source as separate entities, we can model the SfS problem such that the unknown albedo is parameterized and calculated, thus providing a more accurate metric estimation of depth [10].

▶ **Table 1** Best results for travel distance estimation obtained using Kannala and Brandt's method.

Row of pins	Travel distances (cm)		
	Actual	Estimated	Absolute error
1	19.8	20.7	0.9
2	17.4	14.8	2.6
3	19.9	20.7	0.8
4	19.6	20.9	1.3

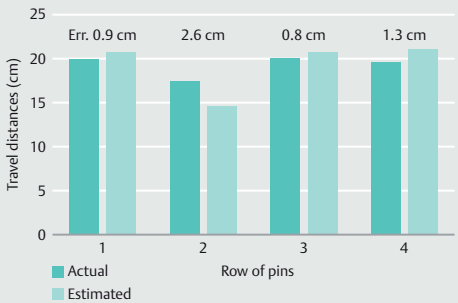

▶ **Fig. 3** Best results in travel distance estimation after calibration per row of thumbtacks. The error between the actual and the estimated travel distance is presented on top of the respective bars.

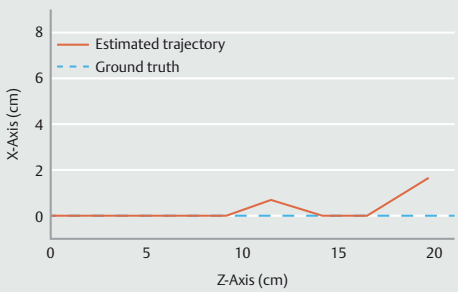

▶ **Fig. 4** Graph showing estimated vs actual CE trajectory.

The ORB-SLAM (Oriented FAST and Rotated BRIEF – Simultaneous Localization and Mapping) is used to estimate the pose (location and orientation) of a camera by finding matching points in image sequences as in videos [11]. From these matching points and the known calibration parameters of the camera, an estimation of the camera's pose as well as a sparse 3D reconstruction (mapping) of the environment can be extracted. Using a sequence of images from the CE video, the entire trajectory ("tracks") of the CE can be estimated. In ORB-SLAM the matching points in consecutive images are extracted using a specific type of customized image features called ORB. ORB features include Features from Accelerated Segment Test (FAST), used for detection of points of interest within the image [12] and Binary Robust Independent Elementary Features (BRIEF) [13], used for the representation of image content at the points of interest. These features offer the advantage of fast calculation, facilitating the real-time operation of SLAM, as well as being invariant to viewpoint rotation and scale changes.

Results

Calibration and travel distance estimation

Seventeen video frames of the checkerboard (▶ **Fig. 2**) were used for calibration. As the capsule was navigated through the model bowel, the number of video frames per movement ranged from 42 to 66, due to the variable frame rate of the capsule. Overall, the MAE in the estimated distance travelled by the capsule was 4.1 ± 3.9 cm, for a camera focal length of 1.16 mm. Minimum error achieved was 1.4±0.8 cm, and the respective results per row of thumbtacks are illustrated in ▶ **Table 1** and ▶ **Fig. 3**.

The 2D reconstruction of the capsule's trajectory through the model bowel is shown in ▶ **Fig. 4**. The solid red line represents the estimated capsule movement, in comparison to the actual path shown by the straight broken line.

3D reconstruction

Both 3D reconstruction methods detailed above were able to achieve a good, but not optimal, reconstruction of the bowel model using information from the CE video alone.

Using the modified SfS technique, the cylindrical shape of the model bowel, with details of the tissue and attached thumbtacks, was successfully reconstructed. Examples of reconstructed bowel lumen, with corresponding original images, are shown in ▶ **Fig. 5**.

The ORB-SLAM method of 3D reconstruction produced good localization of the capsule within the reconstructed model. Results using this method are shown in ▶ **Fig. 6**. The blue triangles, corresponding to the outline of the reconstructed bowel wall from each frame of the video, are positioned in a straight line, with the overall "track" denoted by the green line passing through the triangles. This corresponds with the linear forwards-backwards movement of the capsule in the straight bowel model used.

Discussion

CE technology has progressed significantly since its introduction to routine clinical practice; however, the interpretation of a CE examination in order to reach a diagnosis remains heavily reliant on human readers [14]. Furthermore, the long reading times required also diminish its clinical efficiency. Therefore, further technological developments should aim to reduce CE reading times and minimize variability in CE reading. An ideal way to do so is to develop methods for computer-assisted and eventually automated diagnosis.

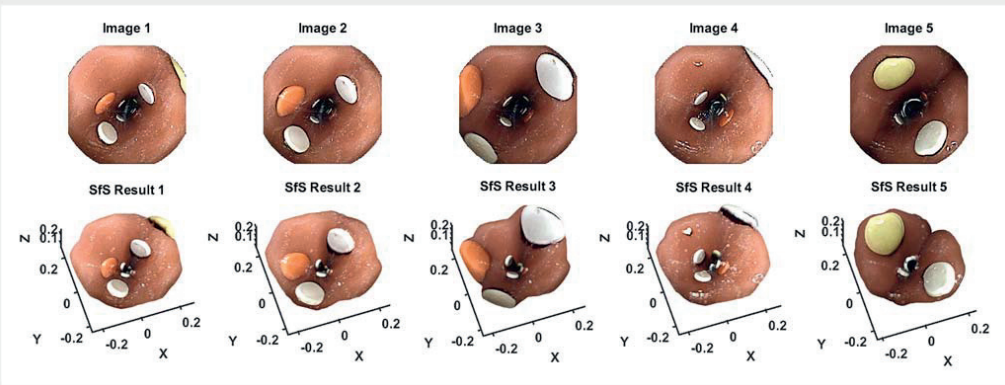

▶ **Fig. 5** Reconstruction results using the modified SfS technique. Selected frames from the CE video are shown above, with the corresponding reconstructions below.

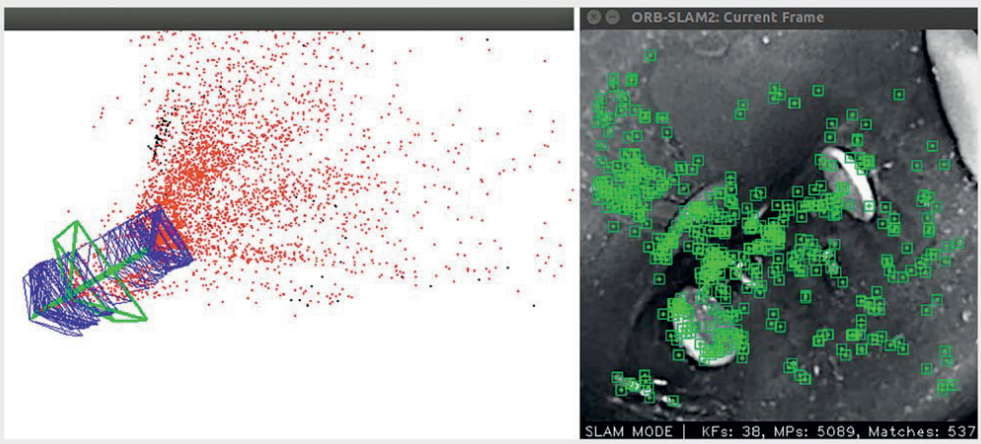

▶ **Fig. 6** Results obtained using the ORB-SLAM algorithm. The location and post of the CE camera is estimated for each frame (current track in green rectangle; previous tracks in blue rectangles). The green line denotes the overall CE trajectory. The sparse 3D reconstruction is illustrated as a point cloud.

A significant limitation of CE is the lack of accurate localization. Current approaches to capsule and hence lesion localization include: transit time estimation from anatomical landmarks, localization in 2D or 3D space with respect to external sensors and radiofrequency triangulation, active magnetic localization, magnetic resonance, ultrasound and positron emission imaging-based approaches [4, 15, 16]. Our method provides comparable performance to methods based on external sensor arrays, without their use. Furthermore, because CE is a wireless minimally invasive system, information is mainly obtained as videos and images. 3D information could facilitate more detailed diagnostic evaluation of lesions seen [17]. Due to the difficulty in accessing the human small-bowel, more invasive investigations or procedures such as deep enteroscopy should be optimally planned.

Typically, in CE, monocular vision provides the only information for 3D reconstruction. Therefore, our modified SfS method uses assumptions more applicable to CE images, obtained in the confined environment of the bowel lumen, and where manual focus is impossible due to the passive nature of capsule propulsion. To determine depth, this method estimates the albedo (whiteness coefficient, or measure of reflection) by using specular highlights and the corresponding surface normals of the reconstructed surface [10].

Our setup has inherent limitations due to currently available technology. First, the intrinsic parameters of the PillCam SB3 are unknown; therefore, vital information such as the focal length of the lens had to be estimated via calibration. Secondly, we assumed that the capsule moved at constant velocity following the centre of the bowel lumen. Finally, the model bowel was linear, immobile and had an elliptical cross-section throughout; furthermore, there was no luminal content. These do not entirely reflect actual human bowel structure and function, nor the usual clinical conditions under which CE operates.

Conclusion

In conclusion, based on our experimental set-up, we present methods for both 2D and 3D localization of a capsule using visual information alone. Such methods are feasible and have potential to be of clinical use. However, there remains a significant margin of error, indicating that much further work is required to refine these processes.

Acknowledgements

The work described in this paper was partially supported by the European Commission within the framework of the endoscopic versatile robotic guidance, diagnosis and therapy of magnetic-driven soft-tethered endoluminal robots Project-H2020-ICT-24-2015 (EU Project-G.A. number: 688592). The authors thank all the collaborators of the EU project.

Competing interests

None

References

[1] Iakovidis DK, Koulaouzidis A. Software for enhanced video capsule endoscopy: challenges for essential progress. Nat Rev Gastroenterol Hepatol 2015; 12: 172 – 186

[2] Grove PM. The Psychophysics of binocular vision. In: 3D-TV System with Depth-Image-Based Rendering. New York, NY: Springer New York; 2013: 347 – 373

[3] Van Rijn JC, Reitsma JB, Stoker J et al. Polyp miss rate determined by tandem colonoscopy: A systematic review. Am J Gastroenterol 2006; 101: 343 – 350

[4] Baptista V, Marya N, Singh A et al. Continuing challenges in the diagnosis and management of obscure gastrointestinal bleeding. World J Gastrointest Pathophysiol 2014; 5: 523 – 533

[5] Spyrou E, Iakovidis DK. Video-based Measurements for Wireless Capsule Endoscope Tracking. Meas Sci Technol 2014; 25: 14

[6] Spyrou E, Iakovidis DK, Niafas S et al. Comparative assessment of feature extraction methods for visual odometry in wireless capsule endoscopy. Comput Biol Med. 2015; 65: 297 – 307

[7] Kannala J, Brandt SS. A generic camera model and calibration method for conventional, wide-angle, and fish-eye lenses. IEEE Trans Pattern Anal Mach Intell 2006; 28: 1335 – 1340

[8] Cool S, Pieters JG, Mertens KC et al. Development of a high irradiance LED configuration for small field of view motion estimation of fertilizer particles. Sensors 2015; 15: 28627 – 28645

[9] Ciuti G, Visentini-Scarzanella M, Dore A et al. Intra-operative monocular 3D reconstruction for image-guided navigation in active locomotion capsule endoscopy. InBiomedical Robotics And Biomechatronics (Biorob), 2012 4th IEEE Ras & Embs International Conference. 2012: 768 – 774

[10] Visentini-Scarzanella M, Stoyanov D, Yang G-Z. Metric depth recovery from monocular images using Shape-from-Shading and specularities. In: 2012 19th IEEE International Conference on Image Processing. 2012: 25 – 28

[11] Mur-Artal R, Montiel JM, Tardos JD. ORB-SLAM: a versatile and accurate monocular SLAM system. IEEE Transactions on Robotics 2015; 31: 1147 – 1163

[12] Rosten E, Drummond T. Machine learning for high-speed corner detection. Computer Vision–ECCV 2006 2006: 430 – 443

[13] Calonder M, Lepetit V, Strecha C et al. Brief: Binary robust independent elementary features. Computer Vision–ECCV 2010 2010: 778 – 792

[14] Lo SK, Mehdizadeh S, Ross A et al. How Should We Do Capsule Reading? Tech Gastrointest Endosc 2006; 8: 146 – 148

[15] Keuchel M, Kurniawan N, Baltes P et al. Quantitative measurements in capsule endoscopy. Comput Biol Med 2015; 65: 333 – 347

[16] Than TD, Alici G, Zhou H et al. A review of localization systems for robotic endoscopic capsules. IEEE Trans Biomed Eng 2012; 59: 2387 – 2399

[17] Sakata S, Grove PM, Stevenson ARL et al. The impact of three-dimensional imaging on polyp detection during colonoscopy: a proof of concept study. Gut 2016; 65: 730 – 731